united nations
educational, scientific
and cultural
organization

international atomic
energy agency

the
abdus salam
international centre for theoretical physics

H4. SMR/1247
Lecture Note: 09

WORKSHOP ON PHYSICS OF MESOSPHERE-STRATOSPHERE-TROPOSPHERE INTERACTIONS WITH SPECIAL EMPHASIS ON MST RADAR TECHNIQUES

(13 - 24 November 2000)

SCATTERING OF RADIO WAVES, AND THE NATURE OF THE SCATTERS

Prof. W. K. Hocking

Dept. of Physics
University of Western Ontario
London, Ontario
CANADA

"Workshop on Physics of Mesosphere - Stratosphere - Troposphere Interactions with Special Emphasis on MST radar Techniques"

13-24 Nov. 2000
Abdus Salam International Center
For Theoretical Physics
Trieste, Italy.
(Invited)

Lecture Material

Prof W. K. Hocking
Dept of Physics
Univ. of Western Ontario
London, Ontario
N6A 3K7
Canada

Scattering of Radio Waves, and the Nature of the Scatters

In the following pages, I am going to examine the process of radio wave backscatter. I am going to assume that you are already familiar with the concepts of "volume scatter", "Specular Reflection" and Fresnel scatter. I want to take out investigation to a deeper level.

To begin, I am going to look at SPECULAR reflection, and develop appropriate mathematical tools to study it. Then I will consider non-specular scatter - both from isotropeé and amisotropic irregularities. In the initial stages, I am not going to be too concerned about why these different structures exist, - rather, I will just assume the **PHYSICAL** reasons for those structures until later. That will then naturally lead to a discussion about turbulence and other small-scale phenomena. I will then discuss the dynamics of these motions, and show how they interact with radio waves. I will also combine this information and then show how the properties allow radars to be able to be used to actually measuring things like turbulence strength.

Scattering Mechanisms in the clear air and Ionosphere.

W. Hocking

The nature of scattering mechanisms in the clear air and ionosphere is a complicated subject. Scattering is NOT simply due to turbulence, and there are many subtle features about the subject which are even now unanswered.

The figure on the next page gives an example of the sorts of complications. You would expect that if turbulence-induced fluctuations were the sole cause of radio-wave scatter, then the received power would not really depend on the direction in which you point your radar beam (at least in a statistical sense). But this figure shows that the signal strengths in this case are much stronger when the beam is pointed vertically than when it is off-vertical.

Indeed, in this case the signal almost disappears when the radar beam is pointed about 1.6 degrees off-zenith. It appears that the scattering entity is not an isotropic body, but is behaving like a reflecting mirror-
though with perhaps a few gentle undulations on it.

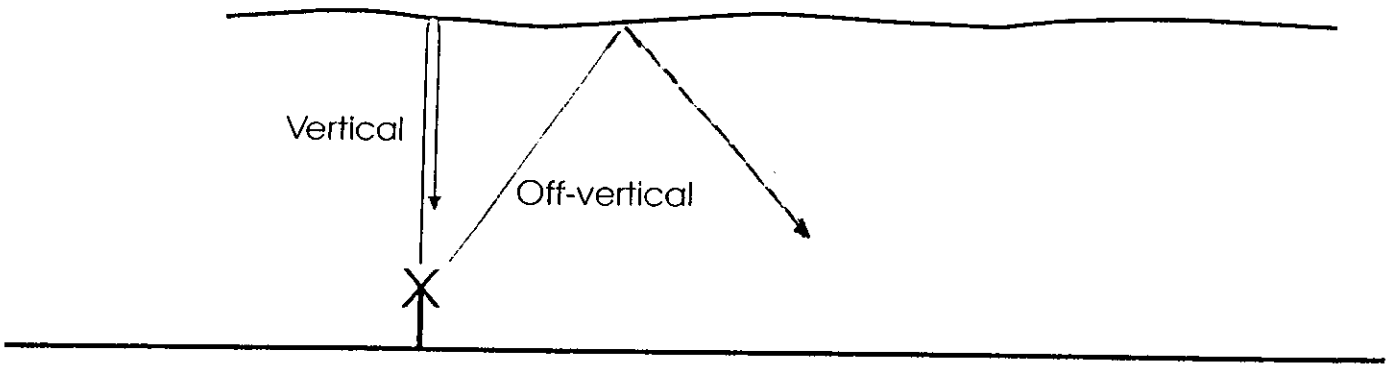

hen if this is so, vertically incident radiation will be reflected back to its source, whereas f-vertical radiation will be reflected away, as in the above diagram.
is type of behaviour is well-known in ionospheric scatter, where the heating of the sun uses the electron density to be approximately stratified.

owever, it also occurs for clear-air scatter in the mesosphere, stratosphere d mesosphere. The reasons for this behaviour (when it does occur) is ll not uderstood. We will consider possible causes shortly.

wever, the fact that these stratified reflectors DO occur means that we need to rn how to deal with them. It turns out that this is moderately simple, because back-scatter equations reduce to a 1-dimensional problem.

To obtain backscattered power, the most common expression for the back-scattered power . essentially sums the backscattered "Huygens' wavelets" from each scattering ctron in the scattering medium. viz.

$$P_s = \frac{k_0^4 P_i}{4\pi^2 R_0^2} \left| \int_V \Delta n(\vec{r}) \exp[i2\vec{k}_i \cdot \vec{r}]\, dV \right|^2 .$$

This works well for a generalized 3-D volume scatter situation.

owever, there is an alternative expression which can be very useful which actually looks e different in form, but which in fact gives a similar result. This special equation works only for stratified media, but is very useful in that case.

Example of Aspect-sensitive Scatter

Buckland Park Radar

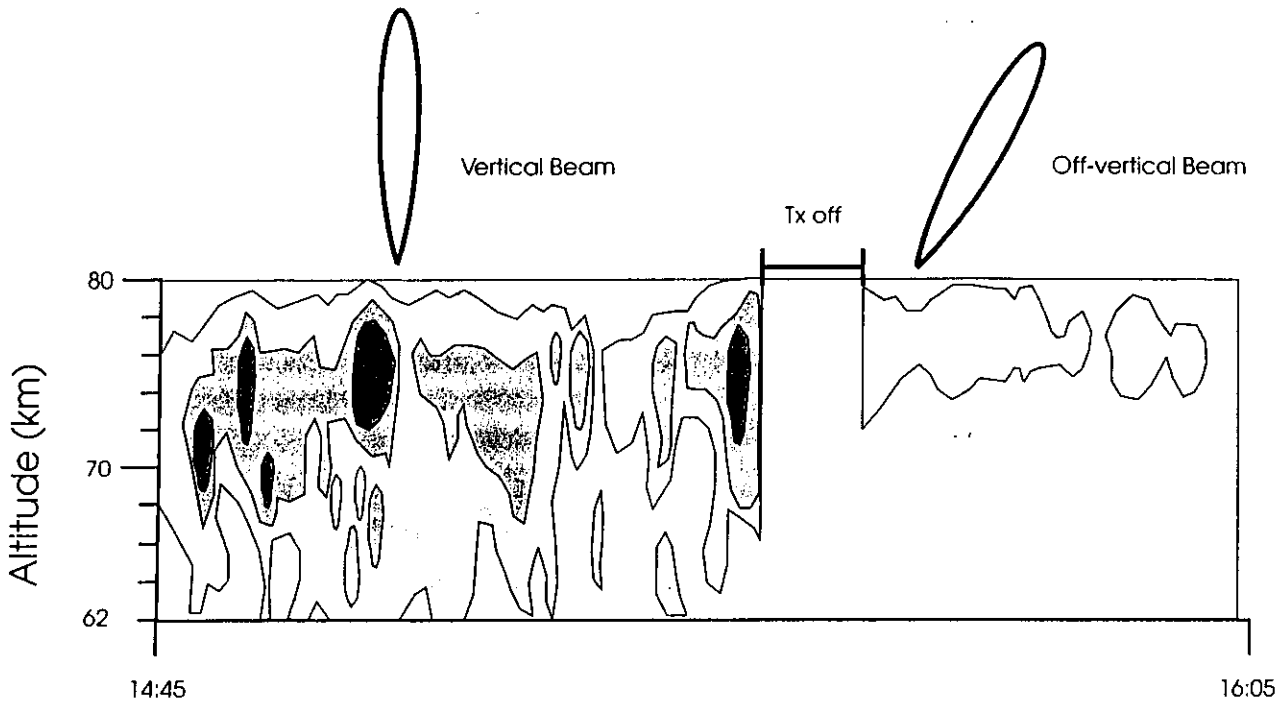

Central Standard Time

Day 151, 1977.

Signal-to-noise Ratio

20 dB
16 dB
12 dB
8 dB
4 dB
0 dB

This graph shows mean powers as a function of height and time measured with a 2 MHz radar. The beam used was moderately narrow (+/- 4.5 degrees half-width), and was pointed first vertically, and then off-vertically.

It was possible to prove that the decrease in power was not simply a temporal change by monitoring the singal strength vertically on a second, broader beam throughout the whole period.

(from Hocking, JGR, 84, 845-851,1979)

This alternative formulation is often easier to work with than the earlier equation. It can most easily be developed by considering the reflection coefficient if a wave as it passes between 2 media separated by a flat surface.

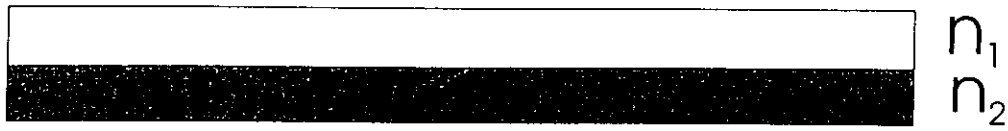

You will recall that the reflection coeffient for radiation incident perpendicular to the surface is given by $(n_2-n_1)/(n_2+n_1)$. We can consider the atmosphere to be a series of such striated layers, as shown below.

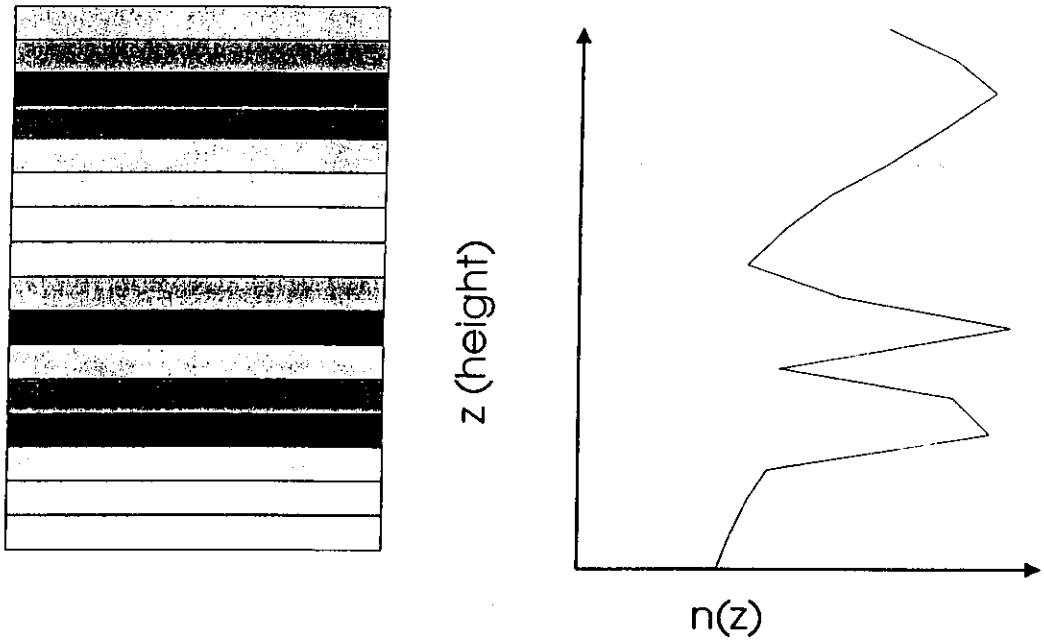

Let us see how these considerations lead us to a new formulation of the scattering problem in one dimension.

(It is also interesting to demonstrate mathematically why the procedures we develop here are in fact the same as equation (79) - I will leave that as an exercise for you. We do not have time to deal with it in this lecture.)

Cant_b2.cdr

The nature of the scattering/reflecting entities

§ IV

The interaction between the radar pulse and the scattering environment.

Horizontally stratified structure

Consider first, and for simplicity, a horizontally stratified atmosphere which has fluctuations in the refractive index in the vertical direction but none horizontally. In fact this is not an unreasonable model to represent the specular reflectors already discussed.

A pulse of the form $g_1(t - z/c)cos[\omega_c(t - z/c)]$ is transmitted, where $f_c = \omega_c/(2\pi)$ is the carrier frequency. At $z = 0$, this is a pulse which varies in time as $g_1(t)cos(\omega_c t)$. This can be written as $g(\xi) = g_z(\xi)cos(k\xi)$ where $k = 2\omega/c = 4\pi/\lambda$ (λ being the radar wavelength) and $\xi = ct/2$ is a length coordinate which closely matches the height of the scatterers (e.g. HOCKING and ROETTGER, 1983). Let the refractive index profile be described by $n(z)$. Imagine a step-like change in refractive index from n_1 to n_2. The the reflection coefficient experienced by a radiowave incident on the step is

$$r'(z) = \frac{n_1 - n_2}{n_1 + n_2} \tag{1}$$

In the limit of small changes, and using the fact that the values of n_i are close to 1, we can write this as

$$r'(z) = \frac{\Delta n}{2} = \frac{1}{2}\frac{dn}{dz}dz \tag{2}$$

We therefore let $r(z) = \frac{1}{2}\frac{dn}{dz}$ be called the reflection coefficient profile, and the reflection coefficient over a step depth dz is $r(z)dz$ (also see HOCKING and VINCENT, 1982a). We will assume that all reflection coefficients are very small, so that by far the bulk of the incident pulse passes right through the reflection level, and only a small portion is reflected.

As the radio pulse approaches this reflection level, the front of it is partially reflected back, and then the trailing bits are reflected until the whole reflected part of the pulse looks like an image of the incident pulse, but turned around and returning to the ground. If there is an other reflecting layer above the first, the same process repeats itself but with a slight time delay compared to the first. Thus the nett reflected echo is the sum of these two reflected pulses, but with a small time delay. If there are multiple reflector levels, it can be readily seen that the resultant amplitude profile is a convolution between the pulse and the reflection coefficient profile.

The reflected complex amplitude as a function of height is then given by

$$a(z) \propto \{\frac{r(z)}{z}\} \otimes g(z) \tag{3}$$

where $\otimes$ stands for convolution. (e.g HOCKING and ROETTGER, 1983, and references therein).

To begin, it is of interest to examine what happens when reflection occurs from a single step of some finite thickness. The easiest step to deal with is one of the type with

$$r(z) \propto e^{\{-\frac{(z-z_0)^2}{d^2}\}}. \tag{4}$$

In this case the refractive index profile is a step of finite thickness, as shown in the following diagram. Note that although d is a measure of the step depth, it is probably not the best measure of this depth. A better measure of the step depth might be the distance between the two points where the reflection coefficient falls to one half of it maximum value, or

$$w = 2\sqrt{ln2}.d$$

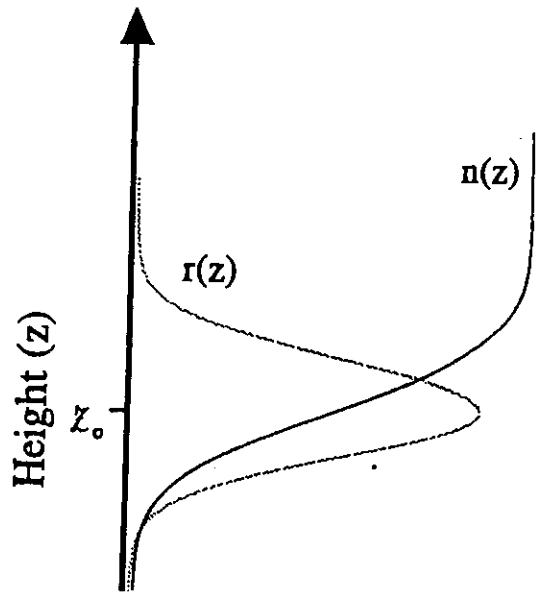

Figure.

The convolution can be done numerically, but it is instructive to examine the process using a slightly different approach. From Fourier theory (e.g. BRACEWELL, 1978) the convolution can be done by Fourier transforming each of $g(z)$ and $r(z)$, multiplying the Fourier transforms $G(k)$ and $R(k)$, and then re-Fourier transforming the product. The process is illustrated diagramatically in the following diagram.

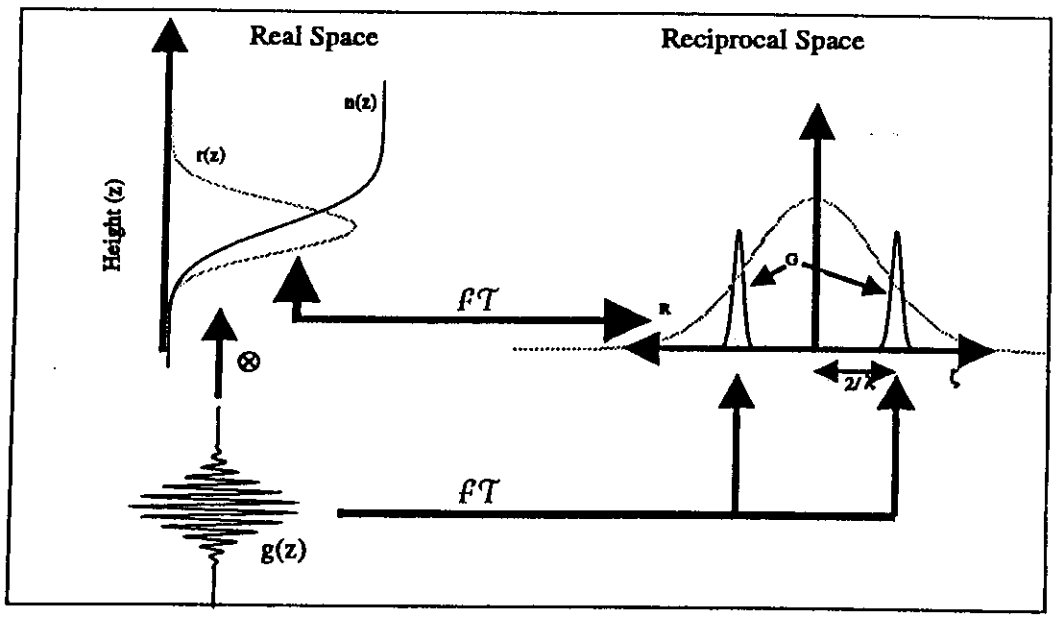

Note that the Fourier transform $G(k)$ of $g(z)$ exists in a narrow band centred at $k_c = 4\pi/\lambda$. Notice also that the narrower the step (smaller d) the wider the function $R(k)$ and so the product of the Fourier transforms is larger. In fact the peak amplitude of the product is

$$A(k_c) \propto e^{-\frac{k_c^2 d^2}{4}} \propto e^{-\frac{4\pi^2 d^2}{\lambda^2}} \tag{5}$$

- so clearly once d exeeds λ, the backscattered power is very small. In fact even if $d = \lambda/4$ ($w = 0.42\lambda$), the reflected amplitude is 0.08 times that for a step of zero width (ie a sharp discontinuity). The power will therfore be reduced by 22 dB compared to a single step. Many authors have taken this to infer that only steps much less than about a quarter wavelength in thickness will ever be seen by radar, and this may well be true for say MF radars. However, with coherent integration and the greater sensitivity of modern radars, particularly VHF radars, it is not so easy to adopt this argument; VHF radars can often see such steps even if reduced in efficiency by 20 dB, and they are indeed capable of detecting layers with a depth d of about $\lambda/4$. However, it is true that beyond this depth, the efficiency falls off remarkably quickly; for example, if $d = \lambda/2$, the power is reduced by 80 dB, and even VHF radars would not normally detect such a step. HOCKING (1987a) has discussed this point and suggests that some "specular reflectors" seen by VHF radars have typical depths with $2d$ = 3 - 4 m, or w between 2.5 and 3 metres; in other words, the steps are right on the edge of the region of detectability.

Another useful model is that of "Fresnel Scatter", a model known for many years in D region MF studies, (eg AUSTIN et al., 1969; MANSON et al., 1969; GREGORY and VINCENT, 1970), but given renewed popularity by GAGE et al (1981) in respect to VHF studies. In this model, horizontal stratification is again assumed, but $n(z)$ is assumed to vary randomly, so the atmosphere can be thought of as a series of thin slabs sitting atop each other, each with slightly different refractive indices. Despite some initial controversy, it is relatively easy to show, using similar procedures to those discussed above, that in this case the backscattered power is proportional to the pulse length (HOCKING and ROETTGER 1983), and if one includes the decrease in reflected power as a function of height z then one finds that the power received by a radar takes the form

$$P_R = \frac{\alpha^2 P_t A_e^2}{4\lambda^2 z^2} \left[F(\lambda)\overline{M}\right]^2 (\Delta z) \tag{6}$$

where P_R is the received power, α is the array efficiency, P_t is the peak transmitted power, A_e is the array effective area, λ is the radar wavelength, z is the height of reflection, $\overline{M}$ is the mean generalized refractive index gradient and $F(\lambda)$ is a "calibration constant" which must be determined empirically for each radar. The term Δz represents the radar pulse-length. In the case that $\overline{M}$ varies substantially within one pulse-length this formula need some modification, as described by HOCKING and ROETTGER (1983). Later developments of this model have been discussed by GAGE et al., (1985) and GREEN and GAGE, (1985).

(+ also requires horizontal fluctuation in depth to be $\leq \frac{1}{8}$ dep$\}$ — not proven)

Complications for the case of MF and HF radio waves

Although approximately applicable in many instances, the above theory does have some serious limitations, which are especially a problem at MF and HF. These complications include the dispersive nature of a wave pulse when the electron density gets high, and also the effects of absorption on the wave packet. In order to address these issues more precisely, we look back at a previous paper by HOCKING and VINCENT, JATP, 44, 843, 1982). This paper shows a more general formulation which enables us to deal with these (and many other) complications.

We will not discuss that aspect any further here.

~~An appropriate extract from that paper now follows, and will be discussed.~~

Non-specular scatter.

In the previous section, we looked at specular reflection. We did this for two reasons - firstly, because it really happens in the atmosphere, and secondly because it is mathematically fairly easy to deal with.

We will now turn to consideration of non-specular scatter. Scatter due to irregularities produced by turbulence is an example of non-specular scatter. Non-specular scatter is in fact more common than specular reflection, and it is somewhat more complex to deal with. It is complicated by the fact that even turbulent scatter can have some aspects of "specularity" about it - we call this feature "aspect-sensitivity".

We will look at turbulence in more detail next lecture, but for now we want to look solely at its properties of directionality of scatter. Before that, though, it is important to look at what a "typical" turbulent irregularity looks like. Turbulent iregularities are in fact very distorted, elongated, string-like features. The tearing motions of the wind shears produce this type of effect. The figure on the next page demonstrates how such irregularities form.

However, despite the fact that we know that turbulent irregularities are distorted like this, we know that if we do a 3-dimensional spatial auto-correlation of the turbulent region, we will get a broadly smooth fall-off in all directions. Generally, we assume that the autocorrelation function falls off in a Gaussian manner in all directions, with (possibly) different rates of "decay" in different orthogonal directions.

Because of this, we often REPRESENT turbulent irregularities (and indeed other quasi-isotropic irregularities) by Ellipsoids which fall off in density in a Gaussian manner as one moves away from their centre.

A 2-D cross-section through such an ellipsoid is shown below. Note that it has been drawn to be longer than it is high. If the ellipse were a circle, then it would indicate isotropic scatter.

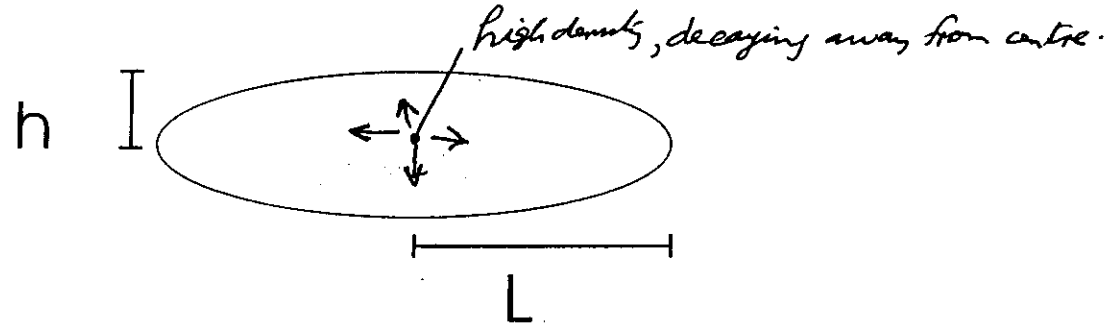

We let the vertical distance over which the refractive index perturbation reaches 1/e of its maximum be h, and the corresponding horizontal distance be L. We will employ this "typical eddy" as a model in our discussions.

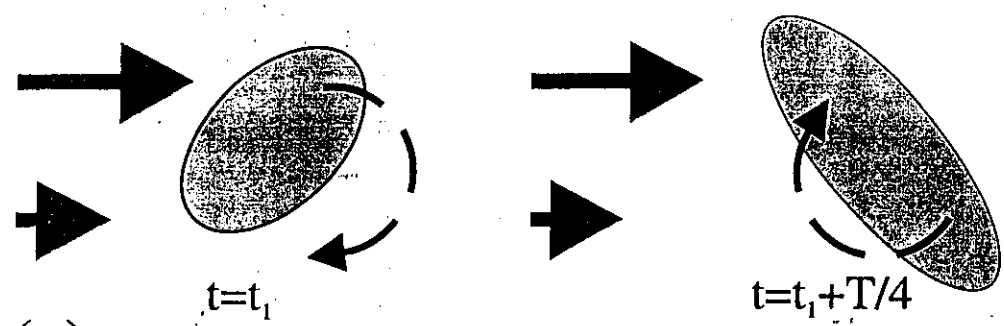

(a)

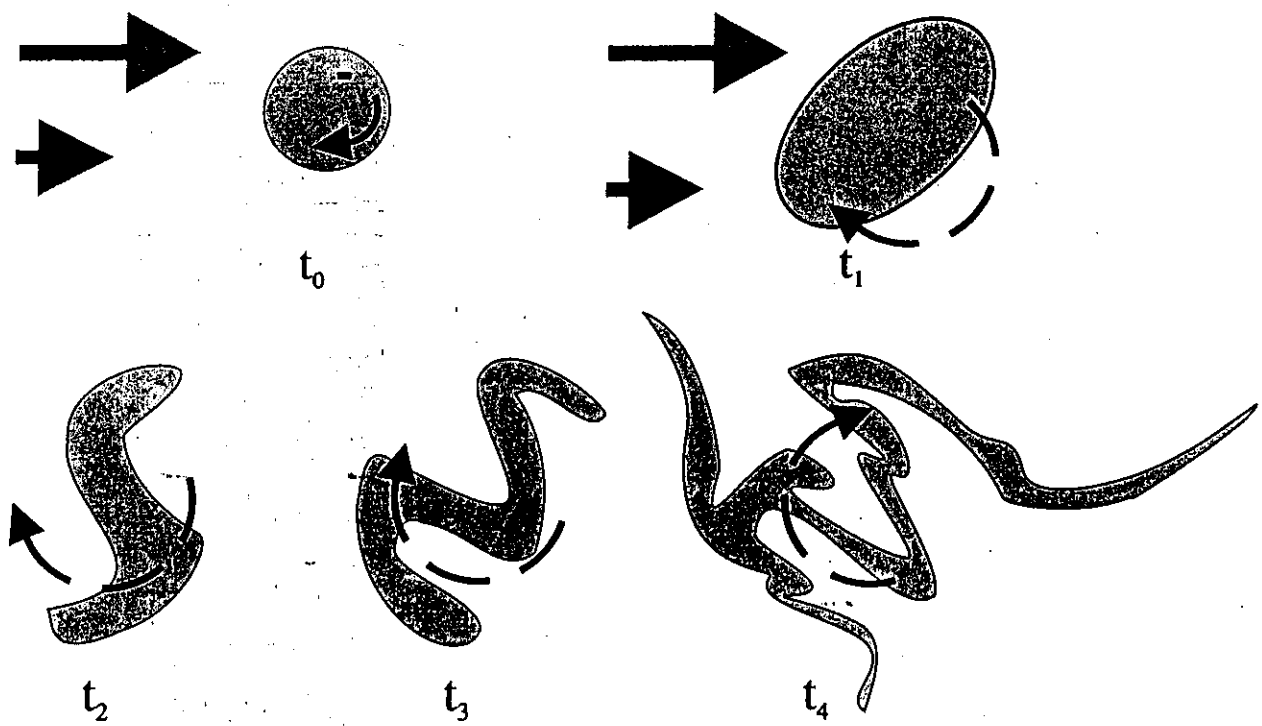

(b)

If we have a model like this for our scatterers, it permits us to predict quite a lot about the scattering properties of the medium. We may then make measurements of the radio wave backscatter to "work backwards" and learn information about the scatterers themselves.

Probably not surprisingly, it turns out that when the scatterers are statistically isotropic, backscatter strength is independent of beam direction, but if the scatterers are "stretched out" horizontally, then the backscatter is strongest when the radar beam is pointed vertically, and becomes weaker as the beam is pointed further from off-vertical. The fall-off often follows a near-Gaussian shape as a function of tilt-angle.

The more stretched out the ellipsoid is horizontally, the more quickly the power falls off as a function of angle.

We represent the power fall-off as a function of angle by

$$B(\theta) \propto \exp\{-(\sin^2\theta)/(\sin^2\theta_s)\}$$

where θ_s is a parameter called the "aspect sensitivity" parameter. (Note that if you measure this parameter, the measured value will be a combination of the effects of the scatterer and of the radar beam.

By measuring this parameter using beam-swinging methods (among others), it is possible to therefore measure the shapes of the scatterers in the scattering region.

The following paper describes some of the mathematical principles behind these determinations. Notice that the radar is also very selective about which scatterers cause backscatter.

We will work through this paper, and "pick out" the most important pieces of information. Notice, however, that equation (1) in the following paper is not derived - this is a complicated derivation.

To see the sort of mathematics involved in producing this relation, you need to refer to the appendices and see the paper by Briggs. This is beyond the scope of this lecture.

Can't_let.cdr

Dealing with anisotropic scatterers from a mathematical perspective

Journal of Atmospheric and Terrestrial Physics, Vol. 54, No. 2, pp. 153–165, 1992.
Printed in Great Britain.

0021-9169/92 $5.00 + .00
Pergamon Press plc

Radar measurements of aspect sensitivity of atmospheric scatterers using spaced-antenna correlation techniques

B. H. Briggs

Department of Physics and Mathematical Physics, University of Adelaide, South Australia 5000, Australia

(*Received in final form* 25 *March* 1991)

Abstract—The theory of spaced-antenna techniques for the measurement of aspect sensitivity of radar backscatter from the atmosphere is considered. Correlation measurements made on the wave field can be used to determine the angular power spectrum of the returned energy in much the same way that aperture-synthesis techniques are used in radio astronomy. After correction for the antenna polar diagrams, this yields the aspect-sensitivity function for the refractive-index fluctuations which are responsible for the scatter. Allowance is made for the possibility that the backscattered power may vary with azimuth angle as well as zenith angle. It is shown that commonly available data from three spaced antennae can give useful information about aspect sensitivity, and can also be used to estimate the effective pointing angle of an off-vertical beam. A method is suggested which may provide increased angular resolution, based on the fact that a single antenna can observe a very long cross-section through a moving ground pattern. The method would be analogous to a synthetic-aperture radar.

1. INTRODUCTION

Much is still unknown about the scattering mechanisms which cause radar echoes from the atmosphere at MF, HF and VHF. It is known that the scatterers are often aspect sensitive. They do not scatter isotropically as spheres would, but give the strongest echoes when the radar beam is directed to the zenith. This suggests that the scatterers have horizontal scales larger than their vertical scales. Some observations have suggested that weakly reflecting horizontal layers which behave almost like mirrors may also occur (Röttger and Liu, 1978; Rastogi and Röttger, 1982). In this case, the zenith-angle dependence of the scattered power would show a narrow 'spike' at the zenith, perhaps superimposed on a broader distribution. On the other hand, some theories of the production of the irregularities predict a sharp minimum or even a null in the scattering at the zenith (Van Zandt and Vincent, 1983; Hocking *et al.*, 1991). Improved measurements of the aspect sensitivity are needed to investigate these possibilities.

In the present paper we consider the theory of various radar techniques which can be used to measure the aspect sensitivity, and suggest some new methods. Allowance is made for the possibility that the scattering may vary with azimuth angle as well as zenith angle, and the term 'aspect sensitivity' will be used to describe both of these effects.

The most direct method of measuring aspect sensitivity is to use a very narrow radar beam and scan it in azimuth and elevation. This method is only practicable at VHF and higher frequencies because only at these frequencies can sufficiently large antenna arrays be built. At MF and HF, and often even at VHF, the required information must be obtained indirectly. A method which can be used employs a broad transmitting beam, directed to the zenith. The returns from scatterers in various directions interfere with each other to form a random distribution of complex wave field over the ground. The statistical properties of this ground pattern are measured using arrays of receiving antennae, each of which has a broad polar diagram directed to the zenith. Correlation measurements between pairs of such antennae can be used to derive the angular distribution of the energy arriving at the ground, as discussed in the following sections. This use of small spaced antennae rather than a large filled array, together with measurements of correlation of the wave field, is analogous to the aperture synthesis techniques used in radio astronomy. The methods to be discussed in the present paper are based on this idea.

In order to find the correlation between the complex wave fields at two spaced points in the ground pattern it is necessary to compute the average value of the product of the two fields. In practice the fields are continually changing due to systematic and random motions of the scatterers. Therefore time averages of the products can be used. The predominant cause of

the time changes is usually a steady motion of the pattern over the ground due to a wind at the scattering level. It can be shown that the pattern moves at twice the speed of the wind (e.g. BRIGGS, 1980).

In Section 2 we consider some basic ideas concerning the radar equation, the scattering cross-section and the addition of powers from randomly positioned scatterers. In Section 3 scatterers are assumed to be randomly distributed throughout the volume probed by the radar, with a particular range interval being selected. The spatial correlation function of the complex wave field over the ground is determined; it depends on the antenna polar diagrams and the degree of aspect sensitivity of the scatterers. Conversely, the aspect sensitivity can be found from correlation measurements made on the wave field, provided the antenna polar diagrams are known. In Section 4 these calculations are repeated for the case of scatterers which are confined to a thin horizontal layer. This might occur if there were a thin layer of turbulence in the atmosphere at a particular height. This case was treated by BRIGGS and VINCENT (1973), but it will be shown that there is an error in that paper.

A common technique is to use a triangle of three spaced antennae to measure the velocity of the ground pattern and hence the wind at the scattering level. The method requires computations of the cross-correlation functions between the signal fluctuations for the three pairs of antennas. A further analysis called full correlation analysis (e.g. BRIGGS, 1984) is then used to determine the velocity of the pattern over the ground. Although the primary objective of this analysis is usually to measure winds, it also gives as a byproduct some statistical parameters which describe the scale of the irregularities in the pattern. In Section 5 it is shown how these parameters can be used to determine the angular distribution of the received energy, and so also the aspect sensitivity of the scatterers. Then, in Section 6, it is shown how these results can also be used to determine the true pointing angle of an off-vertical antenna beam, as often used in Doppler and other radar techniques. The novel feature of Sections 5 and 6 is that allowance is made for the possibility that the scatterers may show aspect sensitivity with respect to azimuth angle as well as zenith angle.

If the pattern over the ground can be shown to be moving at a constant velocity, and without significant changes as it moves, it is possible to observe a very long 'section' through it with only one antenna. In Section 7 we discuss how observations of this type might be used to obtain greatly increased angular resolution. The technique would be similar to that of a synthetic-aperture radar.

2. ECHO POWER FROM A COLLECTION OF SCATTERERS

The polar diagram of scattering from a certain volume of an irregular medium depends upon the three-dimensional correlation function of the refractive-index fluctuations, and the magnitude of the scattered power is proportional to the volume. The equations which follow could be derived on this basis. However, for ease of visualization it is often useful to imagine that the irregular medium is built up from a superposition of randomly positioned identical scatterers. It can easily be shown that the three-dimensional correlation function of the resulting medium is the same as that of the one of the scatterers, while the number of scatterers in a given volume will be proportional to the volume. We will follow this approach. It should be pointed out that it does not imply that the real scatterers all have exactly the same shape, but only that they can be characterized by a certain mean shape, which also characterizes the correlation function and the scattering polar diagram of the medium.

A single scatterer will return a power given by the 'radar equation'

$$P_R = \frac{P_T G_T G_R \lambda^2 \sigma}{64\pi^3 R^4}, \qquad (1)$$

where

P_R = received echo power
P_T = transmitted power
G_T = gain of transmitting antenna
G_R = gain of receiving antenna
λ = radar wavelength
R = range
σ = scattering cross-section of scatterer for backscatter.

For isotropic scatterers σ will be constant, but in general it will depend upon the direction of the incident wave relative to the scatterer. To specify directions the direction cosines (l, m, n) will be used. That is, if a given direction makes angles $(\theta_x, \theta_y, \theta_z)$ with the (x, y, z) axes, then $l = \cos\theta_x$, $m = \cos\theta_y$, $n = \cos\theta_z$. Then $l^2+m^2+n^2 = 1$, and l and m are sufficient to specify a direction. Anisotropy is allowed for by writing $\sigma = \sigma(l, m)$. This function may also be called the 'aspect-sensitivity function', or 'polar diagram for backscatter' and the main aim of the present paper is to show how it may be determined experimentally, using various radar techniques.

Often, when using the radar equation, it is assumed that the antennae are pointed directly at the target, so that G_T and G_R are maximum values. This will not be so in the present work, however, as the antennae are

directed vertically, while the scatter comes from various off-vertical angles. We must therefore regard G_T and G_R as functions of angle, that is, as polar diagrams:

$$G_T = G_T(l, m),$$

$$G_R = G_R(l, m).$$

Note that these are power polar diagrams.

We will not be concerned with the constants in equation (1), and so for present purposes it may be written

$$P_R = \frac{K}{R^4} G_T(l, m) G_R(l, m) \sigma(l, m). \tag{2}$$

When there are many scatterers they are assumed to be in random positions so that the phases of the received echoes are random, and scattered powers may be added. The total received power will therefore be ΣP_R, a sum of terms like (2), one for each scatterer. If the scatterers are all identical, the total power will just be P_R multiplied by the number.

3. VOLUME DISTRIBUTION OF SCATTERERS, WITH RANGE GATING

Assume that the scatterers are uniformly distributed throughout the volume probed by the radar, with density N per unit volume. The radar is assumed to have a range gate such that power is received only from scatterers which lie in the range interval R to $R+\mathrm{d}R$. In equation (2), R is then a constant, the same for each scatterer.

In order to make use of equation (2) we must first find the number of scatterers which lie in directions from l to $l+\mathrm{d}l$ and m to $m+\mathrm{d}m$ (see Fig. 1). The radar 'scattering volume' is $\mathrm{d}V = R^2\,\mathrm{d}\Omega\,\mathrm{d}R$, where $\mathrm{d}\Omega$ is an element of solid angle. The relation between $\mathrm{d}\Omega$ and $\mathrm{d}l\,\mathrm{d}m$ can be obtained by noting that the area of cross-section of the elementary cone, at unit distance from the origin, is $\mathrm{d}\Omega$. This area projects to an area $\mathrm{d}l\,\mathrm{d}m$ on the horizontal plane, and is at an angle θ_z to the horizontal. Therefore

$$\mathrm{d}\Omega = \mathrm{d}l\,\mathrm{d}m/n = \frac{\mathrm{d}l\,\mathrm{d}m}{(1-l^2-m^2)^{1/2}}. \tag{3}$$

The number of scatterers in the range l to $l+\mathrm{d}l$, m to $m+\mathrm{d}m$ is therefore

$$NR^2\,\mathrm{d}\Omega\mathrm{d}R = \frac{NR^2\,\mathrm{d}l\,\mathrm{d}m\,\mathrm{d}R}{(1-l^2-m^2)^{1/2}}. \tag{4}$$

The returned power from the range l to $l+\mathrm{d}l$, m to $m+\mathrm{d}m$ will be denoted by $W(l, m)\,\mathrm{d}l\,\mathrm{d}m$. $W(l, m)$ is the angular power spectrum. From (2) and (4)

$$W(l, m)\,\mathrm{d}l\,\mathrm{d}m = \frac{KN\,\mathrm{d}R}{R^2} \times \frac{G_T(l, m) G_R(l, m) \sigma(l, m)}{(1-l^2-m^2)^{1/2}} \cdot \mathrm{d}l\,\mathrm{d}m. \tag{5}$$

The total received power is therefore

$$\int_{-1}^{+1}\int_{-1}^{+1} W(l, m)\,\mathrm{d}l\,\mathrm{d}m = \frac{KN\,\mathrm{d}R}{R^2} \times \int_{-1}^{+1}\int_{-1}^{+1} \frac{G_T(l, m) G_R(l, m) \sigma(l, m)}{(1-l^2-m^2)^{1/2}} \cdot \mathrm{d}l\,\mathrm{d}m. \tag{6}$$

The spatial correlation function of the complex wave field $f(x, y)$ over the ground is defined as

$$\rho(\xi, \eta) = \frac{\langle f(x, y) f^*(x+\xi, y+\eta)\rangle}{\langle |f(x, y)|^2\rangle}, \tag{7}$$

where the angle brackets denote a time average and the star a complex conjugate. It gives the correlation for an antenna pair with separation ξ in the x-direction and η in the y-direction. With x, y, ξ and η measured in wavelengths, it is the two-dimensional Fourier transform of $W(l, m)$ (RATCLIFFE, 1956). Thus

$$\rho(\xi, \eta) \propto \int_{-1}^{+1}\int_{-1}^{+1} W(l, m) \exp\left[2\pi i(l\xi + m\eta)\right] \mathrm{d}l\,\mathrm{d}m \tag{8}$$

$$\propto \int_{-1}^{+1}\int_{-1}^{+1} \frac{G_T(l, m) G_R(l, m) \sigma(l, m)}{(1-l^2-m^2)^{1/2}} \times \exp\left[2\pi i(l\xi + m\eta)\right] \mathrm{d}l\,\mathrm{d}m. \tag{9}$$

To be identified mathematically with Fourier transforms the limits of the integrals in (8) and (9) should be $\pm\infty$. However, the direction cosines cannot exceed ± 1 and so these limits have been used. The distinction is of no practical importance because $W(l, m)$ will have fallen to a very small value before limits ± 1 are reached.

To obtain the correct normalization which makes $\rho(0, 0) = 1$ the expressions (8) and (9) should be divided by the expression (6). However, to include these normalization factors [which would convert the proportionalities in (8) and (9) to equalities] makes the expressions very cumbersome. The normalization will be omitted, since it can always be reintroduced at any stage by dividing $\rho(\xi, \eta)$ by $\rho(0, 0)$.

Provided the antennae are directed to the zenith, and $\sigma(l, m)$ satisfies $\sigma(l, m) = \sigma(-l, -m)$, $W(l, m)$ will also satisfy $W(l, m) = W(-l, -m)$, that is, the angular power spectrum is centre-symmetric. This

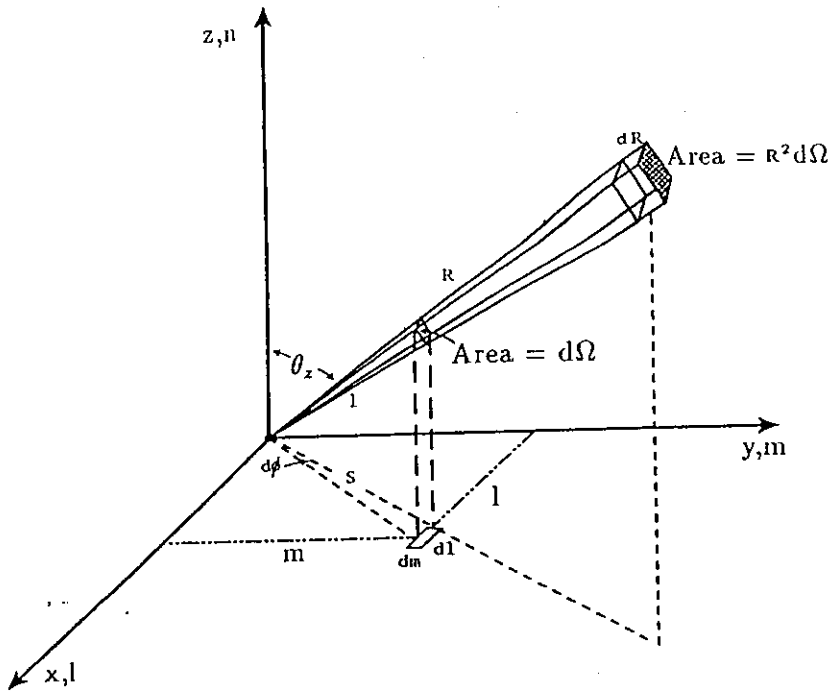

Fig. 1. The geometry for the case of a volume distribution of scatterers, with a range gate extending from R to $R+\mathrm{d}R$.

means that $\rho(\xi, \eta)$ will be real, even though it is computed from complex amplitudes. Not all scattering irregularities will satisfy this condition, however. For example scatterers aligned along the Earth's magnetic field may give a maximum return at some angle away from the zenith, and $\rho(\xi, \eta)$ will then be complex. Another example would be irregularities situated in layers tilted by a few degrees to the horizontal, as observed by RÖTTGER *et al.* (1990) in the troposphere.

Equations (8) and (9) show how $\rho(\xi, \eta)$ can be found when $W(l, m)$ is known. Conversely, $W(l, m)$ is the reverse two-dimensional Fourier transform of $\rho(\xi, \eta)$:

$$W(l,m) = \int_{-\infty}^{+\infty} \int_{-\infty}^{+\infty} \rho(\xi,\eta) \times \exp[-2\pi i(l\xi + m\eta)]\,\mathrm{d}\xi\,\mathrm{d}\eta. \quad (10)$$

When $W(l, m)$ is known, $\sigma(l, m)$ can be found from (5) giving

$$\sigma(l,m) \propto \frac{(1-l^2-m^2)^{1/2}}{G_T(l,m)G_R(l,m)} \times \int_{-\infty}^{+\infty} \int_{-\infty}^{+\infty} \rho(\xi,\eta) \exp[-2\pi i(l\xi + m\eta)]\,\mathrm{d}\xi\,\mathrm{d}\eta. \quad (11)$$

Constants have been omitted, because we are interested only in the form of $\sigma(l, m)$, not its absolute value.

Thus if $\rho(\xi, \eta)$ can be found experimentally, and the antenna polar diagrams are known, the aspect-sensitivity function $\sigma(l, m)$ can be found from (11). If the off-zenith angles of scatter are small enough, the factor $(1-l^2-m^2)^{1/2}$ will be very close to unity. It is then a good approximation to find $\sigma(l, m)$ by dividing $W(l, m)$ by the two antenna polar diagrams.

The above treatment is quite general, and allows for the possibility that $W(l, m)$ is a function of both zenith angle and azimuth angle. This seems to be a likely possibility, because the scale of the irregularities could be different in different directions in the horizontal plane, perhaps related to the wind direction, or the direction of the Earth's magnetic field. It is possible for $W(l, m)$ to have its maximum value at some off-zenith angle; the above treatment will still apply, but $\rho(\xi, \eta)$ will become a complex function.

For simplicity, previous treatments have usually assumed that $W(l, m)$ is a function of zenith angle only, that is, scattered power is independent of azimuth angle. This special case will now be considered. It implies that the scattering irregularities are on the average isotropic in the horizontal plane, but their vertical and horizontal scales may be different.

With this assumption the scattering cross-section $\sigma(l, m)$ depends only on the zenith angle θ_z. It is therefore a function of $\sin\theta_z = s = (l^2+m^2)^{1/2}$. If the antenna polar diagrams are also symmetrical around the vertical they will also be functions of s only. Thus

$$\sigma(l,m) \to \sigma(s)$$
$$G_T(l,m) \to G_T(s)$$
$$G_R(l,m) \to G_R(s)$$
$$W(l,m) \to W(s)$$
$$1-l^2-m^2 \to 1-s^2.$$

The total received power is now

$$\int_{-1}^{+1}\int_{-1}^{+1} W(l,m)\,\mathrm{d}l\,\mathrm{d}m = 2\pi\int_0^1 W(s)s\,\mathrm{d}s. \quad (12)$$

This follows from Fig. 1, since $\mathrm{d}l\,\mathrm{d}m = s\,\mathrm{d}\phi\,\mathrm{d}s$, and the integral with respect to ϕ is 2π. Thus equation (6) for the total received power becomes

$$2\pi\int_0^1 W(s)s\,\mathrm{d}s = \frac{2\pi KN\,\mathrm{d}R}{R^2} \times \int_0^1 \frac{G_T(s)G_R(s)\sigma(s)s\,\mathrm{d}s}{(1-s^2)^{1/2}}. \quad (13)$$

Equation (8) becomes a Fourier–Bessel (or Hankel) transform (Bracewell, 1965; Ratcliffe, 1956):

$$\rho(r)\alpha\int_0^1 W(s)J_0(2\pi rs)s\,\mathrm{d}s \quad (14)$$

$$\alpha\int_0^1 \frac{G_T(s)G_R(s)\sigma(s)}{(1-s^2)^{1/2}}\cdot J_0(2\pi rs)s\,\mathrm{d}s, \quad (15)$$

where $\rho(r)$ is the correlation for a separation r, measured in wavelengths (independent of orientation), and J_0 is the Bessel function of zero order.

As before, $\sigma(s)$ can be found from the inverse transform for $W(s)$, and equation (11) becomes

$$\sigma(s)\alpha\frac{(1-s^2)^{1/2}}{G_T(s)G_R(s)}\int_0^r \rho(r)J_0(2\pi rs)r\,\mathrm{d}r. \quad (16)$$

If the off-zenith angles of scatter are small enough the factor $(1-s)^{1/2}$ will not be important. It is then a good approximation to find $\sigma(s)$ by dividing $W(s)$ by the polar diagrams.

To observe $\rho(r)$ it is sufficient to have a row of receiving antennae along a line. (In practice others would be required to test whether the assumption of isotropy with respect to azimuth was correct.)

4. SCATTERERS CONFINED TO A THIN HORIZONTAL LAYER

A different possibility, in which the scatterers exist only in a thin horizontal layer, will now be considered. In the atmosphere this could occur if, for example, there was a thin horizontal layer of turbulence. It was the case considered by Briggs and Vincent (1973).

Let the layer be at a height h, and assume that the scatterers are uniformly distributed over the layer with a density M per unit area. The geometry is shown in Fig. 2. As before, we must first find the number of scatterers which lie in the range l to $l+\mathrm{d}l$, m to $m+\mathrm{d}m$.

Consider an element of solid angle $\mathrm{d}\Omega$ in the direction (l, m). This will intercept the horizontal layer in an area A given by

$$A = R^2\,\mathrm{d}\Omega/n.$$

As before, $\mathrm{d}\Omega$ is related to $\mathrm{d}l\,\mathrm{d}m$ by

$$\mathrm{d}\Omega = \mathrm{d}l\,\mathrm{d}m/n.$$

Thus

$$A = \frac{R^2\,\mathrm{d}l\,\mathrm{d}m}{n^2} = \frac{R^4}{h^2}\cdot\mathrm{d}l\,\mathrm{d}m,$$

since $n = \cos\theta_z = h/R$.

The number of scatterers in the range l to $l+\mathrm{d}l$, m to $m+\mathrm{d}m$ is therefore

$$MA = \frac{MR^4}{h^2}\cdot\mathrm{d}l\,\mathrm{d}m. \quad (17)$$

This, together with equation (2), gives

$$W(l,m)\,\mathrm{d}l\,\mathrm{d}m = \frac{KM}{h^2}G_T(l,m)G_R(l,m)\sigma(l,m)\,\mathrm{d}l\,\mathrm{d}m. \quad (18)$$

Note that the range dependence $1/R^4$ has been removed by the R^4 in equation (17). For this case the form of $\sigma(l, m)$ can be found without approximations by simply dividing $W(l, m)$ by the antenna polar diagrams.

The total received power is

$$\int_{-1}^{+1}\int_{-1}^{+1} W(l,m)\,\mathrm{d}l\,\mathrm{d}m = \frac{KM}{h^2} \times \int_{-1}^{+1}\int_{-1}^{+1} G_T(l,m)G_R(l,m)\sigma(l,m)\,\mathrm{d}l\,\mathrm{d}m. \quad (19)$$

It is assumed here that the range gate of the radar is wide enough to accept all the returned energy.

As before, the two-dimensional auto-correlation function of the complex wave field over the ground can be found as the two-dimensional Fourier transform of $W(l, m)$:

$$\rho(\xi,\eta)\alpha\int_{-1}^{+1}\int_{-1}^{+1} G_T(l,m)G_R(l,m)\sigma(l,m) \times \exp[2\pi i(l\xi+m\eta)]\,\mathrm{d}l\,\mathrm{d}m. \quad (20)$$

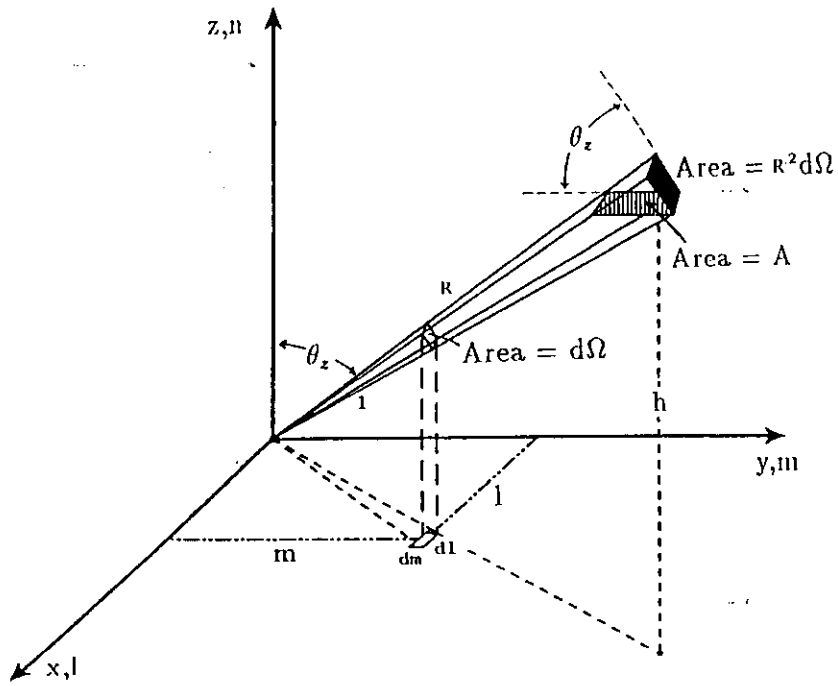

Fig. 2. The geometry for the case of scatterers confined to a thin layer at a height h.

Conversely, $W(l, m)$ is the reverse two-dimensional Fourier transform of $\rho(\xi, \eta)$, and on dividing by the polar diagrams we obtain

$$\sigma(l,m)\alpha \frac{1}{G_T(l,m)G_R(l,m)} \int_{-\infty}^{+\infty}\int_{-\infty}^{+\infty} \rho(\xi,\eta) \times \exp[-2\pi i(l\xi+m\eta)]\,d\xi\,d\eta. \quad (21)$$

For the case in which all the functions have symmetry around the zenith, and depend on zenith angle s only, these equations become:

$$2\pi\int_0^1 W(s)s\,ds = \frac{2\pi KM}{h^2}\int_0^1 G_T(s)G_R(s)\sigma(s)s\,ds \quad (22)$$

$$\rho(r)\alpha\int_0^1 G_T(s)G_R(s)\sigma(s)J_o(2\pi rs)s\,ds \quad (23)$$

$$\sigma(s)\alpha\frac{1}{G_T(s)G_R(s)}\int_0^\infty \rho(r)J_o(2\pi rs)r\,dr. \quad (24)$$

BRIGGS and VINCENT (1973) gave numerical results for the case of scatterers which scattered isotropically in both azimuth and elevation, that is, $\sigma(s) =$ constant. Physically this would require them to have on the average spherical symmetry, or to be very small compared with the wavelength. The zenith-angle dependence of the returned power $W(s)$ is then determined by the antenna polar diagrams alone. To obtain illustrative numerical results it was assumed that these were of Gaussian form, each with a $1/e$ half-width, s_o, that is

$$G_T(s)\alpha \exp(-s^2/s_o^2)$$
$$G_R(s)\alpha \exp(-s^2/s_o^2),$$

so that

$$W(s)\alpha \exp(-2s^2/s_o^2).$$

Then, from (23)

$$\rho(r)\alpha\int_0^1 \exp(-2s^2/s_o^2)J_o(2\pi rs)s\,ds. \quad (25)$$

Due to an incorrect definition of $W(s)$, BRIGGS and VINCENT (1973) obtained

$$\rho(r)\alpha\int_0^1 \exp(-2s^2/s_o^2)J_o(2\pi rs)s^2\,ds. \quad (26)$$

[$W(s)$ was found by assuming that the total power was proportional to $\int W(s)\,ds$ instead of $\int W(s)s\,ds$.]

The correct result (25) gives

$$\rho(r) = \exp(-\tfrac{1}{2}\pi^2 s_o^2 r^2). \quad (27)$$

In Fig. 3 the results from equation (27) are compared with those obtained from equation (26). The oscillatory nature of the results obtained from equation (26) is due to the extra s factor, which places a null at the zenith.

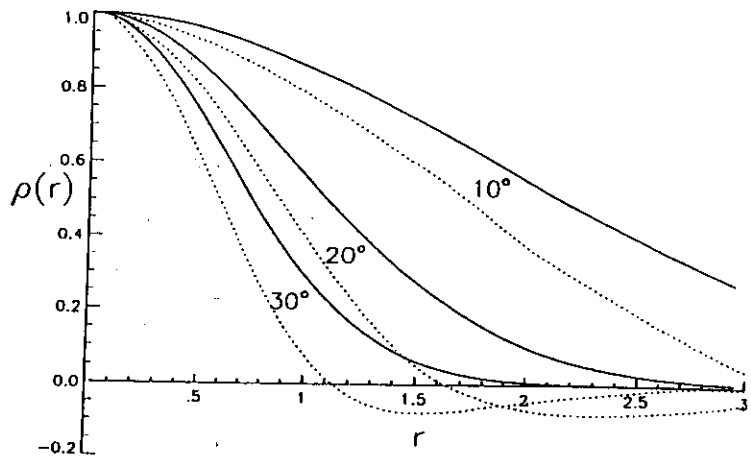

Fig. 3. Spatial correlation functions $\rho(r)$ for isotropic scatterers, and with transmitter and receiver polar diagrams both given by $\exp(-s/s_0^2)$, where $s_0 = \sin\theta_0$. Curves are given for θ_0 values of 10, 20 and 30°. The solid curves are from equation (27), while the dotted curves are from BRIGGS and VINCENT (1973) and are incorrect. r is in wavelengths.

Similar equations can be used to find $\sigma(s)$ when it does have a dependence on zenith angle, provided the dependence is Gaussian. If

$$\sigma(s)\alpha \exp(-s^2/s_1^2)$$

$$G_T(s)\alpha \exp(-s^2/s_2^2)$$

$$G_R(s)\alpha \exp(-s^2/s_3^2),$$

then

$$W(s)\alpha \exp(-s^2/s_4^2),$$

where

$$\frac{1}{s_4^2} = \frac{1}{s_1^2} + \frac{1}{s_2^2} + \frac{1}{s_3^2}. \qquad (28)$$

Then

$$\rho(r) = \exp(-\pi^2 s_4^2 r^2). \qquad (29)$$

Note that measurement of $\rho(r)$ with just one pair of antennas (i.e. for a single value of r) is sufficient to determine s_4 from (29), and s_1 can then be found from (28) if the polar diagram half-widths are known.

A useful result can be derived from equation (29) to relate the antenna separation in wavelengths, $r_{0.5}$, for which $\rho(r) = 0.5$, to the angle θ_4 measured in degrees (where $s_4 = \sin\theta_4$). This relation is, for θ_4 small, $r_{0.5} = 15.2/(\theta_4)$. If a similar result is derived from the incorrect equation (26), the constant obtained is 12.0 rather than 15.2. As the value 12.0 has been quoted and used in the literature [e.g. HOCKING (1987, 1989); HOCKING *et al.* (1989)] the required correction should be noted.

$\rho_{0.5} = 15.2/\theta$

5. METHODS FOR DETERMINING $\rho(\xi, \eta)$ EXPERIMENTALLY, AND A GAUSSIAN MODEL

In the general case, with no assumptions being made about its form, experimental observations of the spatial correlation function $\rho(\xi, \eta)$ require a very large array of antennae.

FELGATE and GOLLEY (1971) used the 1 × 1 km array at Buckland Park, South Australia (BRIGGS *et al.*, 1969) to produce examples of spatial correlation functions for patterns produced by total reflections from the E and E_s ionospheric layers, and also for weak partial reflections from the D-region. These were obtained using a filled array containing 89 antennae connected to 89 separate radio receivers. However, the receivers did not have phase-sensitive detectors, and $\rho(\xi, \eta)$ was computed from amplitude variations only. The observations are not suitable, therefore, for use in equations (11) or (21) to find $\sigma(l, m)$, but they did indicate the size and shape of the features in the amplitude pattern.

If the primary objective is to determine $\rho(\xi, \eta)$, the use of a filled array is not the optimum configuration for a given number of antennae, because many of the vectorial separations (ξ, η) of antenna pairs are duplicated. A more efficient arrangement is to use an array in the form of a cross, as often used in radio astronomy. This allows increased angular resolution of the derived $\sigma(l, m)$ for a given number of antennae. Such a configuration does not appear to have been used for the present purpose, except in small versions such as that used by KELLEHER (1966).

(The rest of the paper by Briggs is not included)

8. CONCLUSIONS AND DISCUSSION

he theory of spaced-antenna radar techniques for measurement of aspect sensitivity has been ewed and generalized. In particular, it has been vn that the commonly used three-antenna tri-ılar configuration can provide useful data for the rmination of the dependence of the scattering s-section on both zenith angle and azimuth angle. nethod which may be able to provide greatly eased angular resolution under suitable con-ons has been described.

or some purposes the aspect-sensitivity function interest in its own right. For example, it has been vn how it can be used to determine the effective ting angle of an off-vertical beam. However, a e fundamental characterization of the scattering ium would be the average shape of a scattering ularity or, equivalently, the form of the three-dimensional correlation function of the medium. A discussion of the relation of the latter to the aspect-sensitivity function is beyond the scope of the present paper, but we may comment here that there is no one-to-one relationship between them. However, with certain assumptions and approximations some useful deductions about the horizontal scales in the scattering medium can be made when the form of the aspect-sensitivity function is known. This has been discussed by BRIGGS and VINCENT (1973), HOCKING (1987, 1989) and HOCKING *et al.* (1990).

Acknowledgements—This work forms part of a program of research on atmospheric dynamics supported by the Australian Research Council. Discussions with members of the Atmospheric Physics Group of the University of Adelaide are acknowledged with thanks. Especially valuable suggestions were made by Dr W. K. Hocking.

REFERENCES

EWELL R.	1965	*The Fourier Transform and its Applications*. McGraw-Hill, New York.
GS B. H.	1980	*J. atmos. terr. Phys.* **42**, 823.
GS B. H.	1984	*Middle Atmosphere Program Handbook* **13**, 166.
GS B. H., ELFORD W. G., FELGATE D. G., OLLEY M. G., ROSSITER D. E. and SMITH J. W.	1969	*Nature* **223**, 1231.
GS B. H. and VINCENT R. A.	1973	*Aust. J. Phys.* **26**, 805.
ATE D. G. and GOLLEY M. G.	1971	*J. atmos. terr. Phys.* **33**, 1353.
A. and PETTERSEN H.	1970	*J. atmos. terr. Phys.* **32**, 397.
ING W. K.	1983	*J. atmos. terr. Phys.* **45**, 89.
ING W. K.	1987	*Adv. Space Res.* **7**, 327.
ING W. K.	1989	*Middle Atmosphere Program Handbook* **30**, 228.
ING W. K., FUKAO S., TSUDA T., YAMAMOTO M., TO T. and KATO S.	1990	*Radio Sci.* **25**, 613.
ING W. K., FUKAO S., YAMAMOTO M., TSUDA T. I KATO S.	1991	*Radio Sci.* (in press).
ING W. K., MAY P. and RÖTTGER J.	1989	*Pure appl. Geophys.* **130**, 571.
ING W. K., RÜSTER R. and CZECHOWSKY P.	1986	*J. atmos. terr. Phys.* **48**, 131.
HER R. F.	1966	*J. atmos. terr. Phys.* **28**, 213.
P. T.	1988	*J. atmos. terr. Phys.* **50**, 21.
GI P. K. and RÖTTGER J.	1982	*J. atmos. terr. Phys.* **44**, 461.
LIFFE J. A.	1956	*Rep. Prog. Phys.* **19**, 188.
GER J.	1981	*J. atmos. terr. Phys.* **43**, 277.
GER J. and LIU C. H.	1978	*Geophys. Res. Lett.* **5**, 357.
GER J., LIU C. H., CHAO J. K., CHEN A. J., C. J. and FU I.-J.	1990	*Radio Sci.* **25**, 503.
ANDT T. E. and VINCENT R. A.	1983	*Middle Atmosphere Program Handbook* **9**, 78.
MAN R. F. and CHU Y.-H.	1989	*Radio Sci.* **24**, 113.

The previous theory deals with single scatterers. But it is important to also consider the number-density of scatterers with particular aspect-ratios. This next paper addresses this issue.

It also briefly re-examines the issue of the existence of specular reflectors, because at the time that this paper was written, there were still many scientists who believed that specular reflectors simply did not exist!

Adv. Space Res. Vol. 7, No. 10, pp. (10)327–(10)338, 1987
Printed in Great Britain.

0273–1177/87 $0.00 + .50

23

pp. 330–333 is the main section to look at. (The rest is for completeness)

RADAR STUDIES OF SMALL SCALE STRUCTURE IN THE UPPER MIDDLE ATMOSPHERE AND LOWER IONOSPHERE

W. K. Hocking

Department of Physics, University of Adelaide, Adelaide, Australia 5000

ABSTRACT

The characteristics of radar backscatter from the height region 60 - 100 km are examined in order to try and better understand the nature and origin of the scatterers. In particular, the evidence for quasi-specular scatter, in which the signal returned from the zenith is found to be much larger than from off-vertical directions, is examined, and some recent results are used to quantify the aspect ratio of the scatterers. The evidence is used to show that both turbulent and quasi-specular scatterers may exist throughout the atmosphere, and it is shown how the radar wavelengths used may selectively single out one or the other type of scatterer in different height regimes. Some models are discussed which may explain the existence of specular scatterers.

INTRODUCTION

In the early 1900's, when transmitter powers were weak and receiver sensitivities poor, studies of the atmosphere with radio waves concentrated almost exclusively on ionospheric total reflection experiments, generally using ionosondes. Nevertheless, evidence was occasionally found for the existence of very weak scatter from heights below 100 km /1,2,3, 4/. The first detailed study of these "partial reflections", was performed by /5/ using a single frequency (2.28 MHz) radar system specifically designed to observe these weak echoes, rather than the ionosondes which had been used previously.

The observations of /5/ were made at a site near Sydney, Australia. They found that scattering layers existed in the range between 60 and 100 km, and that these layers had voltage reflection coefficients varying between about 10^{-5} at 60 and 70 km up to about 10^{-3} at 90 km altitude. They noted that often echoes appeared consistently at particular heights and could persist for periods of hours at those altitudes. The echoes faded with time scales of a few seconds. Below 80 km, the echoes were only seen during daylight hours, but above 80 km they were present at night as well. These workers utilized this scatter to measure the electron density as a function of height in this so-called "ionospheric D-region", by comparing back-scattered signal strengths measured using two different modes of polarization of the radio waves. This was the foundation of the Differential Absorption Experiment.

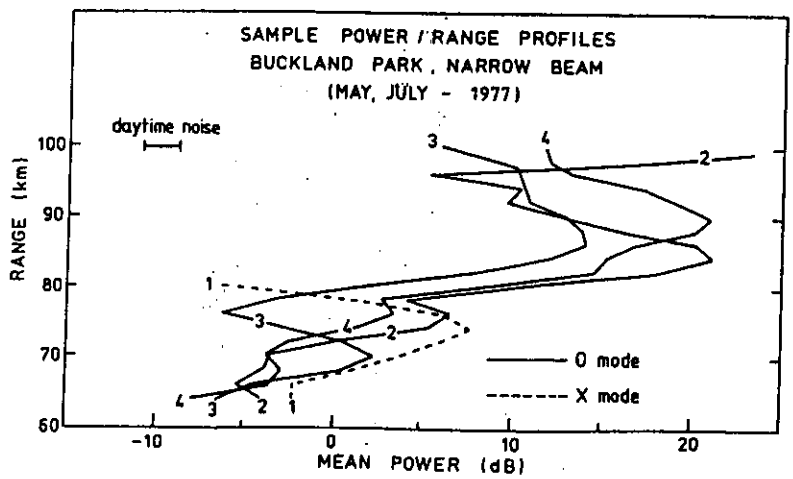

Fig 1. Sample profiles of mean power as a function of range recorded with the 1.98 MHz radar near Adelaide, Australia, at various times in 1977. The averaging times used varied between 1 and 3 mins.

Following the work started by /5/, /6,7/ used a site in New Zealand and a frequency of 1.75 MHz to look more carefully at seasonal variations, and concluded that the echoes were stronger, and occurred more frequently in non-summer months. It also appeared that the echoes occurred preferentially at certain heights, notably around 95 km, 85 km, 75 km, 65-70 km, and occasionally even at 56-57 km, although these preferred heights did appear to vary with season. Other studies /8,9,10/ showed the existence of these scatterers elsewhere around the globe.

Typical height profiles of mean power, recorded with a much more recent system near Adelaide, Australia, are presented in figure 1 /33/. These profiles show the tendency for echo strengths to increase with increasing altitude, and also the tendency for echoes to come preferentially from particular height ranges on any one day. Similar characteristics have also been noted more recently by, for example, /31,33/.

The very existence of these scatterers, and the reason for the preferred heights, were difficult enough to explain, but an extra property soon became apparent which introduced extra problems. It was observed that at times the fading times could become as large as 10s or more, particularly below 80 km altitude. Phase path measurements /11,12/ showed that individual scatterers were sometimes extremely long-lived and very stable in height, varying by less than a few hundred metres in height over time intervals of a few minutes or more. Scatter from any set of irregularities produces a diffraction pattern over the ground, and measurements of the pattern scale of this diffraction pattern /12/ suggested that the scatterers had horizontal dimensions much larger than their vertical extent. These observations implied that the scattering layers should not necessarily be ascribed to turbulence, and that at times the echoes were due to single, well-defined "partial reflectors". Numerical calculations showed that these reflectors would have to have relatively sharp changes in refractive index at their edges /13,14/. Some authors /11,12,14/ suggested that the scatterers acted like partially reflecting "mirrors" which had large horizontal dimension, possibly greater than 1 km across but with sharply bounded horizontal edges. Such horizontally extended structures are often called specular, quasi-specular, or even diffuse-specular reflectors in the literature. The existence or otherwise of "specular" reflectors was for some time a point of debate in the literature, but the consequences of this debate have led to a much greater understanding of the nature of the reflectors, and so this point will be discussed in some detail in the next section. To begin with, only the evidence collected with relatively long wavelength radars will be discussed (MF and HF). In the 1970's, VHF systems became capable of observing these structures, and the observations made with these radars will be discussed in due course.

EVIDENCE FOR "SPECULAR" REFLECTORS AT MF AND HF

Although the issue of whether specular scatterers exist was at one stage a controversial issue /15,16,17,18,19,20,21/, a large volume of evidence now exists in their favour. Often, for parameterization purposes, the scatterers are assumed to take a shape such that the power returned to a monostatic radar as a function of angle from the zenith, θ, takes the form $\exp\{-\sin^2\theta/\sin^2\theta_s\}$. If θ_s is large, then the scatterers are nearly isotropic, whilst if θ_s is small then the function falls off rapidly as a function of θ, and so the scatterers are said to be specular.

A detailed study of the values of θ_s at Adelaide, Australia was performed by /22, 23/, who cross-correlated echoes received at separated aerials on the ground and found that θ_s varied between about 2° and 4° at 60 - 70 km, whilst above 80 km θ_s tended to values more like 10°-15°. Some studies (eg. /19/) showed that much of the time a layer actually comprised several specular scatterers within a horizontal band of narrow vertical extent, rather than a single scatterer, but sometimes the reflectors did exist as single stable extended reflectors. The layers were in general less than 4 km deep, and were often less than 1 km deep, particularly below 80 km altitude. Individual scatterers often seemed to be less than one radar pulse-length in extent.

Working in Ottowa, Canada, /24/ compared signal strengths received with two radars of very different beam widths to estimate values of θ_s. They obtained values of around 9° at 60 - 80 km, and up to 20° at 90 km. Clearly this is evidence of non-isotropic scatter below 80 km, although the anisotropy is not as severe as at Adelaide.

Statistics about the pattern scale of the diffraction pattern of the scatterers on the ground at Adelaide were compiled by /25/, and these can readily be converted to estimates of θ_s, as shown by /13/. That is to say, if the spatial correlation function across the ground is taken to consist (on average) of circular contours, and is given by the function $\rho(\xi)$, where ξ is the spatial lag, then

$$\rho(\xi) \propto \exp\left\{-\tfrac{1}{2}\pi^2 S_s^2 \xi^2\right\} \qquad (1)$$

where $s_s = \sin \theta_s$, . By plotting this function for various θ_s values and finding where it falls to one half of its value at zero lag ($\xi_{0.5}$), it is possible to obtain a graph of $\xi_{0.5}$ as a function of θ_s. When the pattern scales measured by /25/ are converted to values of θ_s, it is found that θ_s is typically about 4° - 6° at 80 km, and 9° - 12° at 90 km. These values are consistent with those found by /22,23/. Pattern scales for heights below 80 km were not presented by /25/.

Using beam-swinging techniques with a radar at Adelaide, Australia, /26/ showed that the power received with off-vertical beams from altitudes below 80 km was weak compared to that received with a vertical beam, whilst above 80 km the scatter was generally more isotropic. Similar results were obtained when comparisons of signal strengths at frequencies of 2 and 6 MHz were made /41/.

It is also possible to use the fading time (or equivalently the spectral width) of the received signal to determine upper limits on the parameter θ_s. It has been shown /27,28/ that a major cause of fading can be horizontal motion of the scatterers through the beam of the radar; the range of radial velocities present because of the finite beam-width causes a spectral broadening. For scatterers moving horizontally through the beam, and with no other motions, the spectral half-power-half-width is equal to

$$f_{1/2} = (1.0) \ \frac{2}{\lambda} \ . \ V. \ \theta_{1/2} \qquad (2)$$

where V is the horizontal wind velocity, $\theta_{1/2}$ is the half-power-half-width of the combined polar diagrams of the radar and the scatterers, and λ is the radar wavelength. For a Gaussian spectrum, the fading time $\tau_{0.5}$ of the complex data series is related to $f_{1/2}$ through the relation $f_{1/2} = 0.22/\tau_{0.5}$, so that the parameter

$$\tau^{B}_{0.5} = \frac{0.22 \ \lambda}{2 \ V \ \theta_{1/2}} \qquad (3)$$

is the fading time expected due to beam-broadening alone. The experimental fading time $\tau_{0.5}$ could be less than $\tau^{B}_{0.5}$ due to random vertical motions (eg. due to turbulence), but never more. Thus if $\tau_{0.5}$ and V are known, it is possible to deduce an upper limit to $\theta_{1/2}$. At some experimental sites, experiments such as beam swinging have not been performed to measure θ_s, but estimates of θ_s can still be made by using equation (3). A radar at Townsville, Australia has been used to study the upper mesosphere /29/, and although θ_s was not specifically measured, the fading times and wind speeds were. Taking data from March, 1979, as an example, fading times during strong bursts of power at around 70 km altitude generally exceeded 5s, and often exceeded 10s. Wind speeds were generally greater than 20 m s^{-1}. Thus $\theta_{1/2}$ was certainly less than 10°, and often less than 5°. At 90 km, typical fading times were 3s or less, and typical $\theta_{1/2}$ values were more like 15°. The half-power-half-width of the combined polar diagrams of the radar and the scatterers is given by $\theta_{1/2}$, where

$$\sin^{-2} \theta_{1/2} = \sin^{-2} \theta_s / \ln 2 + \sin^{-2} \theta_r \ , \qquad (4)$$

and θ_r is the half-power-half-width of the radar beam /30/. For the Townsville system, the radar polar diagram was very wide, so $\theta_s = \theta_{1/2} / \sqrt{\ln 2}$. Thus at Townsville too the scatterers are certainly not isotropic below 80 km.

Measurements of fading times have also been made at Tromso, Norway /31/ in spring and summer. Typical fading times in summer were about 6s at 60 km, 3-4s at 70 km, and as small as 1-2s above 80 km. At 60 - 70 km, typical summertime wind speeds at the latitude of Tromso are greater than 40 m s^{-1}, so that an upper limit of $\theta_{1/2}$ at 60 km is 3° and at 70 km is 5°. The radar polar diagram used was wide, so upper limits for θ_s are 4° at 60 km and 6° at 70 km altitude. At higher altitudes (>80 km) the wind speeds are generally less and θ_s may be larger. In spring, fading times were even longer, although the wind speeds are generally much weaker, and so θ_s values are probably comparable to the summer values. The trend of small θ_s values at 60-70 km increasing to larger values above 80 km is again evident. Similar calculations for Saskatoon, Canada, using fading times from /74/ and mean winds from /75/ give upper limits of θ_s of 4° for January 1978 and 8° for July 1977.

In connection with fading times, some authors have occasionally looked for correlations between strengths of back-scattered signals and the fading times, in the hope of learning something about the scatterers. However, such data must be treated cautiously, particularly if the beam-broadening contribution to the fading time has not been removed, for this term can be a major cause of the fading, and can make such correlations meaningless.

The main point to emerge in this section is that D-region specular scatterers do indeed exist over a wide range of locations, particularly below heights of 80 km. The general picture is that the specular scatterers exist between 60 and 80 km, whilst above that height the scatterers tend to be more isotropic, at least when observed with MF and HF systems.

DETAILED SHAPES OF THE SCATTERERS

When trying to explain the nature of these scatterers, it proves useful to begin with simple models, and add more complexity as needed. To begin, then, two very simple models will be proposed, and these will be used to try and learn a little more about the scatterers using the observations discussed thus far. These models will be called models A and B.

The first model (A) surmises that the refractive index in an individual scatterer varies in a Gaussian manner horizontally, and varies in some equally smooth manner vertically. It is assumed that the gross structure in a vertical plane is ellipsoidal, with circular symmetry in the horizontal plane. Importantly, it is assumed that all scatterers have the same ratio of depth (h) to horizontal scale (L), although scatterers of varying size may exist. Such structures might, for example, represent an "average" shape produced in anisotropic turbulence, and there will be many within the radar scattering volume.

The second model (B) is one in which the scatterers are proposed to be flat partially reflecting "mirrors" which have developed undulations and "wrinkles" on their surface. Such scatterers have been described as "diffuse reflectors" /32/.

Model A

The case of ellipsoidal scatterers, in which the refractive index (over and above the background) takes the form $\exp -[(x^2 + y^2)/L^2 + z^2/h^2]$ has been considered by /13/ (see figure 2a). They found that if such scatterers are uniformly distributed over the sky, and are observed with a monostatic radar, then the backscattered power density as a function of zenith angle θ is proportional to $[\pi^{3/2}.(L^2h)]^2$. P' , where

$$P' = \exp\{-\frac{8\pi^2}{\lambda^2} \cdot (L^2s^2 + h^2(1-s^2))\} \qquad (5)$$

and where $s = \sin\theta$. Similar studies have also been performed by /72/. This formula does not, however, include a term to consider the variations in refractive index for scatterers of different sizes, and nor does it contain a term describing the number density of scatterers; for example small scatterers might have smaller cross-sections of backscatter individually, but if greater in number than the larger ones, they may have a large effect. So assume that the peak refractive index above the background value in any scatterer is a function of h and L/h, n_o (h,L/h) say, and that the number density of scatterers of vertical scale h and aspect ratio L/h is D $(h, \frac{L}{h})$. $dh.d(\frac{L}{h})$. Then the power back-scattered from zenith angle θ by scatterers with vertical scales in the range h to h + dh and aspect ratios in the range L/h to L/h + d(L/h) is proportional to /14/

$$P = n_T^2 (h, \frac{L}{h}).D (h, \frac{L}{h}). P' \quad , \qquad (6)$$

where n_T (h, L/h) = $n_o(h, L/h).\pi^{3/2}.L^2h$ is the total integrated refractive index of the irregularity. The term L^2h will often be considered as $(L/h)^2 . h^3$, since it will be assumed that the ratio L/h is a constant. A profile of this type, with a Gaussian variation in the vertical direction, is not necessarily the best to use, and others will be introduced shortly, but the present case is very useful for illustrative purposes.

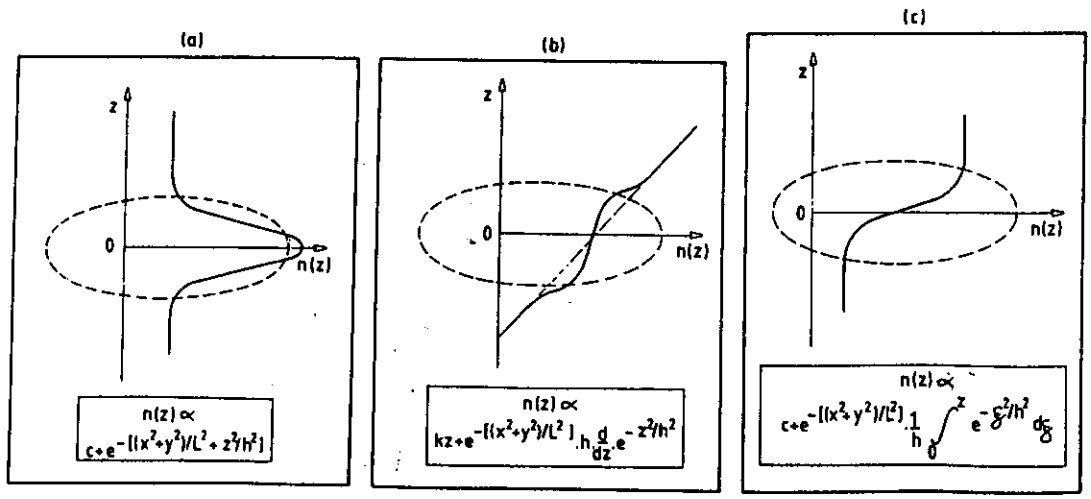

Fig 2. Some hypothetical refractive index variations across scattering irregularities.

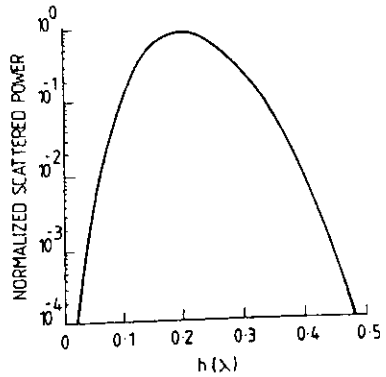

Fig. 3. Normalized scattered power for an overhead irregularity of Gaussian form as a function of the vertical scale parameter h measured in wavelengths λ. The sharp resonance centred on h ≈ 0.2λ indicates that irregularities of this vertical scale are preferentially selected by a probing wave of wavelength λ.

is clear that if, in an experiment, an angular variation of signal strength of the type p $(-\sin^2\theta/\sin^2\theta_s)$ is found (as discussed earlier), and if the scatterers have a shape as scribed by fig. 2a, then

$$\frac{\sin^2\theta}{\sin^2\theta_s} = \frac{8\pi^2}{\lambda^2} \cdot (L^2 - h^2) \cdot \sin^2\theta \qquad (7)$$

or

$$\frac{L}{h} = \sqrt{\left\{ \left(\frac{\lambda}{h}\right)^2 \cdot \frac{1}{8\pi^2 \sin^2\theta_s} + 1 \right\}} \cdot \qquad (8)$$

ius if it is possible to measure h, then θ_s can be used to estimate the ratio of the width the depth (i.e. the aspect ratio L/h) of the scatterers. Can h be determined? In fact can be shown that efficient backscatter only occurs over a limited range of h values, and iis will now be done.

or a fixed value of L/h, and for vertical backscatter, (6) is a maximum when its derivative ith respect to h is zero. Assume that the term $n_0^2(h,L/h).D(h,L/h)$ varies as a function of in the manner h^β. Then (6) is a maximum when

$$\left(\frac{h}{\lambda}\right)_{max} = \sqrt{(6+\beta)}\,/4\pi \cdot \qquad (9)$$

If we take $\beta = 0$, then (6) is a maximum when $h/\lambda = \sqrt{6}/4\pi = 0.195$. A plot of against h/λ is shown in figure 3, and it is clear that P falls to very small values within narrow range of h/λ values - say between .1 and .3.

model which regards turbulent scatterers as an ensemble of spherical irregularities with aussian cross-section has recently been developed by /34/. For Kolmogoroff inertial range urbulence /35, 36/, and assuming that $n_o(h,L/h)$ is independent of h, the number density of rregularities per unit volume in the range h to h+dh is proportional to $h^{-10/3}$. In that odel $n_T(h,L/h)$ is proportional to h^3, and if D is taken to be approximately proportional o $h^{-10/3}$ then $\beta = -10/3$, and $(h/\lambda)_{max} = 0.13$.* In more extreme circumstances, $n_o(h)$ might ncrease with increasing scale, but even if β is as high as 4, $(h/\lambda)_{max} = \sqrt{10}/4\pi$, or about .25. Clearly, over a wide range of β values, the maximum backscattered power occurs in the ange of h = 0.15λ to 0.3λ.

$\otimes\ n_T \propto n_0 \cdot \left(\frac{L}{h}\right)^2 \cdot h^3$

$n_T \propto n_0 h^3$

$\Rightarrow n_0 = \text{const.}$ if $n_T \propto h^3$

$\Rightarrow n_0^2 D \propto h^{-\frac{10}{3}}$

ther possible refractive index profiles with height have also been considered by /33/, lthough it was still assumed that the scatterers had circular shapes horizontally and fell ff in refractive index in a Gaussian manner in the horizontal direction. Such cases are hown in figures 2b and 2c. Figure 2b represents a scatterer which exists in a region where he refractive index increases linearly with height, but tends to be more nearly constant cross the scatterer. Notice that by multiplying $d/dz(\exp\{-z^2/h^2\})$ by h, it has been nsured that the maximum excursion of the refractive index from a straight line is ndependent of the value of h. Likewise in figure 2c, the total change in refractive index cross the scatterer is independent of h.

he backscattered power as a function of L, h, and θ is found by Fourier transforming the efractive index function /13/. The Fourier transform of the derivative of a function can e found by multiplying the Fourier transform of the function by $2\pi i\nu$, where ν is the ppropriate spatial frequency /37/. Hence for figure 2b, the received power is proportional o $n_T^2.D.(2\pi i\nu_3)^2$ times the expression in equation (5), where ν_3 is the vertical spatial requency 2 cosθ/λ. The term n_T is still taken as $n_o \cdot \pi^{\frac{3}{2}}.L^2h$, although in this case n_T does not have as its physical meaning the integrated refractive index over the scatterer.

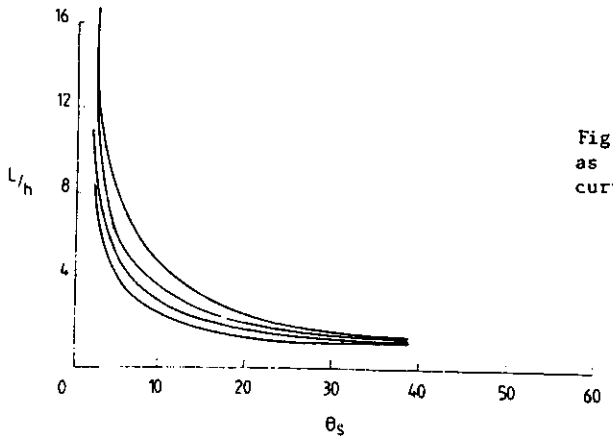

Fig. 4. Aspect ratio of scatterers, L/h, as a function of θ_s, for h = .15λ (upper curve), .195λ, .25λ and .32λ.

For the case described by figure 2c the power received is proportional to $n_1^2.D(2\pi i\nu_3)^2$. P', where P' is the expression in (5). For θ less than say 15°, this multiplicative cosθ can be ignored. Thus for a power law form for $n_1^2.D$, (i.e. h^β), it can be shown that

$$(\frac{h}{\lambda})_{max} = \sqrt{(5+\beta)}/4\pi \text{ for figure 2b,} \quad (9a)$$

and $$(\frac{h}{\lambda})_{max} = \sqrt{(7+\beta)}/4\pi \text{ for figure 2c.} \quad (9b)$$

Over the range of β values 0 to 4, as used previously, $(h/\lambda)_{max}$ still lies in the range 0.15 to 0.3. So clearly for these three quite different scatterer profiles, the optimum scatter depth for backscatter lies between 0.15λ and 0.3λ. Smaller values are inefficient because they are associated with smaller L values, so that the total cross-section is less. Note that all the functions discussed thus far are continuously differentiable; if a discontinuity exists in n(z), or any of its derivative, the picture changes totally, but it has been assumed that viscous effects will prevent the formation of discontinuities.

Thus although h is not known precisely, limits on it are known, and these can be used in equation (8). The relation between L/h and θ_s, as described by equation (8), has been plotted in figure 4 for various values of h in the range 0.15λ to 0.32λ. It will be noticed that all the curves look similar, and although it is not possible to relate L/h to θ_s precisely, it is certainly possible to give a range of L/h values for any specified θ_s value. For example, at 90 km altitude θ_s is typically 12°, and it can be seen from figure 4 that such a value corresponds to a range of L/h of between 2 and 4. This seems quite a reasonable aspect ratio for anisotropic turbulence, and so scatter from around 90 km altitude could be due to turbulence in which buoyancy forces have introduced some asymmetry between the vertical and horizontal scales.

However a value for θ_s of 4° implies an aspect ratio of between 6 and 12, and 2° gives an aspect ratio of between 9 and 18. For example, if a radar wavelength of 150 m is used, the optimum vertical scale would be about 30 m, and the horizontal scale would be between 300 and 600 m. It seems most unlikely that even anisotropic turbulence could create such large irregularities, unless perhaps the turbulence were well into the decay phase.

Model B

Model A seems at least superficially appropriate to describe the scatterers above 80 km, but was not appropriate below 80 km, so model B is now introduced to try and better explain these lower scatterers. In this model, it is assumed that the quasi-specular scatter is due to one or more horizontally stratified steps, possibly with undulations and "wrinkles". The vertical profile of refractive index might look something like that in figure 2c, but there would be little change in refractive index in the horizontal direction, save for the effects of undulation and wrinkles. For such a step, in which the vertical variation in refractive index is proportional to $\exp\{-z^2/h^2\}$, the backscattered power is proportional to $[\Delta n.\exp\{-\pi^2.(2/\lambda)^2.h^2\}]^2$ /38/. Here Δn is the total change in refractive index across the step. Notice that narrow steps where h is much smaller than λ reflect most efficiently, and the reflected power is reduced by 20 dB if the step size is about λ/4. The existence of undulations and wrinkles on the layer, of say root mean square depth d, will tend to spread any incident radiation over a range of angles. The layer can be treated as a phase screen containing random fluctuations of phase with root mean square value $\Phi_{RMS} = 2d/\lambda$ /39/, where d is the RMS depth of undulation.

Calculations have shown that a change in electron density across such a step of about 5%-10% of typical electron densities in the region around 70 km altitude is capable of explaining the observed echo strengths /14, 40/. The major arguments usually proposed against such a model revolve around the problems of forming and maintaining such steps. What would cause

them? Would they not diffuse apart quickly? These questions will be addressed in due course; for the present, it is simply necessary to state that the experimental evidence presented so far is consistent with the scatterers below 80 km being such steps, at least at several different locations around the globe. Indeed /14/ proposed that the step size should be less than 10 m in vertical extent. Further evidence for this statement was supplied by /41/, where comparisons of observations at 2 MHz and 6 MHz suggested that the step sizes were less than one tenth of a wavelength for the 6 MHz radar, or about 5m.

Turbulence

To finish this section, a discussion of the backscattered power expected due to turbulence proves useful. In some ways, this will simply represent a different approach to model A. Given typical energy dissipation rates and typical electron density profiles, the potential refractive index gradient /28/ can be found and so the backscattered power expected due to inertial range isotropic turbulence can be calculated. This has been done by /33/, and for scatter from below 80 km the estimated backscattered signal for the Adelaide MF radar are over 100 times less than the powers actually observed. However these calculations used a "typical" electron density profile /68/ which had relatively poor vertical resolution. If the small scale electron density gradients can be considerably greater than those assumed, then of course the expected backscattered signal will be greater than that estimated, but it is unlikely to increase so much as to explain the echoes below 80 km. For heights above 80 km, the calculations are comparable to the experimentally determined values. This emphasizes even further that the scatter from below 80 km is not just due to turbulence, whilst for the higher altitudes turbulence may well cause the scatter.

VHF OBSERVATIONS OF D-REGION SCATTERERS

In the early 1970's, D-region echoes were observed with radars working with frequencies of about 50 MHz /42,43,51/. These echoes showed several features in common with the scatterers observed with HF and MF radars, including some preference to occur at heights of about 70-75 km and sometimes at 80-85 km, and similar variations of mean power with time. VHF systems generally use shorter pulse lengths than MF and HF systems, and these VHF studies showed that individual scattering surfaces were often very narrow, often less than 300 m deep /32/ and sometimes less than the pulse resolution. However, they also showed some characteristics which were different from the MF and HF observations. In particular, the scatter did not always show a sharp drop-off in power when the radar beam was tilted off-vertical. Certainly in some cases /44, 47/ there was an aspect sensitivity; /44, 47/ found that the powers measured when the beam of the Jicamarca (Peru) VHF radar was pointed to 3.5° off-vertical were between 5 and 15 dB less than those observed with a vertical beam. However /45, 30/ found that powers observed with a beam of the SOUSY radar in West Germany pointed to 7° off-vertical were very similar in magnitude to those found with the vertical beam. Furthermore,/30, 46/ calibrated their radars and made absolute measurements of backscattered power, and found that these values were consistent with turbulent scatter. Thus while HF and MF radars observe specular echoes most of the time, VHF radars see specular scatter only occasionally, whilst at other times they see turbulent scatter.

Thus it must be speculated that neither model A nor model B completely describe the situation below 80 km. Perhaps both turbulent and specular scatterers co-exist in similar regions of the atmosphere, with the turbulence being too weak to be seen by HF and MF radars. If the specular reflectors have step depths h comparable to or greater than the VHF wavelengths, then they would not be seen by VHF radars. Possibly on occasions the step depths may narrow so that VHF radars might be able to detect specular echoes, which might explain the observations of aspect sensitivity found by /44, 47/.

It is also possible that the turbulence may be anisotropic, and indeed /47/ has suggested that all the aspect-sensitivity of scatter observed at all frequencies can be ascribed to anisotropic turbulence. The fall off in power as a function of angle measured with VHF radars by /44, 47/ suggest aspect ratios for the scatterers of between 7 and 20 (figure 4). This would certainly require highly anisotropic turbulence. /24/ found θ_s at 2.7 MHz to be about 9° at heights below 80 km at Ottowa, Canada, implying values of L/h of about 4, so it might be possible that anisotropic turbulence could explain these particular observations. It is very unlikely, however, that such turbulence could explain the HF and MF observations made at Adelaide, Townsville and Tromso discussed earlier.

Model B certainly produces both a vertical component of scatter due to stratification as well as an off-vertical component due to the undulations. As the radar wavelength is decreased it can be anticipated that the signal returned from vertically overhead will diminish because of the finite step depth, but the off-vertical scatter may not decrease so rapidly. Hence model B alone could perhaps explain the observations. Nevertheless, it seems likely that any irregular structure of the step would arise as a result of turbulence, so it might not be surprising if both types of scatterers co-exist. The idea that the off-vertical scatter component is due at least in part to turbulence is reinforced by the fact that absolute measurements of backscattered power at VHF seem consistent with those expected

due to turbulence /30/. Thus it is proposed that both model-A type scatterers and model-B type scatterers co-exist in regions very close to each other. There may be geographic and seasonal variations in the relative importance of each.

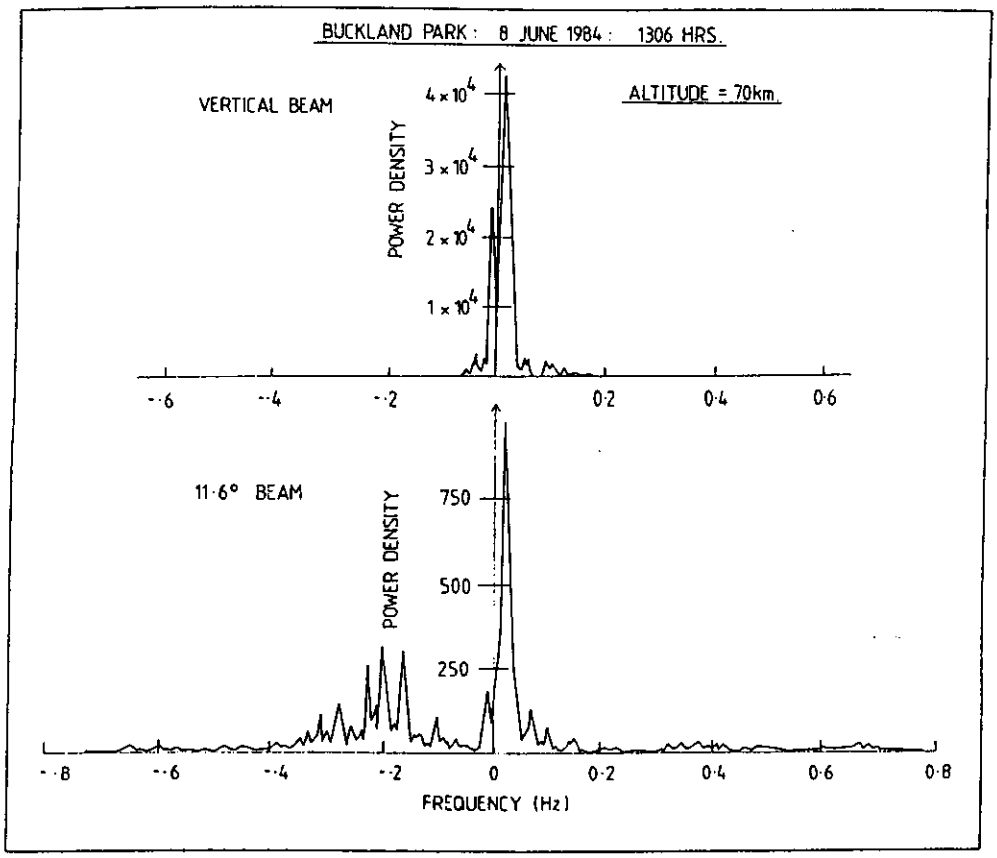

Fig. 5 Spectra recorded with vertical and off-vertical beams of the Buckland Park 2 MHz radar.

Experimental Test of Dual scatterer model

As a test for this model, it was decided to look more carefully for evidence of turbulent scatter with the 2 MHz radar near Adelaide, Australia. As discussed, calculations /33/ have shown that the turbulent scatter should be at least 10 - 20dB weaker in strength than the observed specular echoes if this radar is used. Extrapolation from VHF observations of D-region turbulence /30/ suggest that the turbulent scatter seen by the Adelaide radar should be 25 times less than the specular component and data presented by /26/ showed about a 10-15 dB drop in signal when the radar beam of the 2 MHz radar near Adelaide was tilted by 11.6°.

The following experiment was performed with the Adelaide radar. The radar was configured into two separate receiving beams, one pointing vertically and the other pointing at 11.6° off-vertical in the eastward direction. The angle of 11.6° ensured that the first null of the radar pointed vertically. A very wide beam transmitter array transmitted radio pulses into the ionosphere, and the back-scattered signals were simultaneously recorded with both receiving beams. The time-series were Fourier-transformed into power spectra, and figure 5 shows a comparison of two such spectra recorded simultaneously. The powers recorded with the off-vertical beam were about 15 dB less than those with the vertical beam. Two features should be noted in connection with figure 5. Firstly the parts of the spectra around 0 Hz

are almost identical in shape, even to quite fine details, and secondly the off-vertical beam has a spectral component significantly offset from zero, which is not present in the vertical beam spectrum. Although only a limited data set has been analysed, several examples like this have been found. Clearly the component around 0 Hz for the off-vertical beam is due to leakage of the signal from overhead leaking in through the sidelobes and the edge of the main beam, since it so closely matches that for the vertical beam. This was further verified by examining the actual data time-series, and indeed the signal received by the off-vertical beam looked just like that on the vertical beam, but with a higher frequency component added. The spectral component shifted from 0 Hz and recorded with the tilted beam can be ascribed to more isotropic scatterers producing backscatter through the main lobe of the off-vertical beam, with a Doppler shift due to the large eastward component of the mean wind which existed at the time. Indeed the frequency offset is consistent with this idea. These data therefore represent evidence that specular and quasi-isotropic (possibly turbulent) scatterers do simultaneously exist at 70 km altitude. Specular reflections from the stratosphere have also been observed by VHF radars /48, 49/. These have not been discussed here because of lack of space, but it is worth noting that /50/ presented observations which suggested that turbulence and specular reflectors co-exist in the stratosphere. The above results are the first to show that this is true for the lower D-region.

If it is assumed that the quasi-specular scatter observed with MF, HF and VHF radars is due to stratified steps, and the off-vertical component is largely due to turbulence, it is now possible to estimate the depth of these scattering steps. The power received by a radar due to inertial range turbulence is /28/

$$P_{Rt} = \frac{P_t G_t A_r}{4\pi z^4} \left(\frac{dn}{dN}\right)^2 . C_N^2 . \lambda^{-1/3} . \frac{V}{\ln 2} . B.f \ , \qquad (10)$$

where N represents the electron density, C_N^2 is the electron density structure constant, G_t is the gain of the transmitter, A_r is the receiving area, z is the height of the scatterers, V is the radar volume $(= \pi . (z\,\theta_{1/2})^2 . (0.5\,L_p))$, and f is the fraction of the radar volume filled by turbulence. The term $\theta_{1/2}$ is the half-power-half-width of the transmitting and receiving polar diagrams combined, L_p is the pulse length, and n the refractive index. The term P_t represents the transmitted power, and B represents ionospheric absorption along the ray paths. The power received for specular scatter due to a single sharp step in electron density of change ΔN across the step is /41/

$$P_{Rs} = \frac{P_t G_t A_r}{4\pi (2z)^2} \left(\frac{dn}{dN}\right)^2 . \left(\frac{\Delta N}{2}\right)^2 . B \ . \qquad (11)$$

Thus the ratio of specular to turbulent signal returned from a given height z should be

$$\frac{P_{Rs}}{P_{Rt}} = \frac{\ln 2 . \lambda^{1/3}}{16\pi\, f\, \theta_{1/2}^2 . (0.5\, L_p)} . \frac{\Delta N^2}{C_N^2} \qquad (12)$$

Now compare this ratio for the Adelaide 2 MHz radar and the Jicamarca 50 MHz radar. For the Adelaide 2 MHz radar, $\theta_{1/2}$ is 4.5°, and the pulse-length is about 4 km, whilst for the Jicamarca radar $\theta_{1/2}$ is about 0.35° and L_p about 3 km. The pulse lengths are similar, so it may be expected that the fraction f will be similar in each case, since turbulence seems to occur in extended striated layers. So if the ratio $(\Delta N)^2/C_N^2$ is similar over each radar then the ratio of specular scatter to turbulent scatter for the Jicamarca VHF radar should be about 70 times that for the Adelaide radar. In fact /46/ has proposed that often VHF turbulent scatter comes from irregularities within the viscous range of turbulence, and in this case the ratio should be even greater. However, even assuming that VHF scatter is from the inertial range, the ratio of specular to turbulent scatter for the Jicamarca system should between 30 and 35 dB, based on the observed ratio for the Adelaide radar. This is 15 to 25 dB more than actually observed, and suggests that the "step" observed with the VHF system is not as narrow as one quarter of a wavelength or less.

viz. If the step size is $w = 2\sqrt{\ln 2}\,h$, where the reflection coefficient profile is $r(z) \propto \exp\{-(z-z_0)^2/h^2\}$ (as used earlier), then the reflected amplitude is $\propto \exp\{-4\pi^2 h^2/\lambda^2\}$, and the reflected power is $\exp\{-8\pi^2 h^2/\lambda^2\}$. times less than for a step of thickness much much less than $\lambda/4$. Then using the above observation

that the actual observed specular component is 15-25 dB less than would be expected for a very narrow step allows determination of w, and gives a value of between 2 and 3 m. The common assumption that the step must be less than one quarter of a wavelength in depth is not applicable because VHF radars are such sensitive receivers that they can detect scatter even from the very weak Fourier component of a quite thick step. Recently /52/ has compared powers received by a MF and VHF radar at the same site, and came to a similar conclusion; namely that VHF scatter, could not be due to scatter from a step of depth as narrow as a fraction of a metre.

The above calculations suggest a minimum step depth of ~3-5 m. It is possible that at times the step depth is more, in which case the only significant VHF scatter would be from turbulence. It is also possible that at times this turbulence could itself be anisotropic /47/, in which case the aspect sensitivity at VHF could be entirely due to anisotropic turbulence. In still other cases there might not be any specular reflectors present at all, as in the case of very active turbulence. But undoubtedly the steps do exist, and occur a considerable fraction of the time. A step of depth h can be maintained against molecular diffusion for a time scale of about h^2/ν, where ν is the kinematic viscosity. At 75 km, ν is about 0.3 $m^2\ s^{-1}$, so that a step of depth h = 4m would have a lifetime of about 1 min before being destroyed by molecular diffusion. If, on the other hand, the reflector was a step of depth less than a quarter wavelength (at VHF), then the lifetime would be about 7s or less, and it would quickly be destroyed. This serves as further evidence against step sizes as small as 1 m.

Coexistence of specular and turbulent scatterers

Given that turbulent and specular scatterers co-exist at around 70 km altitude, it must be asked why they should not co-exist together everywhere. Indeed, /33/ has proposed a model in which it is assumed that both types of scatterers do exist at all heights, and has assumed that the size of any step is comparable to the inner scale of turbulence. As the altitude increases, the kinematic viscosity increases exponentially, and so the depth of any specularly reflecting step increases markedly. Hence the steps become less efficient reflectors with increasing height. The turbulent component of the backscattered signal does not fall off so rapidly; at very high heights scatter from turbulence occurs at scales within the viscous range, but this situation only arises at heights much higher than the heights where the "specular" reflections become inefficient. For any radar there is ar upper altitude limit, above which specular reflectors become very inefficient and nc reflected signal is detectable. For a 2 MHz radar, /33/ has shown that the transitior occurs somewhere around 80-85 km, and because of the exponential increase of the kinematic viscosity with height the cut-off is quite abrupt. The cut-off for a VHF radar is lower down, being somewhere between 70 and 75 km, and so specular scatter at VHF is confined tc altitudes of about 70-75 km or less. Thus with a MF system like the Adelaide radar, turbulent scatter should dominate above about 85 km. At heights above 70-75 km the inner scale of turbulence exceeds the Bragg scale for VHF radar wavelengths, so that generally VHF scatter from above 70-75 km is due to irregularities within the viscous sub-range of turbulence /46/. At heights above 85 km the Bragg scale is so far into the viscous sub-range that very little VHF backscatter is seen at all.

It therefore seems reasonable to propose that both specular and turbulent scatterers exist throughout the D-region, with the radars preferentially selecting one type or other, depending on the radar wavelength and the height of scatter. Variations in the intensity of turbulence and the background electron density profile may vary the relative roles of specular and turbulent scatter, and this may explain why sometimes quasi-specular reflections are seen with VHF radars; a change of the step depth to about 3-4 m is all that is required for VHF radars to detect the step. At other times, when the steps are wider than about 5m, they would not be seen by VHF radars, although a MF or HF radar would still detect them.

CAUSES OF THE SCATTERERS

There seems little doubt that the scattering layers are associated with gravity waves o tides. Occasional observations of downward propagation of the layers /30, 53/, and o correlations of gravity wave motions with backscattered powers, have been made in th mesosphere and indeed the stratosphere /30,54,55/.

The details of the creation of these scatterers are as yet elusive. One popular model ha been that due to Bolgiano /56, 31/, in which the turbulence is assumed to mix a backgroun refractive index gradient to be nearly constant within a layer of strong turbulence, and s produce sharp changes in refractive index at the edges. However this model is not entirel appropriate because it should only produce specular scatter; the turbulence is assumed t mix the atmosphere so well that the potential refractive index gradient tends to zero withi the layer, so that no turbulent backscatter should be received. Furthermore, it is no clear in this model what would constrain the turbulence to a narrow band in the first place Indeed /71/ has shown with a series of laboratory experiments in stably stratified fluid that the boundary between turbulent and non-turbulent regions is generally not sharp although it contains large gradients and a substantial spectrum of internal buoyanc waves. /57/ have proposed that the scatter may be due to inertial period buoyancy (gravity waves with wavelengths equal to the Bragg backscatter scale of the radiowaves. For 50 MH radars, this requires gravity waves with vertical wavelengths of 3m. Such waves should b highly damped by viscosity effects at 70 km, although it is perhaps conceivable that thos generated in-situ might survive just long enough to have a weak effect.

Fine steps in density are also known to occur in the oceans /58, 59/ and even in fresh wate lakes /60/. A review of some of the processes which contribute to the steps in the ocea was given by /61/ and while many of the proposals were based on the different rates of

diffusion of salt and momentum (double-diffusive effects), one interesting point emerged from that discussion. It appears that for mechanical turbulence generated in a fluid which was originally statically stable, turbulent mixing tends to occur more in the horizontal direction than the vertical, and when the energy source of the turbulence is removed, mixing becomes almost two-dimensional. Thus in the decay phase of such turbulence, highly elongated structures arise, often with very little horizontal variation in refractive index, but with more rapid irregular variation in the vertical direction /61,62,63,64,65,71/. In one model of the production of turbulence due to the breakdown of Kelvin-Helmholtz waves, /66/ found evidence for the formation of long horizontal "braids" within which the refractive index was fairly constant.

It is therefore possible that the specular reflectors might be large two dimensional "blini" which seem to result as a consequence of decaying turbulence in highly stratified media. Some modelling is required to determine if such a stratified structure with an irregular variation of refractive index vertically is capable of causing the observed backscattered power. Such a model also requires that the turbulence be generated by mechanical rather than convective processes. Inertial scale gravity waves with vertical wavelengths of 1-2 km might be a possible candidate /67/, and since such waves have nearly horizontal wavefronts they might enhance the tendency for horizontal spreading. The reflectors might align themselves along the wavefronts, which might explain observations made by /73/ that the reflectors often have tilts of the order of 1° or 2°. A possible correlation between a strong scattering layer and an inertial scale wave has been noted on at least one occasion /30/. Such a model could be tested by looking for events of strong turbulence followed by strong specular scatter. In this model, the specular and isotropic scatterers would not be in exactly the same volume of space, but would certainly occur in the vicinity of each other.

Gravity wave - mean flow critical level interactions can also produce reasonably sharp steps in refractive index, although whether sharp enough to cause specular reflections is uncertain. Other models have been discussed by /69/, but until now no conclusive evidence has emerged to support any particular model. It is imperative that experiments are carefully designed to test these models, in order to determine the origin of the scatterers. A clearer understanding of the nature of these scatterers will also be aided by closer studies of seasonal variations e.g. /70/, and also by more investigations into the reasons for preferred heights. Carefully performed beam swinging experiments, accurate measurements of backscatter cross-sections, and studies with better height resolution are also important.

CONCLUSIONS

Both specular reflectors and turbulence can co-exist, possibly in close vicinity to each other, throughout the upper middle atmosphere. There may be geographic, seasonal, and day to day variations in the relative strengths of each type of scatter, and it is possible at times that one or the other type might exist alone. The turbulence itself may exhibit anisotropy. The specular reflectors may take the form either of "steps", or perhaps groups of horizontal two-dimensional planes of differing refractive index overlying each other with "steps" between successive planes. Because of the exponential increase in kinematic viscosity with increasing height, the steps have increasingly larger depths as the altitude increases, and become very inefficient reflectors at the higher altitudes. The "ceiling" above which no more specular reflectors are seen depends on the radar wavelength, being higher for larger wavelength radars. At 70 km, the steps are typically 3 - 10 m thick; they are not as narrow as 1m thick, as has been assumed in the past. Turbulent scatter can also be observed throughout the region with MF, HF and VHF radars, but radar scatter for VHF radio waves occurs from scales in the viscous subrange once heights of greater than about 75 km are reached. MF and HF turbulent scatter can also be detected in the entire region 60-100 km, but below 80 km is often swamped by the much stronger specular reflections.

REFERENCES

1. E.V. Appleton, Proc. Roy. Soc. (Lond), A126, 542, (1930)
2. W. Dieminger, J. Atmos. Terr. Phys., 2, 340, (1952)
3. S. Gnanalingam and K. Weekes, Nature, 170, 113 (1952)
4. C. Ellyet and J.M. Watts, J. Res. Nat. Bur. Standards., 63D 117, (1959)
5. F.F. Gardner and J.L. Pawsey, J. Atmos. Terr. Phys., 3, 321, (1953)
6. J.B. Gregory, Aust. J. Phys., 9, 324, (1956)
7. J.B. Gregory, J. Geophys. Res., 66, 429, (1961)
8. J.A. Fejer, J. Atmos. Terr. Phys., 7, 322, (1955)
9. J.A. Fejer and R.W. Vice, J. Atmos. Terr. Phys., 16, 291, (1959)
10. B. Bjelland, O. Holt, B. Landmark and F. Lied, Nature, 184, 973, (1959)
11. J.B. Gregory and R.A. Vincent, J. Geophys. Res., 75, 6387, (1970)
12. G.J. Fraser and R.A. Vincent, J. Atmos. Terr. Phys., 32, 1591, (1970)
13. B.H. Briggs and R.A. Vincent, Aust. J. Phys., 26, 805, (1973)
14. R.A. Vincent, Aust. J. Phys., 26, 815, (1973)

15. J.S. Belrose and M.J. Burke, J. Geophys. Res., 69, 2799, (1964)
16. A.H. Manson, J. Geophys. Res., 71, 3783, (1966)
17. W.R. Piggott and E.V. Thrane, J. Atmos. Terr. Phys., 28, 311, (1966)
18. W.A. Flood, J. Geophys. Res., 73, 5585, (1968)
19. G.L. Austin and A.H. Manson, Radio Sci., 4, 35, (1969)
20. A.H. Manson, M.W.J. Merry, and R.A. Vincent, Radio Sci., 4, 955, (1969)
21. G.L. Austin, R.G.T. Bennett and M.R. Thorpe, J. Atmos. Terr. Phys., 31, 1099, (1969)
22. B.C. Lindner, Aust. J. Phys., 28, 163, (1975)
23. B.C. Lindner, Aust. J. Phys., 28, 171, (1975)
24. R.A. Vincent and J.S. Belrose, J. Atmos. Terr. Phys., 40, 35, (1978)
25. T.J. Stubbs, J. Atmos. Terr. Phys., 39, 589, (1977)
26. W.K. Hocking, J. Geophys. Res., 84, 845, (1979)
27. W.K. Hocking, J. Atmos. Terr. Phys., 45, 89, (1983)
28. W.K. Hocking, Radio Sci., 20, 1403 (1985)
29. R.A. Vincent and S.M. Ball, J. Geophys. Res., 86, 9159, (1981)
30. W.K. Hocking, R. Ruester and P. Czechowsky, J. Atmos. Terr. Phys., 48, 131, (1986)
31. K. Schlegel, A. Brekke and A. Haug, J. Atmos. Terr. Phys., 40, 205, (1978)
32. J. Roettger, P.K. Rastogi and R.F. Woodman, Geophys. Res. Letts., 6, 617, (1979)
33. W.K. Hocking, Ph.D. Thesis, University of Adelaide, Australia, (1980)
34. D.A. de Wolf, Radio Sci., 18, 138 (1983)
35. A.N. Kolmogoroff, Doklady Akad. Nauk USSR, 32, 16, (1941) (German Translation in "Sammelband zur Statistischen Theorie der Turbulens", Akademie-Verlag, Berlin, (1958), p.77)
36. V. Tatarski, Wave propagation in a turbulent medium, (translated from Russian by Silverman) McGraw-Hill, N.Y., 1961
37. R.N. Bracewell, "The Fourier Transform and its applications". McGraw-Hill (1978)
38. W.K. Hocking and J. Roettger, Radio Sci, 18, 1312, (1983)
39. R. Buckley, Aust. J. Phys, 24, 373, (1971)
40. W.K. Hocking and R.A. Vincent, J. Atmos. Terr. Phys., 44, 843, (1982)
41. W.K. Hocking and R.A. Vincent, J. Geophys. Res., 87, 7615, (1982)
42. R.M. Harper and R.F. Woodman, J. Atmos. Terr. Phys., 39, 959, (1977)
43. P.K. Rastogi and S.A. Bowhill, J. Atmos. Terr. Phys., 38, 449, (1976)
44. S. Fukao, T. Sato, R.M. Harper and S. Kato, Radio Sci., 15, 447 (1980)
45. R. Ruester, P. Czechowsky and G. Schmidt, Geophys. Res. Letts, 7, 999, (1980)
46. O. Royrvik and L.G. Smith, J. Geophys. Res., 89, 9014, (1984)
47. O. Royrvik, Radio Sci., 18, 1325, (1983)
48. J. Roettger and C.H. Liu, Geophys. Res. Letts., 5, 357, (1978)
49. K.S. Gage and J.L. Green, Radio Sci., 13, 991, (1978)
50. R.F. Woodman, J. Roettger, T. Sato, P. Czechowsky and G. Schmidt, URSI Conference, Washington, August 1981, session FG1, paper no. 2
51. R.F. Woodman and A. Guillen, J. Atmos. Sci., 31, 493, (1974)
52. O. Royrvik, Radio Sci., 20, 1423, (1985)
53. G. Schmidt, R. Ruester and P. Czechowsky, IEEE Trans. Geosci. Electron., GE-17, 154, (1979)
54. J. Klostermeyer and R. Ruester, J. Geophys. Res., 86, 6631, (1981)
55. T.E. Van Zandt, J.L. Green, W.L. Clark, and J.R. Grant, Geophys. Res. Letts., 6, 429, (1979)
56. R. Bolgiano, Winds and Turbulence in the Stratosphere, Mesosphere and Ionosphere, ed K. Rawer, p. 371. North Holland, Amsterdam
57. T.E. Van Zandt and R.A. Vincent, Map Handbook, vol. 2, p. 78, (1983)
58. J.W. Cooper and H. Stommel, J. Geophys. Res., 73, 5849, (1968)
59. C. Wunsch, Tellus, 24, 350, (1972)
60. J.H. Simpson and J.D. Woods, Nature, 226, 832, (1970)
61. J.S. Turner, "Small scale mixing processes", in Evolution of Physical Oceanography, ed. B.A. Warren and C. Wunsch, Mass. Inst. Tech., p. 235, (1981)
62. D.K. Lilly, J. Atmos. Sci., 40, 749, (1983)
63. R.E. Britter, J.C.R. Hunt, G.L. Marsh and W.H. Snyder, J. Fluid Mech., 127, 27, (1983)
64. T.D. Dickey and G.L. Mellor, J. Fluid Mech., 99, 13, (1980)
65. A.D. McEwan, "Mass and momentum diffusion in internal breaking events", p. 742 in vol II of Proc. second symposium on stratified flows, Int. Ass. for Hydraulic Research. Trodheim, Norway, (1980)
66. R.I. Sykes and W.S. Lewellen, J. Atmos. Sci., 39, 1506, (1982)
67. D.C. Fritts and P.K. Rastogi, Radio Sci., 20, 1247, (1985)
68. E.A. Mechtly, S.A. Bowhill and L.G. Smith, J. Atmos. Terr. Phys., 34, 1899, (1972)
69. J. Roettger, Pure and Appl. Geophys., 118, 494, (1980)
70. B.B. Balsley, W.L. Ecklund and D.C. Fritts, Radio Sci., 18, 1053, (1983)
71. Y-H Pao, Boundary-layer Meteor., 5, 177, (1973)
72. R.J. Doviak and D.S. Zrnic, Radio Sci., 19, 325, (1984)
73. D. Murphy, M. Sc. Thesis, University of Adelaide, (1984)
74. A.H. Manson and C.E. Meek, J. Atmos. Terr. Phys., 42, 103, (1980)
75. A.H. Manson, MAP handbook 16, 239, (1985).

76. B. H. Briggs, JATP, 54, 153, 1992.

Velocity Bias

One important side-effect of anisotropic scatter is that it leads to biases in velocity methods when the so-called "Doppler method" is used for wind determinations.

We have thus far treated primarily the case of vertical beams, but when an off-vertical beam is used, the effect of anisotropy is to "pull" the peak of the beam back towards overhead. This means the beam is not pointing where

the user "thinks" it is, as illustrated in the diagram on the next page. As a result, the radial speed measured is less than it should be, and Doppler estimates of the mean wind are underestimates. Thus knowledge about the aspect-sensitivity parameter is important for proper determinations of wind speeds by radar.

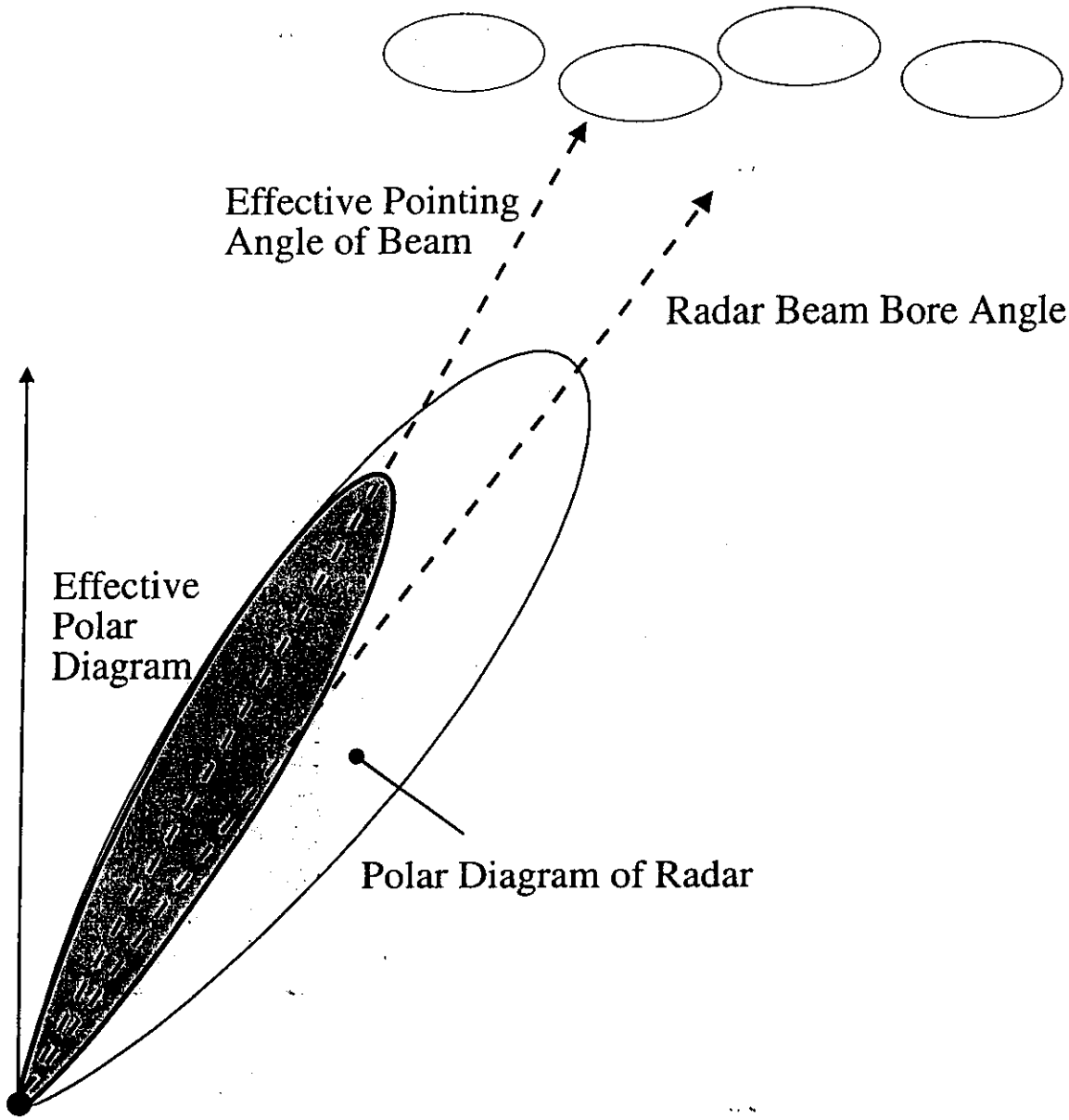
Effective Pointing
Angle of Beam
Radar Beam Bore Angle
Effective
Polar
Diagram
Polar Diagram of Radar

Appendix A: Effective pointing angle and beamwidth for anisotropic scatter

As pointed out by ROETTGER (1981), an anisotropy in the scattering mechanism alters the effective pointing angles for an off-vertical radar. Such anisotropy also alters the effective beamwidth and this is important for the work in this paper. Let the polar diagram of backscatter for the scatterers be

$$P_s(\theta) \propto e^{-\frac{\sin^2\theta}{\sin^2\theta_s}}$$

and the two way polar diagram for a vertically pointing radar be (A1)

$$P_R(\theta) \propto e^{-\frac{\sin^2\theta}{\sin^2\theta_0}} \quad \text{(A2)}$$

Then for a radar pointed off-vertical by angle θ_T in the azimuth direction $\phi = 0$, the polar diagram at angle (θ, ϕ) is

$$P_{RT}(\theta,\phi) \propto e^{\left\{-\left[\frac{(\sin\theta\sin\phi)^2+(\sin\theta\cos\phi-\sin\theta_T)^2}{\sin^2\theta_0}\right]\right\}} \quad \text{(A3)}$$

(Note that the expression $exp[-sin^2(\theta - \theta_T)/sin^2\theta_0)$ (which has in the past been used to represent a tilted beam) is NOT a good approximation, as that describes an annulus around the zenithal point at a mean angle θ_T.) When the effects of the polar diagram of the scatterers are included, the effective polar diagram is the product of (A1) and (A3). This is a maximum when the derivative of the exponent with respect to $sin\theta$ is zero, or at

$$sin\theta_{eff} = sin\theta_T \left[1 + \frac{sin^2\theta_0}{sin^2\theta_s}\right]^{-1} \quad \text{(A4)}$$

For θ_0, θ_s less than about 10°, this approximates to

$$sin\theta_{eff} = sin\theta_T \left[1 + \frac{\theta_0^2}{\theta_s^2}\right]^{-1}$$

Thus the effective pointing angle is given by (A4), and horizontal wind speeds will be underestimated by the factor

$$R_1 = \left[1 + \frac{\theta_0^2}{\theta_s^2}\right] \quad \text{(A5)}$$

if one uses say equation (12) without any correction. This is in fact only approximate - to properly determine the actual measured radial velocity, equation (35) of HOCKING (1983a) should be integrated (including an aspect sensitivity for the scatterers) to produce the expected power spectrum; this will not have a maximum at the exact point described by (A4), but it will be close.

The half-width of the effective beam can be found by finding the angles (θ, ϕ) where the effective polar diagram [i.e. the product of (A1) and (A3)] falls to one half of the value at $(\theta, \phi) = (\theta_{eff}, 0)$. Consider only the line $\phi = 0$. Then the product of (A1)and (A3) gives

$$e^{\left\{-\left[\frac{(\sin\theta-\sin\theta_T)^2}{\sin^2\theta_0}+\frac{\sin^2\theta}{\sin^2\theta_s}\right]\right\}} \quad \text{(A6)}$$

* NB $e^{-\frac{(\sin\theta-\sin\theta_T)^2}{\sin^2\theta_0}}$ is NOT an appropriate model!!

and we seek the two angles $(\theta_{\frac{1}{2}})_{1,2}$ where this falls to one half of the value at $\theta = \theta_{eff}$. Some algebraic manipulation soon shows that a quadratic in $sin\theta$ results, which has two roots at

$$(\theta_{\frac{1}{2}})_{1,2} = sin\theta_{eff} \pm \sqrt{ln2}.sin\theta_0 \left[1 + \frac{\theta_0^2}{\theta_e^2}\right]^{-\frac{1}{2}} \tag{A7}$$

(for θ_0, θ_e less than about 10°), and this shows that the effective half-power half-width is

$$R_2 = \left[1 + \frac{\theta_0^2}{\theta_e^2}\right]^{-\frac{1}{2}} \tag{A8}$$

times the half-width of the radar alone. Notice that this ratio is independent of the radar tilt direction, at least out to angles of 10-15°.

Equivalently, we can write that the effective half-power half-width $\theta_{eff\frac{1}{2}}$ obeys the relation

$$sin^{-2}(\theta_{eff\frac{1}{2}}) = sin^{-2}(\theta_{\frac{1}{2}}) + sin^{-2}(\theta_{e\frac{1}{2}}), \tag{A9}$$

where $\theta_{\frac{1}{2}}$ is the half power half width of the radar beam and $\theta_{e\frac{1}{2}}$ is the half-power half-width of the backscatter polar diagram of the scatterers.

Now let use address the issue of how the power received by the radar changes as a function of tilt angle θ_T. The power received by the vertical beam can be found by integrating over the beam, and for a Gaussian polar diagram this integral is proportional to $(\theta_{eff\frac{1}{2}})^2$ where $\theta_{eff\frac{1}{2}}$ is the effective half-power half-width of the combined polar diagrams of the radar and the scatterers. When the radar beam is phased to look at an off-vertical angle θ_T, the peak power will be reduced by a factor

$$f1 = e^{\{-\frac{(\theta_{eff}-\theta_T)^2}{\theta_e^2}\}}$$

because the peak returned power is returned from θ_{eff} and not θ_T, and then by a further factor

$$f2 = e^{\{-\frac{\theta_{eff}^2}{\theta_e^2}\}}$$

bacause of the reduction in power due to the polar diagram of backscatter of the scatterers.

Thus the total received power will be proportional to the product of $f1$ and $f2$, and then multiplied by the effective beam half-power half-width squared. Thus the received power on the off-vertical beam divided by that received on the vertical beam is equal to

$$\frac{f1.f2.(\theta_{eff\frac{1}{2}})^2}{(\theta_{eff\frac{1}{2}})^2}$$

or

$$\frac{P(\theta_T)}{P(0)} = exp\left\{-\left[\frac{(\theta_{eff}-\theta_T)^2}{\theta_0^2} + \frac{\theta_{eff}^2}{\theta_e^2}\right]\right\} \tag{A10}$$

Note that this final expression corrects an error in the original derivation of HOCKING et al, (1986), in which the factor $f2$ was neglected.

Physical Causes

We now turn to examination of the reasons for the existence of these various radio-wave scatters.

We will begin by examining the cases of specular reflection and anisotropic scatter. I choose these as the first topics because they lead to some fascinating insights into the nature of the atmosphere.

It also happens that these phenomena are still somewhat poorly understood!

The following pages are something of an overview. - more detail will follow later

After this discussion, we will then embark on a more detailed study of turbulence in the atmosphere, because this is still the most common form of radiowave scatter.

Following that, we will return again to specular reflection, and include a few specific models for this phenomenon.

VIII

Aspect sensitivity of the scatterers - possible physical causes

We have seen several times throughout this text that a better understanding about the shapes of the scatterers is necessary in order to better interpret measurements of wind speed, electron densities, and turbulence intensities. It would also naturally help in understanding the cause of the scatterers. The shape of the scattering irregularities has been the subject of active debate over many years. Models have ranged from flat, mirror-like partial reflectors to "pancake-like" scatterers to inertial-range isotropic turbulence, and in this review we will not dwell too much on these arguments. Rather, we will first describe the main models, and then concentrate on the sorts of techniques which might be, and have been, used to determine the shapes of the scatterers.
If it is assumed that the polar diagram of backscatter of the scatterers is of the form

$$B(\theta) \propto e^{-\frac{\sin^2\theta}{\sin^2\theta_s}}, \tag{1}$$

then θ_s gives a measure of how rapidly the backscattered power falls off as a function of zenith angle. If θ_s tends towards 90 ° , it indicates isotropic scatter, whilst if θ_s tends towards 0° then it indicates highly aspect-sensitive scatter.
There are a variety of models which have been advanced, but they basically fall into 2 categories. (e.g. LINDNER, 1975 a,b; BRIGGS and VINCENT, 1975; ROETTGER and LIU, 1978; GAGE and GREEN, 1978; HOCKING, 1979; FUKAO et al., 1980a, b; ROETTGER, 1980b; GAGE et al., 1981; DOVIAK and ZRNIC, 1984; WATERMAN, 1985, amongst others).
(A) The first class assumes that individual scatterers are (on average) ellipsoidal in shape, which may vary in their length to depth ratio as a function of scale. The extremes are spherical shapes (isotropic scatter) and highly elongated structures.
(B) The second class of model assumes a horizontally stratified atmosphere consisting of variations in refractive index in the vertical direction, so one can think of this as a series of "sheets" of different refractive index. Such structures, if truly stratified, would have $\theta_s = 0$, but if we imagine that these sheets are gently "wrinkled", then θ_s will become non-zero (e.g. RATCLIFFE, 1956). In this case, the range of θ_s values relates to the range of Fourier components necessary to describe the wrinkles. Proponents of model B do not claim that the whole atmosphere is like this, but that it is like this in some places at some times, and use the model to describe particular observations.
Sometimes hybrids of the two models are invoked and other, more complicated, models have also been proposed, but they are generally based on the above models. To illustrate these later models, as well as give a feel for how they are explained physically, some examples of such more complicated models are shown below. The first (see over) is due to BOLGIANO (1968), and assumes that an intense turbulent layer might mix the layer so that the potential refractive index across the layer is constant, with sharp edges at the side. These edges might be able to explain the model B reflectors, for example, although doubts about the possibility of a turbulent layer maintaining sharp edges exist.
The second model shown over the page proposes that scatterers near the edges of a confined layer of turbulence are more anisotropic than in the centre. The model has been discussed by HOCKING et al. (1984), noted by HOCKING (1985), and also proposed independently by WOODMAN and CHU (1989). Such a model is physically likely because turbulent layers are often more stable near their edges (e.g. PELTIER et al., 1978; KLAASSEN and PELTIER, 1985), but for the purposes of this paper these models are simply noted as the type of extension to the simple models proposed above which should be borne in mind.

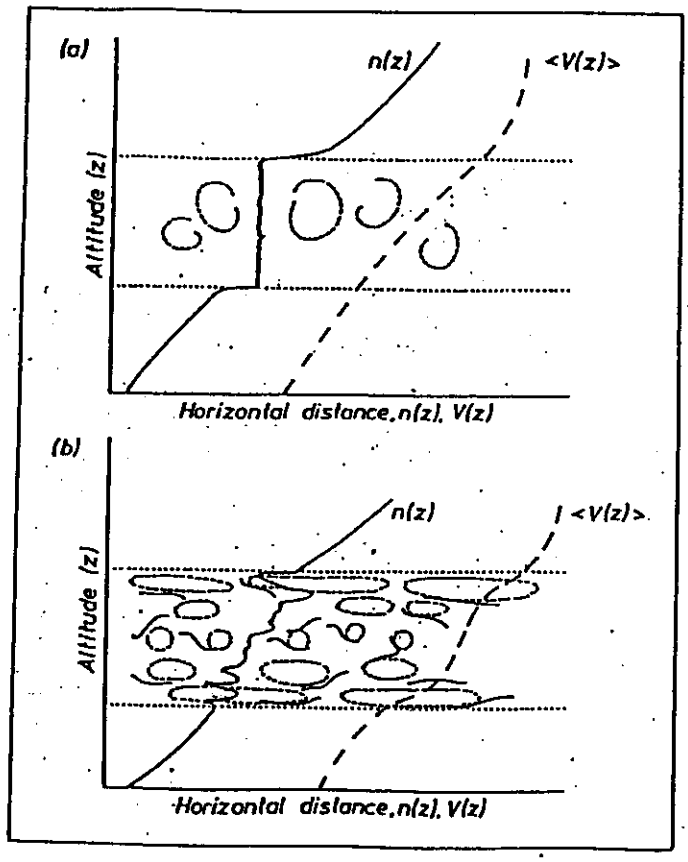

Idealized views of two models for turbulence in the atmosphere. The broken lines represent "eddies", and the solid lines represent scatterering interfaces. The first graph represents an earlier proposal due to Bolgiano (1968), and the second represents a model discussed in the text.

Figure.

Another model which may give a physical basis to model B is the proposal that the specular reflectors might be damped gravity waves (e.g. VANZANDT and VINCENT, 1983; HOCKING, 1987a and references therein) or even viscosity waves HOOKE and JONES, 1986; HOCKING et al., 1991), the latter being capable of existing at very short wavelengths. HOCKING et al. (Radio Sci., "Viscosity waves and thermal-conduction waves as a cause of 'specular' reflectors in radar studies of the atmosphere", Radio Sci., 26, 1281-1303, 1991), have examined the possibility of viscosity waves as specular reflectors in some considerable detail, both at MF and HF in the D-region and at VHF in the stratosphere.

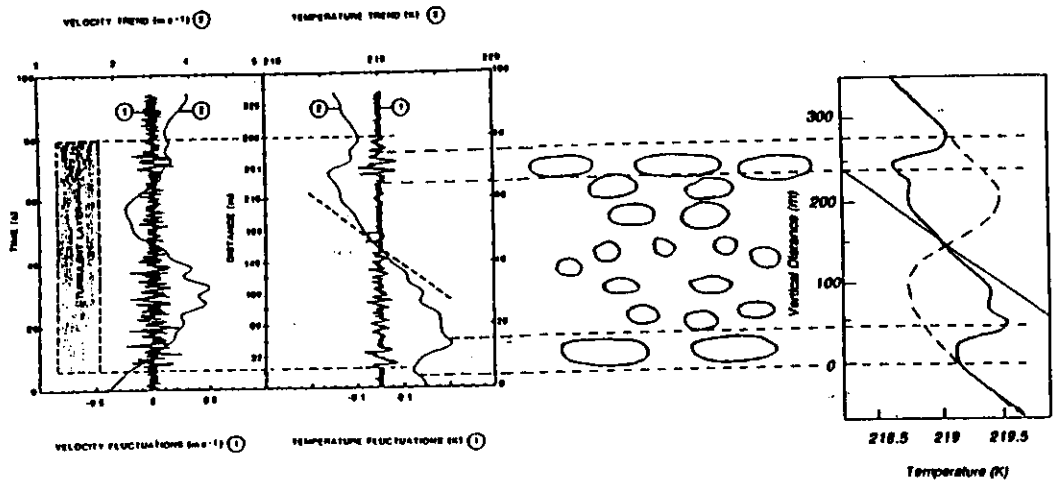

Fig. 6. Collection of diagrams from several sources, all showing evidence in some way of anisotropic turbulence. The left hand side diagrams show experimentally determined velocity and temperature fluctuations through a turbulent layer in the stratosphere, from DALAUDIER and SIDI (1987). The middle section shows a proposal (see text) describing the expected mean degree of turbulent anisotropy within a turbulent layer, and shows greater anisotropy at the edges. The right hand side profile shows the shape of the mean temperature profile in a turbulent layer at two stages of evolution, as predicted by the model of KLAASSEN and PELTIER, (1985a, b), and adapted for comparison with the experimental results shown on the left. The broken line in this last graph shows an initial temperature inversion, and the solid line the profile expected after dynamic turbulence has existed for some time. The straight solid line shows an adiabatic temperature profile for reference. The agreement with experiment is quite remarkable, even in some of the fine detail. The occurrence of very stable temperature gradients at the top and bottom is very pronounced, both in the experimental results and the prediction, and it is in this region that the most anisotropic turbulence is expected. One would also expect the strongest radio-wave backscatter from these sections at the top and bottom, where the fluctuations in temperature as a function of height are the strongest.

The Effects of Middle Atmosphere Turbulence on Coupling between Atmospheric Regions

W. K. HOCKING

J. Geomag. Geoelectr., 43, Suppl., 621–636, 1991

VISCOSITY WAVES: [* To be discussed in more detail later]

Hocking et al., Radio Sci, 26, 1281–1303 (1991)

THEORY

Equations of fluid motion with viscosity and thermal conduction included

The (two-dimensional) equations of motion for small perturbations in a Boussinesq viscous fluid are (for example, HJ):

$$\frac{\partial u'}{\partial t} = -\frac{1}{\rho_0}\frac{\partial p'}{\partial x} + \nu\nabla^2 u' \qquad (1a)$$

$$\frac{\partial w'}{\partial t} = -\frac{1}{\rho_0}\frac{\partial p'}{\partial z} - \frac{\rho' g}{\rho_0} + \nu\nabla^2 w' \qquad (1b),$$

$$\frac{\partial u'}{\partial x} + \frac{\partial w'}{\partial z} = 0 \qquad (1c)$$

$$\frac{\partial \rho'}{\partial t} + w'\frac{\partial \rho_0}{\partial z} = \kappa\nabla^2\rho' \qquad (1d)$$

$$\frac{\partial u'}{\partial t} = \nu\frac{\partial^2 u'}{\partial z^2} \qquad (2a)$$

$$\frac{\partial w'}{\partial t} = \nu\frac{\partial^2 w'}{\partial z^2} \qquad (2b)$$

Assuming a solution of the form

$$u' = u_0' \exp\{i(kx + mz - \omega t)\}$$

and substituting in (2*a*) gives

$$m = \sqrt{\frac{i\omega}{\nu}} \qquad (3a)$$

or

$$m_{1,2} = \left(\frac{1}{\sqrt{2}}\sqrt{\frac{\omega}{\nu}} + \frac{i}{\sqrt{2}}\sqrt{\frac{\omega}{\nu}}\right), \left(-\frac{1}{\sqrt{2}}\sqrt{\frac{\omega}{\nu}} - \frac{i}{\sqrt{2}}\sqrt{\frac{\omega}{\nu}}\right) \qquad (3b)$$

The solution u' therefore describes a heavily damped sinusoidal variation in the vertical with wavelength

$$\lambda_z = \sqrt{8}\,\pi(\sqrt{\nu/\omega}) = 2\sqrt{\pi}(\sqrt{\nu T}) \qquad (4)$$

and with an exponential decay. In this case, T is the period of the wave, $= 2\pi/\omega$.

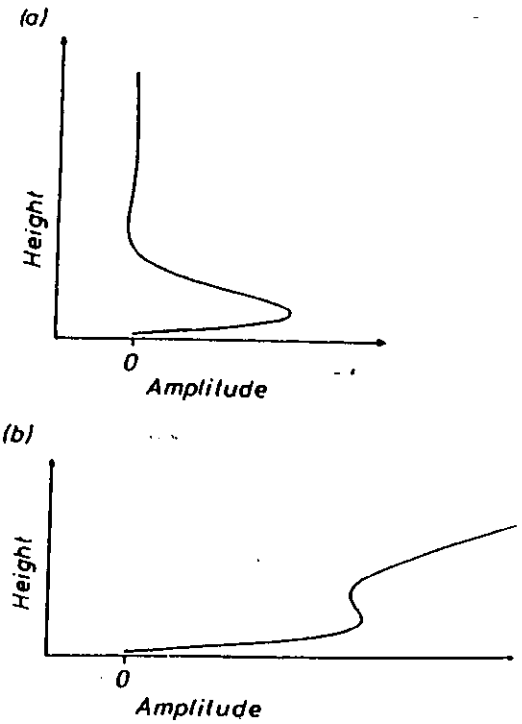

Fig. 5. (*a*) "Amplitude" (which may represent velocity, temperature, density, etc.) as a function of height for a typical viscosity wave. (*b*) A similar wave superimposed on a mean gradient.

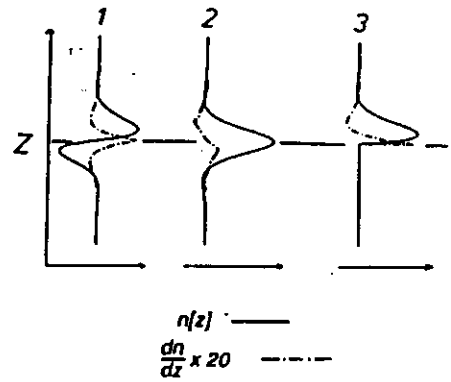

(Specular reflectors and anisotropic scatterers)

Having now established that both models have some physical basis, let us concentrate on the simpler models, since these form an excellent basis for later discussion of any of the more complex models. With regard to model A, it should be noted that θ_s gives a direct measure of the length to depth ratio of the scatterers. The following figure, from HOCKING (1987a), shows this relationship. What techniques, then can be used to determine the nature of these scatterers?

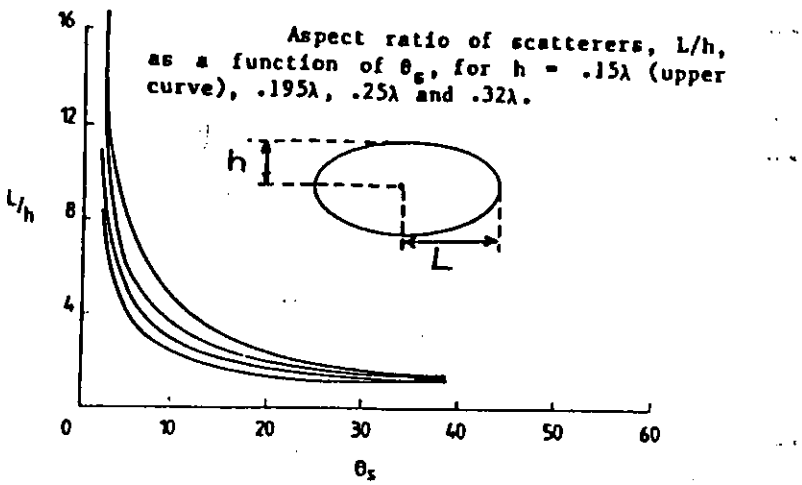

Fig.

VIII.1 Experimental techniques to determine the nature of the scatterers

In the following section a variety of techniques which may be used to determine information about the nature of the scatterers are described and some of the results obtained so far discussed. The list is not, however, exhaustive.

VIII.1.1 Methods utilizing different beam configurations

One of the simplest methods to investigate the aspect sensitivity of the scatterers is to simply point a narrow beam vertically, and then at several off-vertical angles. The variation in power P as a function of beam tilt angle θ, is then related to θ_s. In fact it can be shown that

$$P(\theta_T) \propto e^{-[\frac{(\theta_{eff}-\theta_T)^2}{\theta_0^2}+\frac{\theta_{eff}^2}{\theta_s^2}]} \tag{2}$$

where θ_{eff} is defined by equation (16), θ_T is the beam tilt direction from the vertical, and the polar diagram of the radar beam is assumed to be of the form $exp\{-(sin^2\theta)/(sin^2\theta_0)\}$ [e.g. appendix A; HOCKING et al (1986); note that the derivation in appendix A corrects an error made in HOCKING et al 1986, in that the important term $\frac{\theta_{eff}^2}{\theta_s^2}$ was neglected in the exponent of e in that paper].

A typical experiment which might be performed is to compare the powers received with a vertical and an off-vertical beam, and use this to deduce θ_s. Utilizing equations (A4) and (A10)),it is possible to derive the following simple relation between $P(\theta_T)/P(0)$, θ_T and θ_0. If R is defined to be $ln\{P(0)/P(\theta_T\}$ (or $R = 0.23026R_{dB}$, where R_{dB} is the ratio of $P(0)/P(\theta_T)$ expressed in dBs), then

$$\theta_s^2 = \frac{\theta_T^2}{R} - \theta_0^2$$

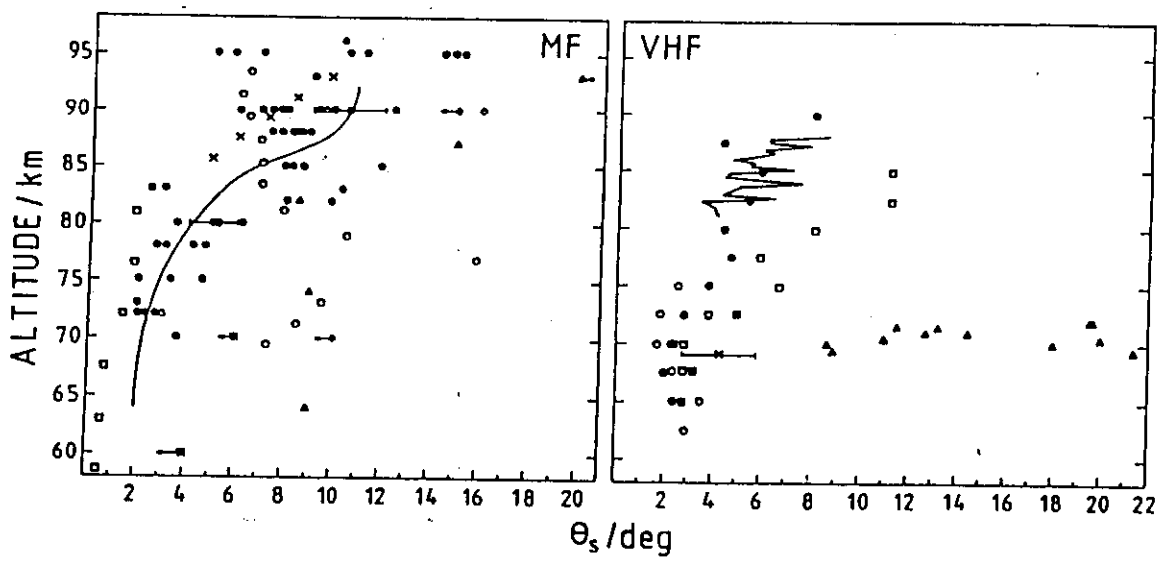

Fig. 8. Values of θ_S observed at MF and VHF at a number of locations. MF symbols represent the following studies: asterixes (Tromsø, 69°N), closed diamonds (Townsville, 16°S), closed squares (Adelaide, 35°S), all from /7/; open squares (Boot Lake, 40°N) /24/; closed circles and continuous line /86,87/, open diamond /88/, open triangles /89/, all from Adelaide; closed triangles (Ottawa, 45°N) /90/; crosses /91/ and open circles /94/, both from Adelaide. VHF symbols represent: cross (Arecibo, 19°N) /1/; open and closed circles and squares (Jicamarca, 12°S) /62,63/; open and closed triangles (Kyoto, 35°N) /95/; and continuous line (Andenes, 69°N, summer) /85/.

$$B(\theta) \propto e^{-\frac{\sin^2\theta}{\sin^2\theta_s}}$$

46

Hooper and Thomas (JATP, 1995) have shown that if the powers on 2 beams, pointed at angles θ_1 and θ_2 from off-vertical, are measured, then the value of θ_s can be found as

$$\theta_s = sin^{-1}\sqrt{\left\{\frac{sin^2\theta_2 - sin^2\theta_1}{ln[P(\theta_1)/P(\theta_2)]} - sin^2\theta_0\right\}} \qquad (3)$$

Typical variations of $P(\theta)$ show an approximately Gaussian fall-off out to about 5° - 10° , and then an approximately constant value beyond this, indicating possibly isotropic turbulence with more anisotropic scatterers either embedded or nearby (e.g. DOVIAK and ZRNIC, 1984). Typical values of θ_s are often in excess of 8° in the troposphere, whilst in the stratosphere at VHF values can be as small as 3° - 4° .

In the mesosphere, θ_s is typically 4° for VHF scatter below 75 km, although on occasions isotropic scatter is also seen. Above 80 km, VHF measurements give θ_s to be about 6° - 8° . At MF, θ_s is typically 2° - 5 ° below 80 km, increasing to about 8 - 15° above 80 km (e.g. LINDNER, 1975a,b; VINCENT and BELROSE, 1978. REID (1989) has summarized the various mesospheric measurements.

An alternative means which may be used to determine θ_s is to utilize equation (16). By comparing wind speeds deduced using the DBS method for a beam pointed at say 5° off-zenith to one at say 15° off zenith, it is possible to deduce θ_s from (A4), assuming that the value deduced with the 15° beam is the true wind speed. An alternative is to use spaced antenna methods to determine the true wind speed, and then comparisons with the DBS measurements may allow determination of θ_s. Another interesting determination of θ_s was made by VINCENT and BELROSE (1978), who compared the powers received on two beams of different polar diagram widths, and used the resultant ratios of powers to determine θ_s. The method yielded results consistent with determinations made by other techniques discussed in this section.

III .2.

47

Applications of these theories in the D-region

Measurements of θ_S are moderately straight-forward, once the above procedures are applied. it is also possible to convert these measurements to other useful parameters, which will now be listed.

The spatial lag at which the autocorrelation of the refractivity structure falls to one half of its max is

$$\rho_{0.5} \simeq \frac{7.6\lambda}{\theta_s} \quad (8)$$

(†)

where θ_s is in degrees.
If we think of the scatterers as ellipsoids, then their horizontal e^{-1} full-length is

$$L \simeq \frac{0.11\lambda}{sin\theta_s}. \quad (9)$$

One of the most important parameters is the length to depth ratio of the scatterers, and this is given by

$$\left(\frac{L}{h}\right)^2 \simeq \left(\frac{\lambda^2/h^2}{8\pi^2 sin^2\theta_s} + 1\right) \quad (10)$$

The most comprehensive practical applications of these theories for D-region (MF and HF) work have been produced by *Lesicar and Hocking, JATP, 54, 295-309, (1992)* and *Lesicar et al., JATP, 56, 581-591, (1994)*. Related works for the VHF include Hocking et al., Radio Sci., 25, 613-627, (1990).
Note that the above theory breaks down when the reflectors become highly distended (θ_s of the order of 0.5°), and in this case the more elaborate Fresnel theory of Doviak and Zrnic (Radio Sci., 19, 325-336, (1984)) can be used. However, the simplicity of the preceding formulations often makes their application much more straight-forward.

Examples are given here and in the following diagrams.

†) Note the factor here is 7.6 = $\frac{1}{2}$ × 15.2. This difference arises because the factor 15.2 (seen earlier) was for the auto-correlation function over the ground whereas the case in equation (8) is for the in-situ correlation function. The difference arises due to the "point-source" effect.

48

(Lesicar and Hocking)

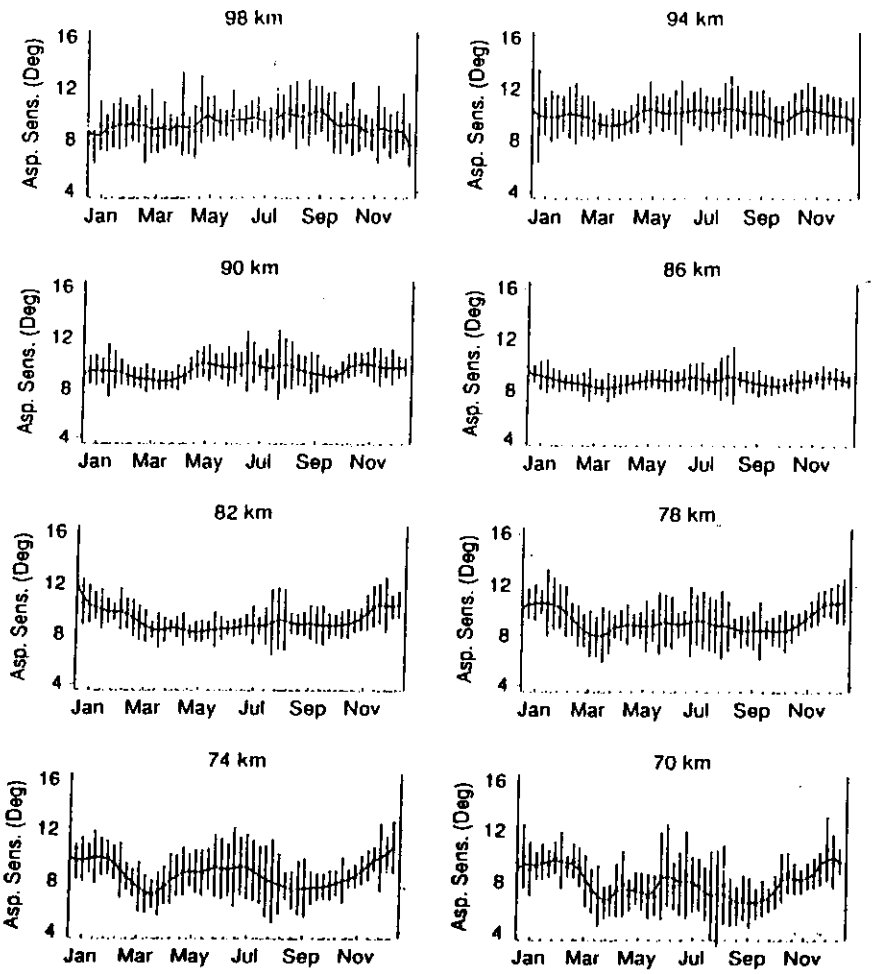

~10°

~6°

Aspect Sensitivity calculated from the Spatial Correlation
Three year average with a smoothed running mean
for the years 1986, 1987 & 1988

θ_c has been calculated from values of the spatial correlation function.

(taken from Spaced antenna analysis)

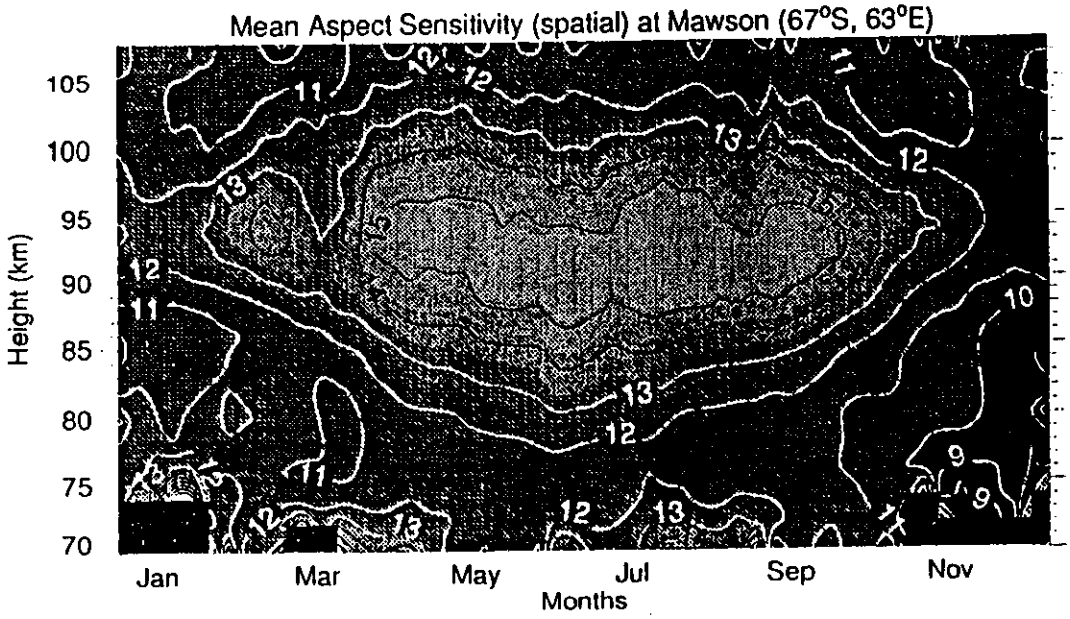

Fig. 3. Image and contour plot of one week averages for θ_x as a function of year for heights of 70–108 km from data collected at Mawson, Antarctica for 4 yr (1985–1988). θ_x was calculated from the spatial correlation method, and is in degrees.

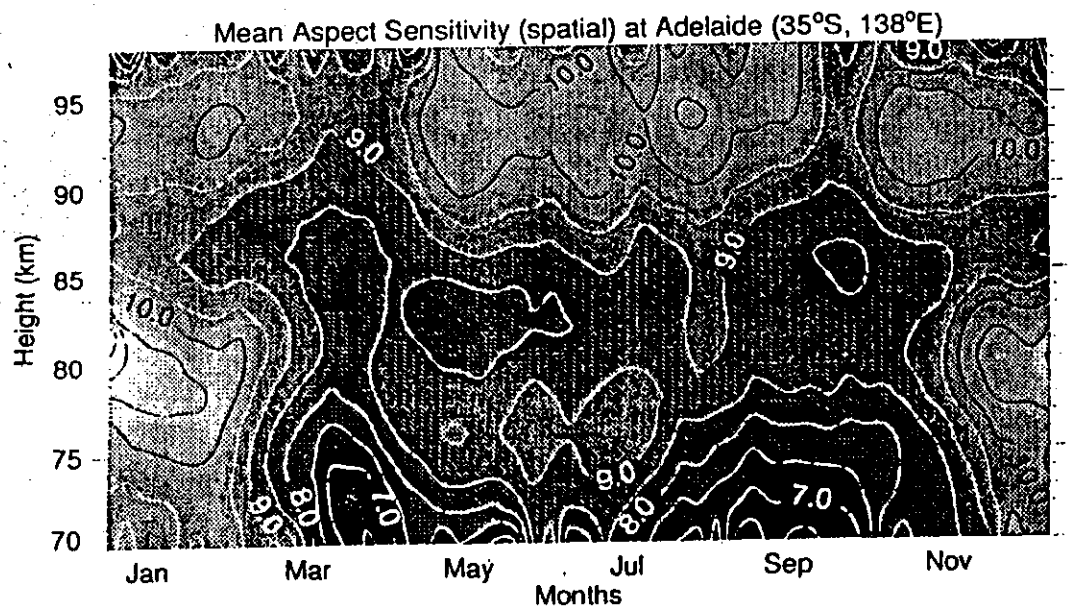

Fig. 4. As for Fig. 3, but for 3 yr of Adelaide data (1986–1988). Note that the height only extends up to 98 km.

58

The following references may be used to track down at least some of the papers cited in the text - the list is not complete, and probably also contains references not cited - but makes a good starting point.

References

Adams, G.W., D.P. Edwards and J.W. Brosnahn, The imaging Doppler interferometer; Data analysis, *Rad. Sci., 20*, 1481-1492, 1985.

Atlas, D., *Advances in Geophysics*, vol 10, 317 pp,Academic New York, 1964.

Atlas, D., R.C. Srevastava and P.W. Sloss, Wind shear and reflectivity Gradient effects on Doppler radar spectra, II, *J.Appl.Meteor.,8*, 384-388, 1969.

Austin, G.L., R.G.T. Bennett,and M.R. Thorpe, The phase of waves partially reflected from the lower ionosphere, *J.Atmos.Terr.Phys., 31*, 1099-1106, 1969.

Barat, J., Some characteristics of clear air turbulence in the middle stratosphere, *J.Atmos.Sci., 39*, 2553-2564, 1982.

Batchelor, G.K., *The theory of homogeneous turbulence*, Cambridge University Press, New York, 1953.

Bohne, A.R., Radar detection of turbulence in precipitation environments,*J.Atmos.Sci., 39*, 1819-1837., 1982.

Bolgiano, R., Jr., *The general theory of turbulence - turbulence in the atmosphere, in "Winds and turbulence in the stratosphere, mesopshere and ionosphere"*, ed K. Rawer, p371, North-holland, Amsterdam, 1968.

Bracewell, R.N., *The Fourier Transform and Its Applications*, 444pp.,McGraw-Hill, New York, 1978.

Briggs, B.H., Radar observations of atmospheric winds and turbulence: a comparison of techniques, *J.Atmos.Terr.Phys., 42*, 823-833, 1980.

Briggs, B.H., The analysis of spaced sensor records by correlation techniques, *Handbook for MAP, vol.13*, Ground based techniques, 166-186, Univ. of Illinois, Urbana, 1984.

Briggs, B.H. and R.A.Vincent, Some theoretical considerations on remote probing of weakly scattering irregularities, *Aust.J.Phys., 26*, 805-814, 1973.

Budden, K.G., Effect of electron collisions on the formulas of magnetoionic theory, *Radio Sci., 69D*, 191-211, 1965.

Caughey S.J. ,B.A. Crease, D.N. Asimakapoulos, and R.S. Cole, Quantitative bistatic acoustic sounding of the atmospheric boundary layer, *Q. J. R. Meteorol. Soc, 104*, 147-161, 1980.

Crane, R.K., A review of radar observations of turbulence in the lower stratosphere, *Radio Sci., 15*. 177-194, 1980.

Croft, T.A., Sky-wave backscatter: a means of observing our environment at great distances. *Revs. Geophys. Space Phys., 10* , 73-155, 1972.

Dewan, E.M., Turbulent vertical transport due to thin intermittent mixing layers in the stratosphere and other stable fluids, *Science, 211*, 1041-1042, 1981.

Doviak, R.J., and D.S. Zrnic, Reflection and scatter formula for anisotropically turbulent air, *Radio Sci., 19*, 325-336, 1984.

Farley, D.T., H.M. Ierkic, and B.G. Fejer, Radar interferometry : a new technique for studying plasma turbulence in the ionosphere, *J.Geophys.Res., 86*, 1467-1472, 1981.

Fukao, S., K.Wakasugi, and S.Kato, Radar measurement of short-period atmospheric waves and related scattering properties at the altitude of 13-25 km over Jicamarca, *Radio Sci., 15*, 431-438, 1980a.

Fukao, S., T.Sato, R.M. Harper,and S. Kato, Radio wave scattering from the tropical mesosphere observed with the Jicamarca radar,*Radio Sci., 15*, 447-457, 1980b.

Fukao, S., T. Sato, P.T. May, T. Tsuda, S. Kato, M. Inaba, and I. Kimura, A systematic error in MST/ST radar wind measurement induced by a finite range volume effect,1, Observational results, *Radio Sci., 23*, 59-73, 1988a.

Fukao, S., M. Inaba, I. Kimura, P.T. May, T. Sato, T. Tsuda, and S. Kato, A systemic error in MST/ST radar wind measurement induced by a finite range volume effect,2, Numerical considerations, *Radio Sci.,23*, 74-82, 1988b.

Gage, K.S., and Balsley, B.B., Doppler radar prob-ing of the clear atmosphere,*Bull. Am. Meteorol. Soc., 59*, 1074-1093, 1978.

Gage,K.S., and J.L.Green, Evidence for specular reflection from monostatic VHF radar observations of the stratosphere, *Radio Sci., 13*, 991-1001, 1978.

Gage, K.S., J.L.Green, and T.E.VanZandt, Use of Doppler radar for the measurement of atmospheric turbulence parameters from the intensity of clear air echoes, *Radio Sci., 15*, 407-416, 1980.

Gage,K.S., B.B. Balsley, and J.L. Green, Fresnel scattering model for the specular echoes observed by VHF radars, *Radio Sci., 16*, 1447-1453, 1981a.

Gage, K.S., W.L. Ecklund, and B.B. Balsley, A modified Fresnel scattering model for the parameterization of Fresnal returns, *Radio Sci., 20*, 1493-1502, 1985.

Green, J.L., and K.S.Gage, Observations of stable layers in the troposphere and stratosphere using VHF radar, *Radio Sci., 15*, 395-405, 1980.

Green, J.L. and K.S. Gage, A Re-examination of the range resolution dependence of backscattered power observed by VHF radars at vertical incidence, *Radio Sci., 20*, 1001-1005, 1985.

Gregory, J.B., and R.A. Vincent, Structure of pertially reflecting regions in the lower ionosphere, *J. Geophys. Res., 75*, 6387-6389, 1970.

Hitschfeld, W., and A.S.Dennis, *Measurement and calculation of fluctuations in radar echoes from snow* , Sci. Rep. MW-23, McGill Univ., Montreal, Canada, 1956.

Hocking, W.K., Angular and temporal characteristics of partial reflections from the D-region of the ionosphere, *J.Geophys. Res., 84*, 845-851, 1979.

Hocking,W.K., and R.A. Vincent, Comparative observations of D region HF partial reflections at 2 and 6 MHz, *J.Geophys. Res., 87*, 7615-7624, 1982a.

Hocking, W.K. and R.A. Vincent, A comparison between HF partial reflection profiles from the D-region and simultaneous Langmuir probe electron density neasurements,*J. Atmos. Terr. Phys., 44*, 843-854, 1982b.

Hocking W.K., On the extraction of atmospheric turbulence parameters from radar backscatter Doppler spectra I, Theory, it J. Atmos. Terr. Phys., 45, 89-102, 1983a.

Hocking, W.K., Mesospheric turbulence intensities measured with a HF radar at 35°S, II, *J.Atmos. Terr.Phys., 45*, 103-114, 1983b.

Hocking, W.K. The spaced antenna drift method, *Handbook for MAP, vol.9*, 171-186, Univ. of Illinois, Urbana, 1983c.

Hocking, W.K., and J. Roettger, Pulse-length dependence of radar signal strengths for Fresnel backscatter,*Radio Sci., 18*, 1312-1324, 1983.

Hocking, W.K., G. Schmidt, and P. Czechowsky, *Absolute calibration of the SOUSY VHF stationary radar*, Max-Planck-Instut fur Aeronomie report MPAE-W-00-83-14, Katlenburg-Lindau, F.R.G., 1983

Hocking, W.K., R. Ruester and P. Czechowsky, *Observation and measurement of turbulence and stability in the middle atmosphere with a VHF radar*, University of Adelaide internal report ADP-335, University of Adelaide, Adelaide, S.A. Australia, 1984

Hocking, W.K., Measurement of turbulent energy dissipation rates in the middle atmosphere by radar techniques: a review, *Radio Sci., 20*, 1403-1422, 1985.

Hocking W.K., R. Ruester and P. Czechowsky, Absolute reflectivities and aspect sensitivities of VHF radio wave scatterers measured with the SOUSY radar, *J.Atmos.Terr.Phys., 48*, 131-144, 1986.

Hocking, W.K., Observation and measurement of turbulence in the middle atmosphere with a VHF radar,*J.Atmos. Terr. Phys., 48*, 655-670, 1986.

Hocking, W.K., Radar studies of small scale structure in the upper middle atmosphere and lower ionosphere, *Adv. Space Res., 7*, 327-338, 1987a

Hocking, W.K., Reduction of the effects of non-stationarity in studies of amplitude statistics of radio wave backscatter, *J. Atmos. terr. Phys., 49*, 1119-1131, 1987b

Hocking, W.K., Two years of continuous measurements of turbulence parameters in the upper mesosphere and lower thermosphere made with a 2-MHz radar,*J. Geophys. Res., 93*, 2475-2491, 1988

Hocking, W.K., May, P.T., and Roettger, J., Interpretation, reliability and accuracies of parameters deduced by the spaced antenna method in middle atmosphere applications, *Pure and Appl. Geophys.*, 1989, in press.

Hooke, W.H., and R.M. Jones, Dissipative waves excited by gravity-wave encounters with the stably stratified Planetary Boundary Layer, *J. Atmos. Sci., 43*, 2048-2060, 1986.

Klaassen, G.P., and W.R. Peltier, Evolution of finite amplitude Kelvin-Helmholtz billows in two spatial dimensions, *J. Atmos. Sci., 42*, 1321-1339, 1985.

Klostermeyer, J. and R. Ruester, Radar observation and model computation of a jet stream-generated Kelvin-Helmholtz instability, *J. Geophys. Res., 85*, 2841-2846, 1980.

Klostermeyer, J. and R. Ruester, Further study of a jet stream-generated Kelvin-Helmholtz instability,*J. Geophys. Res., 86*, 6631-6637, 1981.

Kuo, F.-S.,C.-C. Chen, S.I. Liu, J. Roettger, and C.H. Liu, Systematic behaviour of signal statistics of MST radar echoes from clear air and their interpretation, *Radio Sci., 22*, 1043-1052, 1987.

Labitt, M., *Some basic relations concerning the radar measurement of air turbulence*, Mass. Inst. of Technol., Lincoln Lab., Work. Pap. 46WP-5001, 1979.

Lilly, D.K., D.E. Waco and S.I. Adelfang, Stratospheric mixing estimated from high-altitude turbulence measurements,*J. Appl. Meteorol., 13*, 488 - 493, 1974.

Lindner, B.C., The nature of D-region scattering of vertical incidence radio waves, I. Generalized statistical theory of diversity effects between spaced receiving antennas, *Aust.J.Phys., 28*, 163-170, 1975a.

Lindner, B.C., The nature of D-region scattering of vertical incidence radio waves, II., Experimental observation using spaced antenna reception, *Aust.J.Phys., 28*, 171-184, 1975b.

Manson, A.H., M.W.J. Merry, and R.A. Vincent, Relationship between the partial reflection of radio waves from the lower ionosphere and irregularities as measured by rocket probes, *Radio Sci., 4*, 955-958, 1969.

Mathews J.D., J.H. Shapiro and B.S. Tanenbaum, Evidence for distributed scattering in D-region partial-reflection processes, *J.Geophys. Res. 78*, 8266. 1973.

Mathews, J.D., J.K. Breakall, and M.P. Sulzer, The moon as a calibration target of convenience for VHF-UHF radar systems, *Radio Sci., 23*, 1-12, 1988.

May, P.T., S. Fukao, T. Tsuda, T. Sato and S. Kato, The effect of thin scattering layers on the determination of wind by Doppler radars, *Radio Sci., 23*, 83-94, 1988.

Ottersten, H., Radar backscattering from the turbulent clear atmosphere, *Radio Sci., 12*, 1251-1255, 1969.

Peltier, W.R., J.Halle, and T.L.Clark, The evolution of finite-amplitude Kelvin-Helmholtz Billows, *Geophys. Astrophys. Fluid Dyn., 10*, 53-87, 1978.

Pfister, W., The wave-like nature of inhomogeneities in the E-region, *J.Atmos.Terr.Phys., 33*, 999-1025, 1971.

Rastogi P.K. and O. Holt, On detecting reflections in presence of scattering from amplitude statistics with application to D-region partial reflections,*Radio Sci. 16*, 1431-1443, 1981.

Rastogi, P.K. and J. Roettger, VHF radar observations of coherent reflections in the vicinity of the tropopause,*J. Atmos. Terr. Phys., 44*, 461-469, 1982.

Ratcliffe, J.A., Some aspects of diffraction theory and their application in the ionosphere, *Rep. Prog. Phys., 19*, 188-267, 1956.

Rayleigh, Lord(J.W.Strutt),*Theory of Sound*, vol.1, pp.35-42. Macmillan, New York, 1894.

Reid, I.M., R. Ruester and G. Schmidt,*Nature*, 327, 43, 1987.

Reid, I.M., Radar observations of stratified layers in the mesosphere and lower thermosphere (50-100 km), *Adv. Space Res.*, 1989 (in press).

Rice,S.O., Mathematical analysis of random noise, *Bell Syst, Tech.J., 23*, 282-332, 1944.

Rice,S.O., Mathematical analysis of random noise, *Bell Syst. Tech.J.,24*, 46-156, 1945.

Roettger, J., Reflection and scattering of VHF radar signals from atmospheric refractivity structures, *Radio Sci., 15*, 259-276, 1980a.

Roettger, J., Structure and dynamics of the stratosphere and mesosphere revealed by VHF radar investigations, *Pure Appl. Geophys., 118*, 494-527, 1980b.

Roettger, J., Investigations of lower and middle atmosphere dynamics with spaced antenna drifts radars, *J.Atmos.Terr.Ph 43*, 277-292, 1981.

Roettger, J., and C.H.Liu, Partial reflection and scattering of VHF radar signals from the clear atmosphere, *Geophys. Res. Lett., 5*, 357-360, 1978.

Roettger, J. and G. Schmidt, High-resolution VHF radar soundings of the troposphere and stratosphere, *IEEE Trans. Geosci. Electron., GE-17*, 182-189, 1979

Roettger, J. and H.M. Ierkic, Postset beam steering and interferometer applications of VHF radars to study winds, waves and turbulence in the lower and middle atmosphere, *Radio Sci., 20*, 1461-1480,1985.

Sato,T., and R.F.Woodman, Fine altitude resolution observations of stratospheric turbulent layers by the Arecibo 430 MHz radar, *J.Atmos. Sci., 39*, 2553-21564, 1982.

Sheen D.R., C.H. Liu and J. Roettger, A study of signal statistics of VHF radar echoes from clear air,*J. Atmos. Terr. Phys., 47*, 675-684, 1985.

Sloss,P.W.,and D.Atlas, Wind shear and reflectivity gradient effects on Doppler radar spectra, *J.Atmos.Sci., 25*, 1080-1089, 1968.

Tatarski, V.I.,*Wave propagation in a turbulent medium*, McGraw-Hill, New York, 1961.

Tatarski, V.I., *The effects of the turbulent atmosphere on wave propagation*, Keter Press, Jerusalem, 1971.

Thrane, E. V., and B. Grandal, Observations of finescale structure in the mesosphere and lower thermosphere, *J. Atmos. Terr. Phys., 43*, 179-189, 1981.

VanZandt,T.E., J.L.Green, K.S.Gage, and W.L.Clark, Vertical profiles of refractivity turbulence structure constant: Comparison of observations by the Sunset radar with a new theoretical model,*Radio Sci., 13*, 819-829, 1978.

VanZandt,T.E., K.S.Gage and J.M.Warnock, An improved model for the calculation of profiles of and in the free atmosphere from background profiles of wind, Temperature and humidity, paper presented at *20th Conference on Radar Meteorology, Am.Met.Soc.*, Boston, Mass., Nov.30-Dec.3,1981.

Van Zandt, T.E., and R.A. Vincent, Is VHF Fresnel reflectivity due to low frequency buoyancy waves?, *Handbook for MAP, vol. 9*, p 78-80, Univ. of Illinois, Urbana, 1983.

Vincent, R.A., The interpretation of some observations of radio waves scattered from the lower ionosphere, *Aust.J.Phys., 26*, 815-827, 1973.

Vincent, R.A. and J.S. Belrose, The angular distribution of radio waves partially reflected from the lower ionosphere,*J. Atmos. Terr. Phys., 40*, 35-47, 1978

Vincent, R.A., and I.M. Reid, HF Doppler measurements of mesospheric gravity wave momentum fluxes, *J. Atmos. Sci., 40*, 1321-1333, 1983.

Vincent, R.A., B. Candy and B.H. Briggs, Measurements of antenna polar diagrams and efficiencies using a phase-switched interferometer, *Handbook for MAP, vol. 20*, p409-409, Univ. of Illinois, Urbana, 1986

Von Biel, H.A., Amplitude distributions of D-region partial reflections, *J. Geophys. Res, 76*, 8365-8367, 1971.

Von Biel, H.A., A statistical assessment of synoptic D-region partial reflection data,*J. Atmos. Terr. Phys., 43*, 225-230, 1981

Waterman, A.T., Techniques for measurement of vertical and horizontal velocities; monstatic vs. bistatic measurements, *Handbook for MAP, vol 9*, 164-169, Univ. of Urbana, 1983.

Waterman, A.T., T.Z. Hu, P. Czechowsky and J. Roettger, Measurement of anisotropic permittivity structure of upper troposphere with clear-air radar, *Radio Sci., 20*, 1580-1592, 1985

Weinstock, J., On the theory of turbulence in the buoyancy subrange of stably stratified flows, *J.Atmos.Sci., 35*, 634-649, 1978a.

Weinstock,J., Vertical turbulent diffusion in a stably stratified fluid, *J.Atmos.Sci., 35*, 1022-1027, 1978b.

Weinstock,J., Using radar to estimate dissipation rates in thin layers of turbulence, *Radio Sci., 16*, 1401-1406, 1981.

Woodman, R.F.and A.Guillen, Radar observations of winds and turbulence in the stratosphere and mesosphere, *J.Atmos. Sci., 31*, 493-505, 1974

Woodman, R.F. and P.K.Rastogi, Evaluation of effective eddy diffusive coefficients using radar observations of turbulence in the , stratosphere, *Geophys. Res. Letts., 11*, 243-246, 1984.

Woodman,R.F., Spectral moment estimation in MST radars, *Radio Sci., 20*, 1185-1195, 1985.

Woodman, R.F. and Y-H Chu, Aspect sensitivity measurements of VHF backscatter made with the Chung-Li radar: plausible mechanisms, *Radio Sci.*, 1989 (accepted)

Yamamoto, M., T. Tsuda, S. Kato, T. Sato, and S. Fukao, A saturated inertia gravity wave in the mesosphere observed by the middle and upper atmosphere radar, *J. Geophys. Res., 92*, 11993-11999, 1987.

Yamamoto, M., T. Tsuda, S. Kato, T. Sato, and S. Fukao, Interpretation of the structure of mesospheric turbulence layers in terms of inertia gravity waves, *Physica Scripta, 37*, 645-650, 1988.

Zrnic,D.S., Estimation of spectral moments for weather echoes, *IEEE Trans. Geosci. Electron., GE-17*, 113-128, 1979.

The following
article gives an overview
of the more important
contributions which radar has
made to understanding
atmospheric turbulence

RADAR CONTRIBUTIONS TO UNDERSTANDING THE STRUCTURE OF ATMOSPHERIC TURBULENCE – A BRIEF HISTORY.

W.K. Hocking[1] and J. Röttger[2]

1. Dept. of Physics and Astronomy, University of Western Ontario, London, Ont. Canada, N6A 3K7.
2. Max Planck Institut für Aeronomie, D-37191 Katlenburg-Lindau, Germany.

1. Introduction.

Radars depend on scatter or reflection from perturbations in radio refractive index in order for them to be able to function as tools for atmospheric studies. One primary cause of such fluctuations is atmospheric turbulence, both in the neutral atmosphere and in ionized parts of the air. Because the processes which produce this radar scatter are often turbulence-related, it must also be true that, over many years of studies, radars should have contributed substantially to our understanding of atmospheric turbulence. Our intent here is to review the various contributions which radars have made to this understanding. We will discuss here only turbulence in the neutral atmosphere. Scatter from plasma turbulence and plasma waves in the ionosphere will not be treated; we refer to Sahr and Fejer (1996) for a corresponding review of ionospheric turbulence.

Radars have been especially good for looking at the larger-scale nature of atmospheric turbulence, and these results will be described here. However, despite the strong dependence of radar backscatter on turbulence, it has in fact been rather difficult to deduce certain other types of information about turbulence from these radar studies. This is especially true with respect to studies at very small scales, particularly at sizes less then the pulse length used by the radars. Therefore, many of the most useful studies have incorporated a mixture of special radar observations, in-situ studies, and careful deduction.

In this short discussion, we will highlight some of the main advances in radar-related understanding of atmospheric turbulence, and incorporate in-situ studies and modeling where they are required to support the radar studies. We will concentrate on the period up to the mid-1990's, before the advent of large three-dimensional computer simulations (e.g. Fritts et al., 1994; Werne and Fritts, 1999). Those 3-D modeling studies essentially heralded a new (but not unprecedented) emphasis on three-dimensional modeling efforts in studies of atmospheric turbulence, but we will not consider them in this review. Rather, our objective here is to summarize what was known up until the beginning of these particular modeling developments, since these earlier developments have not been adequately represented (and indeed have even been largely ignored) in the more recent literature. Yet these earlier studies still have much to offer in helping us to understand atmospheric turbulence, and it is important that the concepts developed in these earlier works be properly recognized. It is also foreseen that new developments and continuous refinements of these valuable radar concepts will significantly contribute to further understanding of atmospheric turbulence in the future.

When we talk here about scales of turbulence, we need to recognize that radar backscatter results from scales in the turbulence spectrum (which in turn determines the radio refractive index variation spectrum), which are equal to one half of the radar wave length (the so-called Bragg scale). The backscattered power is the ensemble average over the total illuminated volume, often (but not always) consisting of a multitude of such so-called "scatterers". Such scatterers can be quite arbitrarily and inhomogeneously distributed in the volume. The

volume and the distribution of the scatterers is usually much larger than the Bragg scale. The radars can never really resolve turbulence structures at the Bragg scale itself, but they can resolve larger scales which are still much smaller than the volume filled by the turbulence. The actual resolution is often defined by the radar pulse length, but on occasions, with suitable special techniques, it is possible to do better. These special techniques are summarized in this article, together with the description of the radar-observed turbulence structures and their morphology.

2. Large-scale studies (> 100m).

Perhaps the most obvious feature that is clear from radar studies is the very horizontally striated nature of turbulence in the neutral atmosphere, at least at scales of more than a few hundred meters. Fig. 1(a) shows some radar observations of the mesosphere carried out by Czechowsky et al., (1979), for both summer and winter conditions, and the stratified nature of the scatter is quite evident. This is very common. For comparison, fig. 1(b) (from Bondarev et al., 1992) shows some in-situ smoke trails released by 4 rockets simultaneously into the atmosphere (in this case the results refer to the stratosphere). The layering in the wind-field is quite evident, with adjacent trails being very similar in shape. Fig. 1(c) shows more radar observations of thin layers, also called sheets or laminae, in this case for the troposphere and lower stratosphere (from Hocking and Röttger, 1983). It is clear that layered and stratified phenomena are common in the atmosphere. Similar results have been observed using rocket releases in the mesosphere (e.g. Blamont and Barat, 1967).

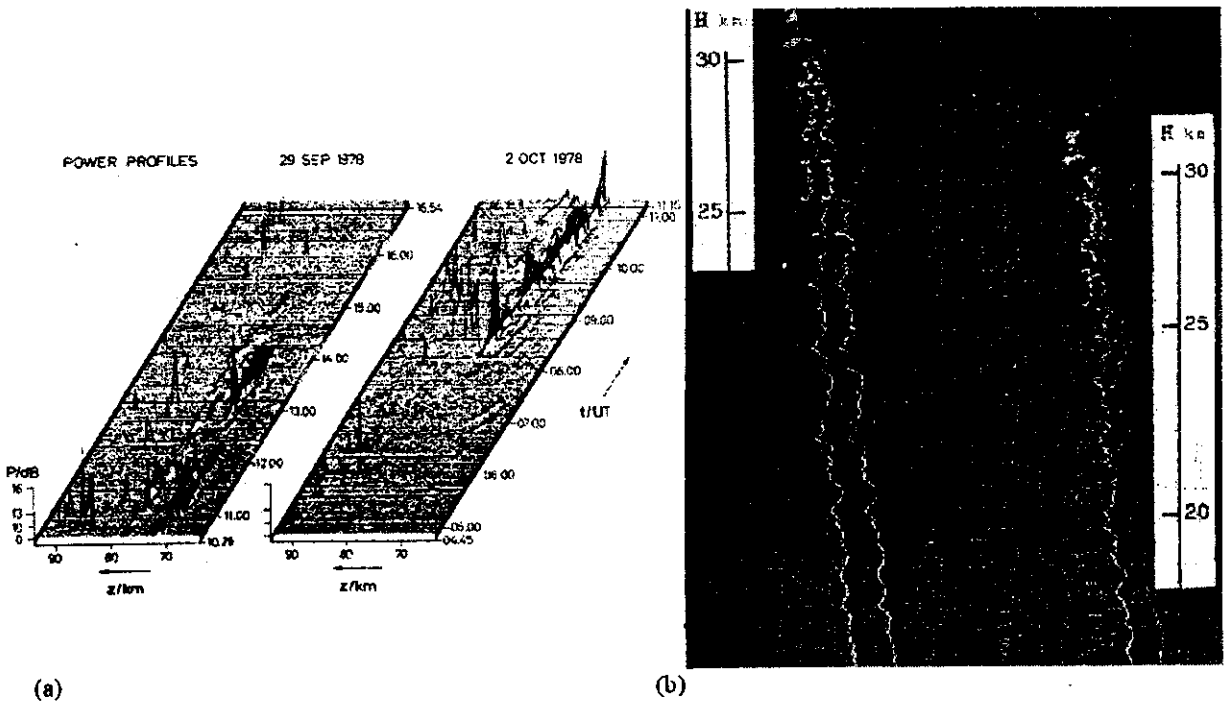

(a) (b)

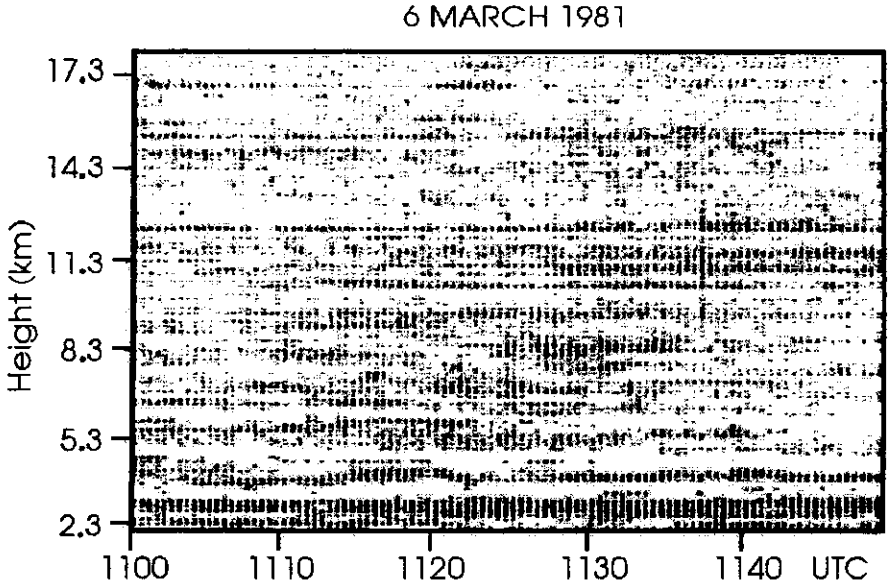

(c)

Fig. 1. (a) Illustration of stratification of radar echoes at VHF in the mesosphere (from Czechowsky et al., 1979). (b) Evidence of horizontal stratification of atmospheric winds using in-situ techniques (smoke trails). (c) Stratification of persistent thin sheets in the troposphere and lower stratosphere (from Hocking and Röttger, 1983).

Radars have played an important role in demonstrating the prevalence of atmospheric stratification. When combined with suitable modeling studies, it is even possible to make some estimate of the expected degree of stratification and structure in the atmosphere. Fig. 1b shows not only a high level of stratification, but also evidence for wave-like structures in the wind field. These are associated with a spectrum of gravity waves (e.g. VanZandt, 1982; Hines 1991a,b). The interactions between these waves, and with the background wind-field, are often responsible for the generation of turbulence in the mesosphere and stratosphere. (Indeed, radar studies of wind fluctuations played a very important role in establishing the importance of gravity waves in the atmosphere, but that topic is not within the scope of this article). If it is assumed that these waves satisfy a so-called "universal spectrum", and that there are many waves propagating up and down with various (random) phases, then the velocity and temperature fields associated with these waves will add in such a way that, on occasion, they will produce a regime in which turbulence will naturally develop (Richardson number less than 0.25). It is possible to produce a statistical investigation of the likelihood of such levels developing, and thereby obtain a statistical summary of the likely depths of these layers, their frequency of occurrence, and their likely vertical spacing. Fig. 2 shows an example of such statistics (from Hocking, 1991, after adaptation from Desaubies and Smith, 1982). Similar calculations have been performed by Fairall et al., (1991) for the troposphere, and by Hines (1991a,b,c) for the mesosphere.

Radars have not only been useful in helping us understand the distribution of turbulence, but have also been useful in helping to describe and parameterize the processes of diffusion in the atmosphere. They have been used regularly, for example, to determine the energy dissipation rates associated with turbulence (e.g. for reviews of these methods see Hocking and Mu, 1997; Hocking, 1999). We will not consider this application in any detail here, since the focus of the paper is related to the structure of turbulence.

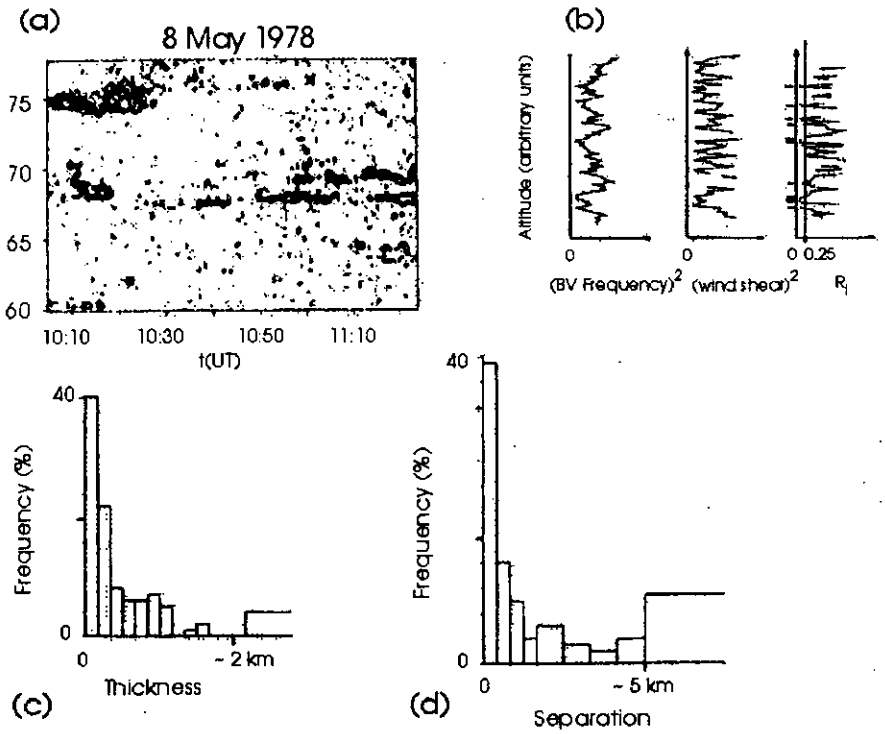

Fig. 2. (a) Another example of stratified radar echoes. (b) Typical profiles of Brunt-Vaisala frequency, wind shears, and resultant Richardson numbers, for a sample gravity wave field. (c) Distribution of the thicknesses of layers of turbulence expected in the stratosphere. Scales are only representative, and somewhat larger in the mesosphere than in the stratosphere. (d) Expected layer spacings. This graph has been adapted from Hocking, (1991).

Radars can also be used to study the rates of turbulent diffusion in the atmosphere, and again we will not consider this in too much detail. However, there is one aspect related to the issue of diffusion that we do wish to discuss, and this is the mechanism of diffusion itself, since it relates closely to the issue of the spatial and temporal morphology of turbulence in the atmosphere.

Particulates and chemicals may diffuse across a patch of turbulence in the classically accepted manner, being driven along a "random walk" by the velocity field embodied in the turbulence. However, this only permits counter-gradient diffusion across the layer itself. What about diffusion over vertical scales much deeper than a typical layer thickness – how can diffusion occur over such large scales? To understand this process, we must return to fig. 2. Layers of the type shown in fig. 2a form at various intervals of time, and have various lifetimes. Diffusion can occur across such a layer, but once a particle diffuses to the edges, it can go no further. It then waits until, purely by chance, another layer forms on top of the particle, but displaced vertically relative to the previous nearby layer. Diffusion may then occur across this new layer, until the particle reaches an upper or lower edge (depending on the direction of diffusion) or until the layer dissipates. Thus the rate of vertical diffusion over scales deeper than the typical layer depths depends on factors including the depth of the layers, and the frequency of occurrence of the layers, (as well as the strength of turbulence within the layers). More details about this process can be found in Dewan (1981), Woodman and Rastogi (1984), and Hocking (1991, 1999) (among others). This understanding of turbulent diffusion has been developed in part due to the contributions of radar observations,

and radar observations offer one of the best tools to implement calculations of diffusion in this manner, as described by Woodman and Rastogi (1984).

3. Intermediate-scale studies (10m – 100m).

While radars have made important contributions to our understanding of the large-scale structure of turbulence, they have also made contributions at smaller scales. Interestingly, this has been a difficult challenge, since it often involves examination of scales which are less than the radar pulse length. Various specialized techniques must be employed in order for these scales to be observed with high resolution, including techniques like frequency-domain interferometry (FDI), which is a simplified FM/CW radar technique, as well as more sophisticated deconvolution procedures (e.g. Palmer et al., 2000).

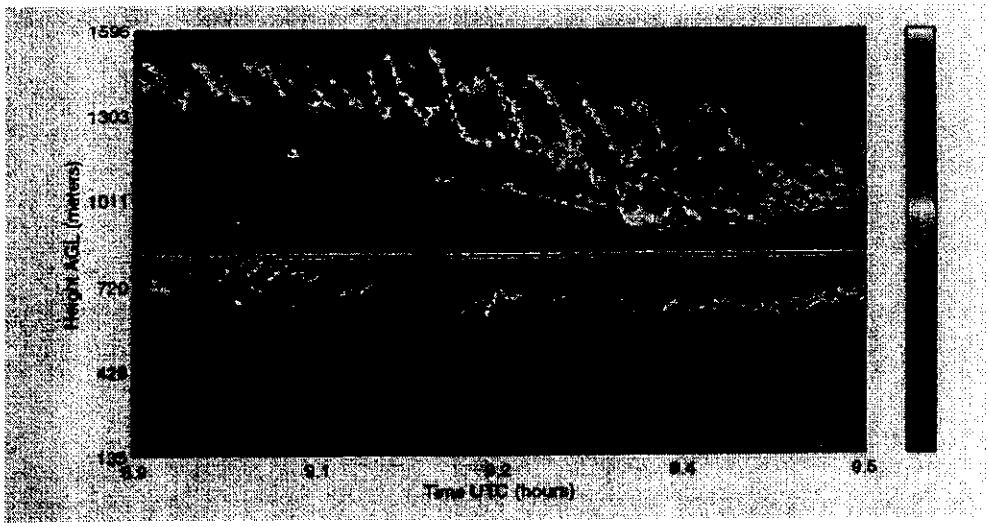

Fig. 3. FMCW radar images of low level turbulence, in this case showing Kelvin-Helmholtz billows (from Eaton et al., 1995)

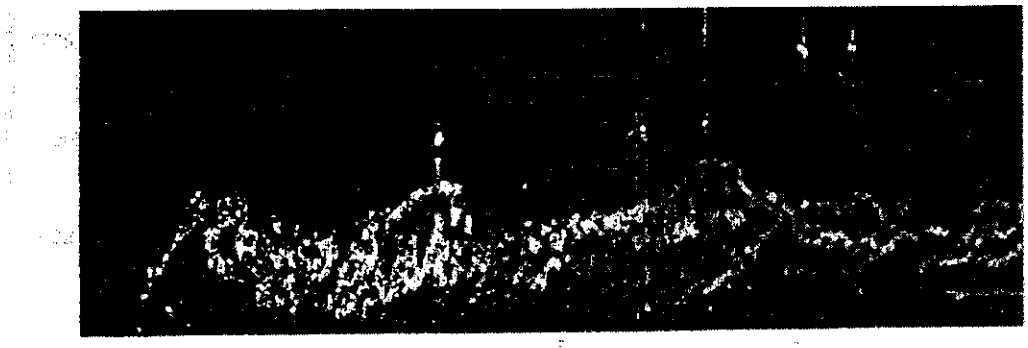

Fig. 4. Another FMCW radar image of low level turbulence, in this case showing frontal turbulence with no sign of K-H billows (again adapted from Eaton et al., 1995). The entire picture covers a period of one hour in duration, and covers the height range from 40 meters altitude to 1.8 km altitude.

It is possible to look at meter-size scales if a radar has sufficiently high frequency, with a correspondingly short wavelength. At these higher frequencies, large bandwidths are possible, thereby allowing very good range resolution. For example, powerful FM-CW radar

have been used to obtain high resolution studies of turbulent events in the atmospheric boundary layer (e.g. Gossard et al., 1970, 1978; Eaton et al., 1995). Figs. 3 and 4 show examples of such observations, taken from Eaton et al., (1995).

These pictures are very informative, and show excellent resolution. However, such images are generally only possible in the lowest few kilometers of altitude of the atmosphere, since the radars used for these studies receive very little backscatter from higher altitudes. They demonstrate that "cat's-eye" structures are not uncommon in the atmosphere as a precursor to turbulence breakdown (fig. 3), and such structures are often associated with Kelvin-Helmholtz (K-H) billows. However, K-H need not be the only mechanism responsible for the formation of cats-eye billows; Smyth and Peltier (1989) have indicated that other mechanisms, such as the Holmboe instability, can also generate such structures. Indeed, K-H instabilites are only dominant in weakly stratified flows, whereas the Holmboe instability is more likely in strongly stratified flows. Furthermore, there can be occasions when other mechanisms of breakdown can be responsible for the turbulence, as seen in fig. 4 (cat's-eye structures are visually impressive, so they tend to dominate the literature – but it is not clear whether they are in fact the main mode of turbulence break-down at all!). Thus while high-resolution studies of the type shown in figs. 3 and 4 are very useful, it is still not clear how relevant these boundary layer studies are to understanding turbulence generation in the stratosphere and mesosphere. Cho et al., (1996) have made higher level, high resolution studies using astronomical antennas, and Woodman (1980) has used the Arecibo 2380 MHz radio telescope to perform high resolution studies of stratospheric layers. Such studies are rare. Nevertheless, we recognize that radars are at least able to make some useful studies of turbulence at high resolution, and have already been very useful in this regard. More such studies are sorely needed.

For many studies of atmospheric dynamics, radars with frequencies in the range 2 to 900 MHz are common. These radars cannot achieve the resolution of FM/CW radars operating in the Gigahertz frequency range (discussed above), but they can achieve a better height coverage. VHF radars can detect signals as high as 90 km altitude in the middle atmosphere. These radars are often pulsed, with pulse-lengths in the range 150 m to 2 km. Normally these radars cannot resolve structure at scales less than the pulse length. However, there are certain procedures which can be used to improve the resolution under certain circumstances. One example is shown in fig. 5, which demonstrates the application of deconvolution procedures (Röttger and Schmidt, 1979).

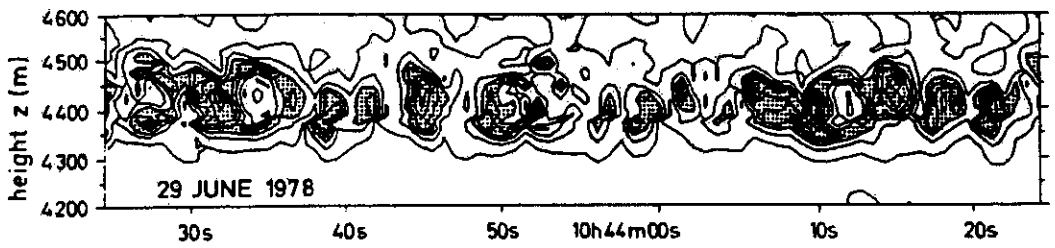

Fig. 5. Results of the application of deconvolution procedures to achieve sub-pulse-length resolution with a VHF radar. Cats-eye structures are evident.

Reid et al., (1987) have shown high-resolution studies of cat's-eye like structures in the mesosphere using a VHF radar. Other procedures also exist to achieve better spatial resolution, such as FDI (e.g. Kudeki and Stitt, 1987; Chilson and Schmidt, 1996, among

others), SDI (Spatial Domain Interferometry e.g. Pan and Röttger (1996) (also see Hocking, 1997)) and newly developed signal processing methods (e.g. Luce et al., 2000; Palmer et al., 2000 (see this issue)). However, it should also be noted that the advantages of improved vertical resolution can be negated if there is not a corresponding improvement in horizontal resolution, and the ideal procedure would be to apply both FDI and SDI simultaneously to produce improvements in both vertical and horizontal resolution (see Röttger et al., 2000, this issue).

4. Small-scale studies (<10m).

At scales of meters and less, radars provide even less direct information than at intermediate scales. Again, however, suitable combinations of observations and theory, together with special radar experiments, still permit useful information to be gleaned even at scales of the order of 1 meter. While the FMCW radars that we spoke of earlier are capable of resolution down to a meter, they are most useful at revealing the dynamics of the turblence at scales of several meters and more. However, it is desirable to use radars to look at scales which are even smaller than this. For example, fig. 6 shows streak-photographs of small scale motions taken in a laboratory setting (in this case for two-dimensional turbulence, so it may not be entirely representative of small-scale atmsopheric turbulence). Eddy motions are clear in both figures, and some ellipticity is evident in some eddies. However, it is important to know just how representative these pictures are of atmospheric processes. Can radars reveal anthing about the motions at these smallest scales? In fact they can, at least indirectly, and one area in which radars have made very important contributions is in the area of studies of anisotropy.

To demonstrate the issue at hand here, we show fig. 7. This figure, (adapted from Pao, 1968), shows flow around an object in salt-stratified water, at points close to the object as well as futher downstream, and the issue to be emphasized here is the way in which the turbulence tends to "striate" and stratify as it dies out. The initial, active turbulence is clearly isotropic at the smaller scales, while the weaker, decaying turbulence is more anisotropic. We therefore ask the question: to what level do we expect atmospheric turbulence to be isotropic? Do the "eddies" shown in fig. 6 form, and if so, do they exhibit any form of anisotropy i.e. do they tend to be elongated horizontally relative to their vertical extent? This is an area where radar studies have made substantial contributions.

To understand the contributions of radars in this field, it is necessary to show how "eddy anisotropy" is parameterized. This is illustrated in fig. 8a. As seen in fig. 6, velocity trajectories are often elliptical in shape, but individual refractive index "entities" (radar scatterers) are not always so organized. Even an initially "organized" shape is quickly torn in various directions by the underlying velocity field, so that individual refractive index "entities" within a turbulent region often have stretched and distorted string-like shapes – just as one can see different "shapes" and structures within an ordinary water vapor cloud. Hocking and Hamza (1997) have discussed this process in some detail. However, despite the fact that individual entities may be distorted in shape, the spatial correlation function of the refractive index fluctuations does have a broadly elliptical shape with a smoothly varying cross-section, where the cross-sectional profile is often assumed to be Gaussian. In determining the general properties of radar back-scatter, it is often this correlation function which is most important (e.g. see Doviak and Zrnic, 1984). Thus we often represent atmospheric radio-wave sacatterers as if they were ellipsoids, since the spatial correlation function of a field of ellipsoidal scatters with Gaussian cross-section is also an ellipsoidal function with Gaussian cross-section. We can therefore can represent the refractive index

12 fluctuations in a turbulent field as if it were comprised of such structures, as shown in fig. 8a (also see de Wolfe, 1983).

When we recognize that such anisotropy exists, then it also becomes clear that a monostatic radar will produce back-scattered power that varies as a function of the beam bore direction.

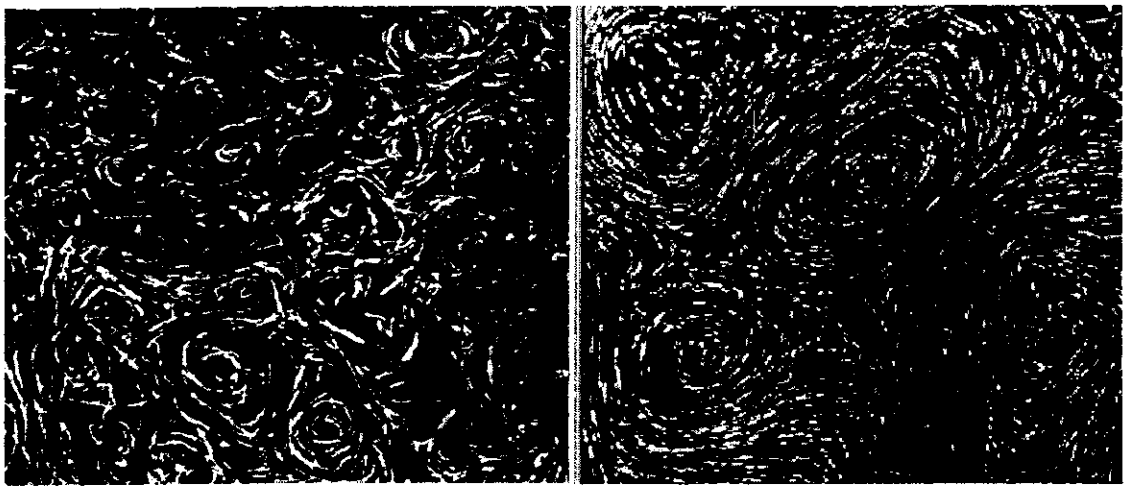

Fig. 6. Streak photography images of small scale turbulence (in this case the graphs are for two-dimensional turbulence). The graphs refer to different conditons of stability. From Hopfinger (1987), who adapted it from Maxworthy et al., (1985).

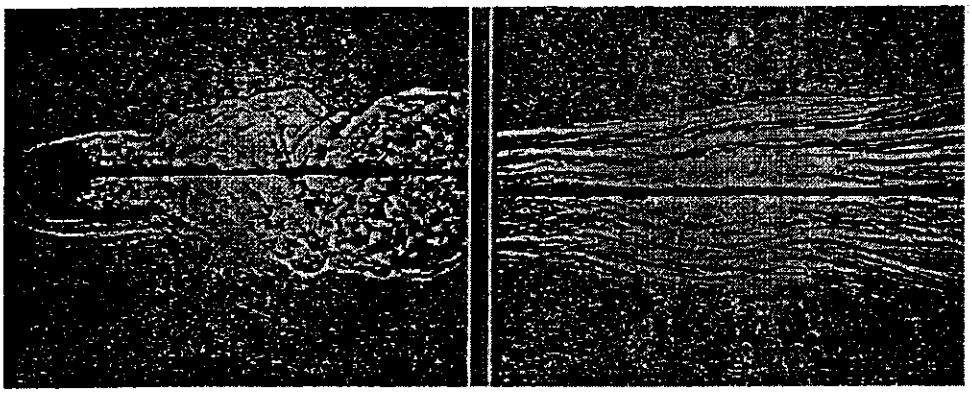

Fig. 7. Photographic images of turbuence generated by flow around an object (Pao, 1968). The left hand panel refers to the flow close to the object, and is clearly fairly isotropic at the smaller scales. The right panel shows the flow further downstream, as the turbulence dies out, and stratification is clearly evident.

When the radar beam is pointed vertically, backscattered power will be a maximum, whilst backscattered power will diminish as the beam is pointed further and further off-vertical. This is a very common feature of radars operating at wavelengths of larger than a few meters with antenna beams pointing to, or close to, the vertical. Such aspect sensitivity has so far not been detected with radars operating at wavelengths of less than about one meter. For scatterers of the type described, the power falls off proportionally to $\exp\{-\sin^2\theta / \sin^2\theta_s\}$, where θ is the angle of tilt of the antenna beam from vertical and θ_s is referred to as the "aspect-sensitivity" parameter. Smaller values of θ_s refer to more anisotropic scatterers, when the ratio L/h (fig 8a) is largest. By measuring the power received as a function of angle,

it is possible to determine this parameter. Other methods may also be used which involve comparison of signal characteristics recorded with radar beams pointed at different zenithal angles. An example of such measurements is shown in fig. 8b, in this case for a 2-MHz radar. More extensive discussions of the conversions between L/h and θ_s can be found in Hocking (1987a), Lesicar et al., (1994) and Hocking and Hamza (1997), among others.

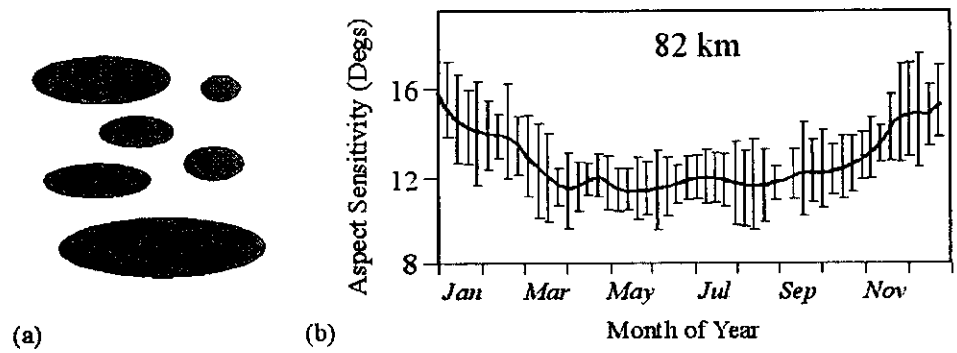

Fig. 8. (a) Illustration of the representation of atmospheric scatterers within a patch of turbulence. (b) Aspect sensitivity parameter θ_s as a function of month of the year for a 2MHz radar detecting scatter from 82 km altitude in the mesosphere (from Lesicar and Hocking, 1992).

A word of warning must be noted here, however. Not all atmospheric radio scatterers take the form of turbulent entities. There are also other, highly structured so-called "specular reflectors" in the atmosphere, which produce "mirror-like" reflections. In calculating θ_s, it is necessary to be certain that such specular reflectors do not co-exist near the turbulence, thereby contributing a non-turbulent component to the radar signal. It is still uncertain what the cause of these thin sheets or laminae is, although various suggestions have been made (e.g. Hocking et al., 1991). Röttger (1980b) and others have suggested that it would be useful to compare such radar observations with observations of similar structures in the ocean. For improved understanding of these atmospheric structures high-resolution radar observations combined with high-resolution in-situ measurements are required (e.g., Luce et al., 1995). We will not discuss these specular reflectors in this article, but they have been considered as early as almost fourty years ago (Atlas, 1964; Beckmann and Spizzichino, 1963). Their existence and the fact that the reflection is from a rough or corrugated surface must be recognized. Further discussions about them can be found in Gage (1990), Röttger and Larsen (1990), Hocking et al., (1991) and Hocking (1996) (among many others). How these corrugated sheets and laminae are generated and how they are related to turbulence remains a challenging question to be solved.

It has also been found that these scatterers have an azimuthal asymmetry, and this is also an area of some interest. For example, Hocking (1987b) showed an azimuthal variation of the so-called "Rice parameter" which may indicate preferential stretching of the scatterers according to the wind direction, and Tsuda et al. (1997) also found anisotropy in the backscattered power as a function of azimuth. Nevertheless, considerable extra work is required in this area, but the point remains that radars have a lot to offer in this regard.

Thus, with due care, radars can be used to measure the degree of anisotropy in a turbulent regime. This is an important parameter which cannot be otherwise easily accessed. It also

needs to be recognized that the aspect-sensitivity parameter is generally scale-dependent, as described by Hocking and Hamza (1997). Multiple frequency radar studies can help examine this scale dependence.

There is yet another feature which needs to be recognized in regard to the turbulence anisotropy, and this is the fact that the degree of anisotropy has long been recognized to be a function of position within the turbulent layer. Several authors have recognized this (e.g. Peltier et al., 1978; Röttger et al., 1981; Hocking, 1985; Woodman and Chu, 1989; Hocking, 1991). Fig. 9 shows one such illustration of the expected variation of anisotropy across the layer, with more anisotropic scatterers towards the edges. Other authors have presented similar diagrams (e.g. Röttger, 1981; Lesicar and Hocking, 1992; Lesicar et al., 1994). Some of these deliberations have their origin in initial proposals by Bolgiano (1968) about the structure of the atmospheric turbulence (and especially with regard to the edges of the layers). We note that the recent modelling work using super computers (Werne and Fritts, 1999; Gibson-Wilde et al., 2000) just confirm the principles, which had been developed and have emerged from radar observations over the past decades.

Fig 10 shows the expected structure across a turbulent layer in even greater detail. This graph, adapted from Hocking (1991), combines data from modeling studies (Klaasen and Peltier, 1985a,b), in-situ observations (Dalaudier and Sidi, 1987), and knowledge about aspect sensitivity deduced from radar observations.The right-hand profile (solid line) shows the expected mean temperature profile across a typical turbulent layer, as determined by modeling studies (Klaasen and Peltier, 1985a,b). Note in particular the relatively sharp edges of the layer, and the near-adiabatic conditions in the middle of the layer. The consequences of this structure are to produce more anisotropic scatterers at the edges, where the background temperature is horizontally stratified but highly fluctuating in the vertical direction (therefore containing large gradients), and more isotropic scatterers towards the center, where the temperature profile is closer to adiabatic. This is illustrated by the central part of the figure, which shows anisotropic scatters at the edges and more isotropic ones towards the center. The graph on the left shows the wind fluctuations and temperature fluctuations measured by a balloon passing through such a turbulent layer. Note that the wind fluctuations are similar throughout the layer, but the temperature fluctuations are much larger at the edges, and smaller in the adiabatic portion. This is to be expected, because as parcels of air are displaced vertically by the turbulence, they change temperature in an adiabatic manner, and thus do not change much at all from the temperature of the background when the background profile is adiabatic. Hence perturbations are minimized in this case.

The fact that the temperature fluctuations are small near the center of the layer has important implications for radar scatter as well. The refractive index depends on upon the temperature, humidity and electron density. If the mean temperature gradient is adiabatic, and the temperature fluctuations are therefore small or zero, and if the atmosphere is dry and electron-free (as in the upper troposphere and startosphere), then there will be no associated refractive index fluctuations and the turbulent layer will be "invisible" to the radar. If a layer exists like the one in fig. 10, then only the edges of the layer will actually be seen by a radar, giving rise to an apparent "dual layer". Thus one needs to take care with the interpretation that the strongest scattering layers are layers of strongest turbulence – indeed sometimes the more intense layers can be least easily seen with radar. This fact was recently also raised by Gibson-Wilde et al., (2000), using computer simulations, although unfortunately these authors did not draw a parallel between their observations and the extensive references and types of discussions considered above.

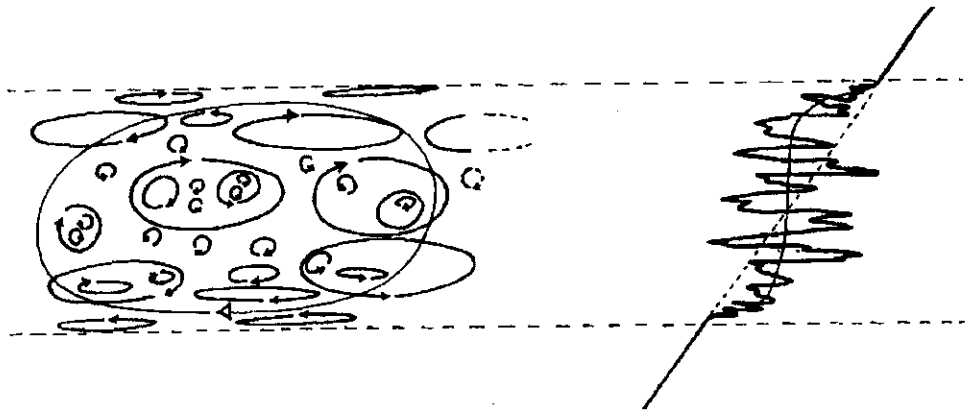

Fig. 9. Illustration from Woodman and Chu (1989) showing a proposal for the structure of radio-wave scatterers with in a turbulent layer. More anisotropic scatterers are expected near the top and bottom of the layer.

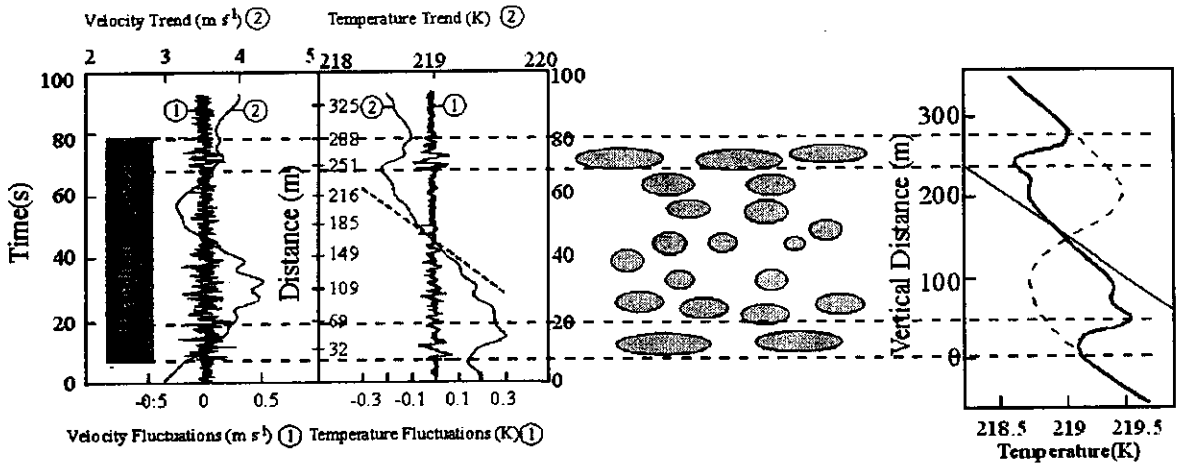

Fig. 10. Expected behaviour of velocity, temperature, and refractive index inhomogeneities within a turbulent layer. In the left hand two graphs, the smoother lines represent the mean wind and temperature profiles (labelled (2)), while the more rapidly varying lines passing up through the center (labelled (1)) represents fluctuations of the appropriate parameter about the mean. In the right hand graph, the broken line represents an intitial temperature profile and the solid one represents the profile after the turbulence is established (from modeling studies). Note that the vertical scalings are slightly different in the left and right-hand profiles, because each comes from a different source. We have adjusted the scalings so that the temperature profiles look similar. See text for other details.

5. Conclusions.

By utilizing radar data, in-situ data, and early modeling studies, it has been possible to deduce significant information about the large and medium scale structure, and the internal structure, of turbulent layers in the atmosphere. Radars are especially useful for displaying the large-scale morphology of turbulence, and by using sophisticated processing techniques they can also be useful in describing the medium and small scale structures. They are especially powerful for studying the anisotropy and morphology at different scales of turbulent atmospheric regions. This paper has concentrated especially on the role which

radars have made to these determinations and how they can contribute further. Combination with in-situ and modeling techniques will certainly supplement these investigations.

REFERENCES

Atlas, D., Advances in Radar Meteorology, *in Adv. Geophys.,10,* eds. Landsberg and Miegham,Academic Press, 317-478, 1964.

Beckman, P., and A. Spizzichino, The scattering of electromagnetic waves from rough surfaces, *Pergamon Press*, Oxford, pp.503, 1963.

Blamont, J. E., and J. Barat, Dynamical structure of the atmosphere between 80 and 120 km, from "*Aurora and Airglow*", ed. B. M. McCormmac, p 159, Reinhold Publ. Co., 1967.

Bolgiano, R., The general theory of turbulence. Turbulence in the atmosphere, in *Wind and Turbulence in Stratosphere, Mesosphere and Ionosphere,* ed. K. Rawer, North Holland Publ., Amsterdam, 371-400, 1968.

Bondarev, V. D., V. N. Lebedinets, V. P. Prorok and A. M. Sarkisyan, Investigation of a fine layered wind field structure in the atratosphere by the artificial luminous cloud method, *Adv. Space Res., 12(10)*, 161-163, 1992.

Chilson, P.B. and G. Schmidt, Implementation of frequency domain interferometry at the SOUSY VHF radar: first results, *Radio Sci., 31*, 263-272, 1996.

Cho, J. Y. N., R. F. Jurgens and M. A. Slade, High-resolution stratospheric dynamics measurements with the NASA/JPL Goldstone solar system radar, *Geophys. Res. Letts., 23*, 1909-1912, 1996.

Czechowsky, P., R. Ruester, and G. Schmidt, Variations of mesospheric structure in different seasons, *Geophys. Res. Letts., 6*, 459-462, 1979.

Dalaudier F., and C. Sidi, Evidence and interpretation of a spectral gap in the turbulent atmospheric temperature spectra, *J. Atmos. Sci., 44*, 3121-3126, 1987.

de Wolfe, D. A., A random-motion model of fluctuations in a nearly transparent medium, *Radio Sci., 18*, 138-142, 1983.

Desaubies, Y., and W. K. Smith, Statistics of Richardson number and instability in oceanic internal waves, *J. Phys. Oceanography, 12*, 1245-1259, 1982.

Dewan, E.M., Turbulent vertical transport due to thin intermittent mixing layers in the stratosphere and other stable fluids, *Science, 211*, 1041-1042, 1981.

Doviak, R. J., and D. S. Zrnic, Reflection and scatter formula for anisotropically turbulent air, Radio Sci., 19, 325-336, 1984.

Eaton, F. D., S.A. McLaughlin and J. R. Hines, A new frequency-modulated continuous wave radar for studying planetary boundary layer morphology, *Radio Sci., 30*, 75-88, 1995.

Fairall, C.W., A. B. White, and D.W. Thomson, A stochastic model of gravity-wave-induced clear-air turbulence, *J. Atmos. Sci., 48*, 1771-1790, 1991.

Fritts, D. C., J. R. Isler and O. Andreassen, Gravity wave breaking in two and three dimensions, 2, Three dimensional evolution and instability structure, *J. Geophys. Res., 99*, 8109-8123, 1994.

Gage, K. S., , Radar observations of the free atmosphere: Structure and dynamics, in *Radar in Meteorology; Battan Memorial and 40th Anniversary Radar Meteorology Conference*, edited by D. Atlas, *pp 534-565*, Amer. Meteorol. Soc., Boston, Mass., 1990.

Gibson-Wilde, D., J. Werne, D. Fritts and R. Hill, Direct numerical simulation of VHF radar measurements of turbulence in the mesosphere, *Radio Sci., 35*, 783-798, 2000.

Gossard, E. E., J. H. Richter, and D. Atlas, Internal waves in the atmosphere from high-resolution radar measurements, *J. Geophys. Res., 75*, 3523-3536, 1970.

Gossard, E. E., R. B. Chadwick, K. P. Moran, R. G. Strauch, G. E. Morrison, and W.C. Campbell, Observation of winds in the clear air using an FM-CW Doppler radar, *Radio Sci., 13*, 285-289, 1978.

Hines, C.O., The saturation of gravity waves in the middle atmosphere. Part I: Critique of linear instability theory", *J. Atmos. Sci., 48*, 1348-1359, 1991a.

Hines, C.O., The saturation of gravity waves in the middle atmosphere. Part II: Development of Doppler-spread theory, *J. Atmos. Sci., 48*, 1360-1379, 1991b.

Hines, C.O., The Saturation of gravity waves in the middle atmosphere. Part III: Formation of the Turbopause and of turbulent layers beneath it, *J. Atmos. Sci., 48*, 1380-1385, 1991c.

Hocking, W.K., Measurement of turbulent energy dissipation rates in the middle atmosphere by radar techniques: a review, *Radio Sci., 20*, 1403-1422, 1985.

Hocking, W. K., Radar studies of small scale structure in the upper middle atmosphere and lower ionosphere, *Adv. Space Res., 7(10)*, 327-338, 1987a.

Hocking, W. K., "Reduction of the effects of non-stationarity in studies of amplitude statistics of radio wave backscatter", *J. Atmos. Terr. Phys., 49*, 1119-1131, 1987b.

Hocking, W.K., "The effects of middle atmosphere turbulence on coupling between atmospheric regions", *J. Geomag. Geoelectr., 43*, Suppl., 621-636, 1991.

Hocking, W.K., S. Fukao, M. Yamamoto, T. Tsuda, and S. Kato,Viscosity waves and thermal-conduction waves as a cause of 'specular' reflectors in radar studies of the atmosphere, *Radio Sci., 26*, 1281-1303, 1991.

Hocking, W.K., and J. Röttger, Pulse length dependence of radar signal strengths for Fresnel backscatter, *Radio Sci., 18*, 1312-1324, 1983.

Hocking, W.K., Some new perspectives on viscosity and thermal conduction waves as a cause of `specular' reflectors in radar studies of the atmosphere, *STEP Handbook, Proceedings of the Seventh Workshop on Technical and Scientific Aspects of MST Radar, Hilton Head Island S.C. USA*, Nov 7-11, 1995, ed. B. Edwards, 82-85, 1996.

Hocking, W. K., Recent advances in radar instrumentation and techniques for studies of the mesosphere, stratosphere, and troposphere, *Radio Sci., 32, 2241-2270*, 1997.

Hocking, W.K. and K.L. Mu, Upper and Middle Tropospheric KineticEnergy Dissipation Rates from Measurements of C_n^2 - Review of Theories, in-situ Investigations, and experimental Studies using the Buckland Park Atmospheric Radar in Australia", *J. Atmos. Terr. Phys, 59*, 1779-1803, 1997.

Hocking, W.K., and A.M. Hamza, A Quantitative measure of the degree of anisotropy of turbulence in terms of atmospheric parameters, with particular relevance to radar studies, *J. Atmos. Solar Terr. Phys., 59*, 1011-1020, 1997.

Hocking, W.K., The dynamical parameters of turbulence theory as they apply to middle atmosphere studies, *Earth Planets Space, 51*, 525-541, 1999.

Hopfinger, E. J., Turbulence in stratified fluids: a review, *J. Geophys. Res., 92*, 5287-5303, 1987.

Klaassen, G.P., and W.R. Peltier, The onset of turbulence in finite-amplitude Kelvin-Helmholtz billows, *J. Fluid Mech., 155*, 1-35, 1985a.

Klaassen, G.P., and W.R. Peltier, Evolution of finite amplitude Kelvin-Helmholtz billows in two spatial dimensions, *J. Atmos. Sci., 42*, 1321-1339, 1985b.

Kudeki, E., and G.R. Stitt, Frequency domain interferometry: a high resolution radar technique for studies of atmospheric turbulence, *Geophys. Res. Letts., 14*, 198-201, 1987.

Larsen, M. F., and J. Röttger, VHF and UHF Doppler radars as tools for synoptic research, *Bull. Amer. Meteorol. Soc., 63*, 996-1008, 1982. ***** Does not appear in main text – yet to add *****

Lesicar, D., and W.K. Hocking, Studies of seasonal behaviour of the shape of mesospheric scatterers using a 1.98 MHz radar, *J. Atmos. Terr. Phys., 54*, 295-309, 1992.

Lesicar, D., W.K. Hocking and R.A. Vincent, Comparative studies of scatterers observed by MF radars in the Southern Hemisphere mesosphere, *J. Atmos. Terr. Phys., 56*, 581-591, 1994.

Luce, H., M. Crochet, F. Dalaudier, and C. Sidi, Interpretation of VHF ST radar vertical echoes from in-situ temperature sheet observations, *Radio Sci., 30*, 1002-1025, 1995.

Luce, H., M. Yamamoto, S. Fukao, D. Helal and M. Crochet, "A frequency domain interferometric imaging (FII) technique based on high resolution methods", *Ninth International Workshop on Technical and Scientific Aspects of MST Radar – MST9 combined with COST-76 Final Profiler Workshop*, Toulouse, France, March 13-18, 2000.

Maxworthy, T., Ph. Caperan and G. R. Spedding, Two-dimensional turbulence and vortex dynamics in a stratified fluid, *Third International Symposium on Density-Stratified Flows*, Caltech, Pasadena, USA, 1985.

Palmer, R.D., P.B. Chilson, A. Muschinski, G. Schmidt, T.-Y. Yu and H. Steinhagen, "Range imaging using frequency diversity: theory and application", *Ninth International Workshop on Technical and Scientific Aspects of MST Radar – MST9 combined with COST-76 Final Profiler Workshop*, Toulouse, France, March 13-18, 2000.

Pan, C.-J., and J. Röttger, Structures of polar mesosphere summer echoes observed with the EISCAT VHF radar in the interferometer mode, *in Proceedings of the 7th Workshop on Technical and*

Scientific Aspects of MST Radar, edited by B. Edwards, pp. 252-255, STEP Hnadbook, Natl. Oceanic and Atmos. Admin., Boulder, Colo., 1996.

Pao, Y.-H., *Document D1-82-0959*, Boeing Scientific Laboratories, 1968.

Peltier, W. R., J. Halle and T. L. Clarke, The evolution of finite-amplitude Kelvin-Helmholtz billows, *Geophys. Astrophys. Fluid Dyn., 10*, 53-87, 1978.

Reid, I.M., R. Ruester and G. Schmidt, VHF radar observations of Cat's-eye-like structures at mesospheric heights, *Nature, 327*, 43-45, 1987.

Röttger, J. and G. Schmidt, High-resolution VHF radar soundings of the troposphere and stratosphere, *IEEE Trans. Geosci. Electron., GE-17*, 182-189, 1979.

Röttger, J., Reflection and scattering of VHF radar signals from atmospheric refractivity structures, *Radio Sci., 15*, 259-276, 1980a. ***** Does not appear in main text – yet to add ******

Röttger, J., Structure and dynamics of the stratosphere and mesosphere revealed by VHF radar investigations, *Pure Appl. Geophys., 118*, 494-527, 1980b.

Röttger, J., The dynamics of stratospheric and mesospheric fine structure investigated with an MST VHF radar, *Middle Atmosphere Program Handbook*, ed. S. K. Avery, *SCOSTEP Secretariat*, University of Illionois, Vol. 2, pp. 341-350, 1981.

Röttger, J. P. Czechowsky, and G. Schmidt, First low-power VHF radar observations of tropospheric, stratospheric and mesospheric winds and turbulence at the Arecibo Observatory, *J. Atmos. Terr. Phys., 43*, 789-800, 1981.

Röttger, J., and M. F. Larsen, UHF/VHF radar techniques for atmospheric research and wind profiler applications, in *Radar in Meteorology; Battan Memorial and 40th Anniversary Radar Meteorology Conference*, edited by D. Atlas, *pp 235-281*, Amer. Meteorol. Soc., Boston, Mass., 1990.

Röttger, J., H. Luce, M. Yamamoto, S. Fukao, C.H. Liu, C.J. Pan, S.Y. Su and C.H. Wu, Combined high-time resolution SDI-FDI experiments with VHF radars, *Ninth International Workshop on Technical and Scientific Aspects of MST Radar – MST9 combined with COST-76 Final Profiler Workshop*, Toulouse, France, March 13-18, this issue, 2000.

Sahr, J.D., and B.G. Fejer, Auroral electrojet plasmairregularity theory and experiment: A critical review of present understanding and future directions, *J. Geophys. Res., 101*, 26893-26909, 1996.

Smyth, W. D., and W. R. Peltier, The transition between Kelvin-Helmholtz and Holmboe instability: an investigation of the over-reflection hypothesis, *J. Atmos. Sci., 46*, 3698, 1989.

Tsuda, T., W. E. Gordon and H. Saito, Azimuth angle variations of specular reflection echoes in the lower atmosphere observed with the MU radar, *J. Atmos. Solar-Terr. Phys., 59*, 777-784, 1997.

Van Zandt, T.E., A universal spectrum of buoyancy waves in the atmosphere, *Geophys. Res. Letts., 9*, 575-578, 1982.

Werne, J., and D. C. Fritts, Stratifed shear turbulence: Evolution and statistics, *Geophys. Res. Letts., 26*, 439-442, 1999.

Woodman, R. F., High-altitude-resolution stratospheric measurements with the Arecibo 2380-MHz radar, *Radio Sci., 15*, 423-430, 1980.

Woodman, R.F. and P.K. Rastogi, Evaluation of effective eddy diffusive coefficients using radar observations of turbulence in the stratosphere, *Geophys. Res. Letts., 11*, 243-246, 1984.

Woodman, R. F., and Y.-H. Chu, Aspect sensitivity measurements of VHF backscatter made with the Chung-Li radar: plausible mechanisms, *Radio Sci., 24*, 113-125, 1989.